Dissipation dynamics within quantum integrable models

Michiel Larmuseau

Supervisor: Prof. dr. Dimitri Van Neck
Counsellors: Dr. Stijn De Baerdemacker, Pieter Claeys, Dr. ir. Sebastian Wouters

Master's dissertation submitted in order to obtain the academic degree of
Master of Science in Engineering Physics

Vakgroep Fysica en Sterrenkunde
Chair: Prof. dr. Dirk Ryckbosch
Faculty of Engineering and Architecture
Academic year 2015-2016

UNIVERSITEIT
GENT

This research was conducted at the Center for Molecular Modeling.

Preface

Although my decision to study physical engineering was mostly due to the lack of interesting alternatives rather than because of my eagerness to study physics or sincere interest in it, I have no doubt that I would make the same choice if I had to. The road towards graduating was paved with some challenging, yet very interesting courses. It was a beautiful journey along the fundamentals of science. After these five years of study, I'm more than ever convinced that physics is one of the greatest, if not the greatest achievement of mankind. I got especially intrigued by the mysteries of quantum mechanics and many-body problems. The complexity of these problems is such that even with the current computational resources it is very hard to get an understanding of them. Feynman's famous quote "I think I can safely say that nobody understands quantum mechanics" is still valid today, although rapid progress is made in the area. The conviction that true insight can only be obtained by looking at exactly solvable, non-perturbative models is what made this thesis subject so appealing to me. I sincerely hope that this thesis might help to shed more light on how these exactly solvable models behave.

I would like to thank Pieter Claeys for his commitment and incessant support, Stijn De Baerdemacker for his enthusiasm and his physical insights, Professor Van Neck for his aid with the calculations and useful corrections. I would also like to thank all the members of the CMM and my fellow thesis students Yentl, Senne, Titus, Pieter and Klaas for the great atmosphere. A last word of thanks goes to my classmates who have endured the same existential crises as I during our studies of "applied" physics.

Michiel Larmuseau

Michiel Larmuseau

Ghent, 1 June 2016

Dissipation dynamics within quantum integrable models

Larmuseau Michiel

Supervisor: prof. dr. Dimitri Van Neck
Counsellors: dr. Stijn De Baerdemacker and ir. Pieter Claeys

Master's dissertation submitted in order to obtain the academic degree of
Master of Science in Engineering Physics

Faculty of Engineering and Architecture – Ghent University
Center for Molecular Modeling
Academic year 2015–2016

Abstract
We study the dynamics of an integrable $p + ip$ system interacting with a bath. We start by considering the harmonic oscillator to obtain insight into the dynamics of open quantum systems, after which we make the connection with classical damping to facilitate the interpretation of the underlying physics. These insights are then applied to the integrable $p + ip$ system. We numerically analyze the dynamic behavior of this system by looking at the time evolution of the relevant physical properties. The phase transition in the isolated model plays an important role in the dynamics of the model.

Keywords. Harmonic Osillator, Quantum Dynamics, Dissipation, Integrable models

Dissipation dynamics within quantum integrable models

Michiel Larmuseau
Supervisor: prof. dr. Dimitri Van Neck
Counsellors: dr. Stijn De Baerdemacker and ir. Pieter Claeys

Abstract. **We study the dynamics of an integrable $p + ip$ system interacting with a bath. We start by considering the harmonic oscillator to obtain insight into the dynamics of open quantum systems. These insights are then applied to the integrable $p + ip$ system.**
Keywords. **Harmonic Osillator, Quantum Dynamics, Dissipation, Integrable models**

I. Introduction

Dissipation and decoherence in quantum systems is a highly relevant topic in quantum computing. Even at very low temperatures, current quantum computers can only remain in a coherent state for a time of the order of milliseconds [1]. This is because the coherent state decoheres due to the interaction with the environment. It is hence very important that the interaction of the quantum computer with its environment can be modeled in an adequate manner. We present a method to model the dynamics of dissipation and decoherence in a non-perturbative way using integrable models. Before starting the discussion of the integrable model, however, we first consider dissipation in the harmonic oscillator system. The availability of analytic solutions for this system greatly facilitates the interpretation of the underlying physics and contributes strongly to the understanding of damping in open quantum systems.
When considering the integrable models, we focus on the $p + ip$ model. This is mainly because this model exhibits a rich quantum phase diagram and because of its potential for quantum computation in quantum computing [2]. We first consider the isolated system and then add bath-interaction terms to the Hamiltonian.

II. The quantum harmonic oscillator

We consider the following Hamiltonian

$$\hat{H} = \hbar\omega(\hat{a}^\dagger\hat{a} + \frac{1}{2}) + \beta\hat{a}^\dagger + \gamma\hat{a}, \qquad (1)$$

where $\hat{a}$ and $\hat{a}^\dagger$ are the conventional ladder operators. The first two terms correspond to the regular quantum harmonic oscillator and preserve the number of quanta in the system. The last two terms break the conservation of quanta in the system and can therefore be interpreted as an interaction with the environment. As we do not impose that $\gamma = \beta^*$, this Hamiltonian is not hermitian in general. This has a few important consequences:
1. For a hermitian operator, one has that the eigenvalues have to be real. For non-hermitian operators this is no longer the case. This implies that the eigenenergies can become complex, which can lead to dissipation or amplification.
2. The eigenfunctions of a hermitian operator are mutually orthogonal and form a complete set. When the operator is non-hermitian, this is no longer guaranteed. This implies that we may lose the possibility to expand every wavefunction in terms of the eigenfunctions of the Hamiltonian.
3. When $\hat{H}$ is non-hermitian, the time evolution operator $e^{\frac{i\hat{H}t}{\hbar}}$ will no longer be unitary. This causes the norm of the wavefunctions to change through time.
4. When $\hat{H}$ is hermitian, we have that $(\hat{H}|\psi\rangle)^\dagger = \langle\psi|\hat{H}$. In the non-hermitian case this will not hold anymore and we will have to make a distinction between the left and the right eigenstates.

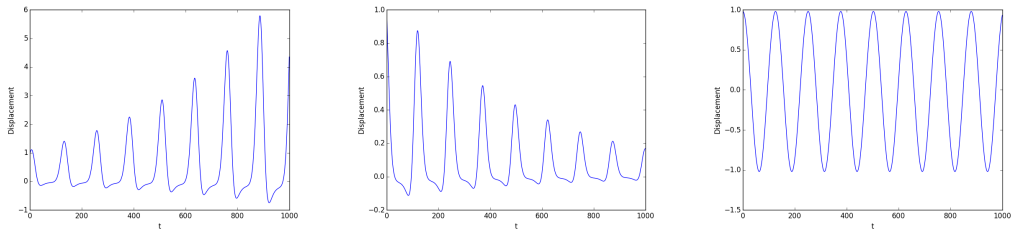

(a) $\beta = 9 + 4i, \quad \gamma = 5 + 3i$ (b) $\beta = 9 + 4i, \quad \gamma = 5 + 3i$ (c) $\beta = 5 + 3i, \quad \gamma = 5 - 3i$

Figure 1: The three different types of time evolution of the displacement: amplification, damping and oscillation. For all figure the following values were chosen $\omega = 50$, $\alpha = 5$ and $m = 1$.

In order to be able to interpret the damping effects, we would like to make a connection to the classical case. We therefore introduce the Glauber state $|\alpha\rangle$, which by definition satisfies

$$\hat{a}\,|\alpha\rangle = \alpha\,|\alpha\rangle\,. \tag{2}$$

It turns out that for this state, the norm evolves as

$$\langle\alpha'(t)|\alpha'(t)\rangle = e^{4|\alpha'||\frac{\gamma-\beta^*}{\hbar\omega}|\sin(\frac{\omega t}{2}-\phi)\sin\frac{\omega t}{2}\times} \tag{3}$$
$$e^{i\frac{\gamma\beta-\gamma^*\beta^*}{\hbar^2\omega^2}\omega t}.$$

The two exponentials have a very different behavior. The first one is causing the norm to oscillate, but doesn't contribute to damping or oscillating on the long term. This is the case for the latter factor, which clearly causes an exponential damping as $\frac{\gamma\beta-\gamma^*\beta^*}{\hbar^2\omega^2}$ is imaginary. Each expectation value with respect to the Glauber state will be proportional to the norm of the Glauber state. In Figure 1, we show the time evolution of the displacement as an example. Depending on the values of β and γ we can obtain a damped, an amplified or an oscillating regime.

It turns out that all the obtained results can straightforwardly be generalized to a system of coupled oscillators.

Because of the difficulties with the interpretation of non-normalized wavefunction, we also briefly consider different methods to introduce dissipation in a quantum system. We find that the most natural way is by employing the density operator formalism, in which the Hilbert space of the system can be easily embedded in a bigger Hilbert space, which represents the environment. Not coincidentally, this formalism is often employed in describing decoherence.

III. Integrable models

We consider the $p + ip$ Hamiltonian

$$\hat{H}_{p+ip} = \sum_{i=1}^{L} \epsilon_i^2 \left(\hat{S}_i^0 + \frac{1}{2}\right) + g \sum_{\substack{i,k \\ k\neq i}}^{L} \epsilon_i \epsilon_k \hat{S}_i^\dagger \hat{S}_k, \tag{4}$$

where each of the L single-particle levels i has a single-particle energy ϵ_i and closes an $su(2)$ algebra $\{\hat{S}_i^\dagger, \hat{S}_i, \hat{S}_i^0\}$.

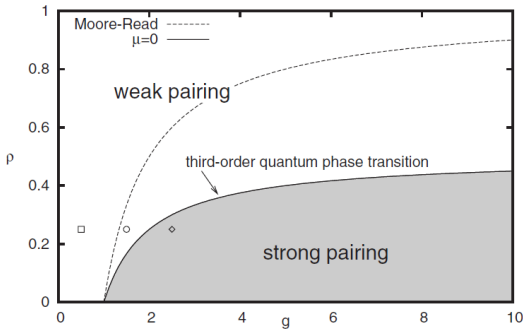

Figure 2: The quantum phase diagram of the $p_x + ip_y$ model [3].

The model has a rich phase diagram as shown in Figure 2. The two lines on the figure are called the Moore-Read line and the Read-Green line. At the Read-Green line, there is a rare third order phase transition. At these lines,

there appear degeneracies in the eigenenergies. To obtain an expression for the eigenstate of the Hamiltonian, we propose the following ansatz for the wavefunction

$$|\psi\rangle = \prod_{\alpha=1}^{N} \hat{S}_\alpha^\dagger |\theta\rangle\,, \tag{5}$$

which is known as the Bethe ansatz wavefunction [4]. $|\theta\rangle$ is the vacuum state, N is the number of excitations of the state and $\hat{S}_\alpha^\dagger$ is the generalized creation operator, given by

$$\hat{S}_\alpha^\dagger = \sum_{i=1}^{L} \frac{\epsilon_i}{\epsilon_i^2 - E_\alpha} \hat{S}_i^\dagger. \tag{6}$$

It is found that this wavefunction is indeed an eigenstate with the eigenenergy given by

$$E = \sum_\alpha E_\alpha - \sum_k \epsilon_k^2 d_k, \tag{7}$$

when the rapidities satisfy the following set of equations

$$1 + 2g \sum_i \frac{\epsilon_i^2 d_i}{\epsilon_i^2 - E_\alpha} - 2g \sum_{\beta \neq \alpha} \frac{E_\alpha}{E_\beta - E_\alpha} = 0, \tag{8}$$

which should hold for each α and with d_i the degeneracy of the orbital. Throughout this work, we will only consider the case $d_i = \frac{1}{2}\ \forall i$. These equations are called the Richardson-Gaudin equations. Solving the eigenvalue problem is hence reduced to solving a set of L algebraic equations in E_α. However, the Richardson-Gaudin equations contain so-called singular points that cause numerical instabilities when solving for the rapidities. In order to sidestep this problem, it is convenient to rewrite the Richardson-Gaudin equations in terms of eigenvalue-based variables $\Lambda_i = \sum_{\alpha=1}^{N} \frac{\epsilon_i^2}{E_\alpha - \epsilon_i^2}$. Expressed in terms of these new variables, the Richardson-Gaudin equations can be solved straightforwardly [5]. Once a solution for eigenvalue-based variables is obtained, it is possible to retrieve the rapidities from them [5], although many physical properties can be computed by solely relying on the eigenvalue-based variables.

From equation (7), it is clear that in case of a finite number of particles degeneracies appear whenever one of the rapidities E_α becomes zero. At the Moore-Read line all the rapidities collapse to zero, whereas at the Read-Green line exactly one rapidity becomes zero. The following relation between the coupling strength g and the number of excitations N holds at the Moore-Read points [3]

$$\frac{1}{g} = 2N - L - 2, \tag{9}$$

whereas at the Read-Green points

$$\frac{1}{g} = N - L - 1. \tag{10}$$

In a completely analogous manner as for the harmonic oscillator, we can now introduce interaction to an environment by breaking the particle-number conservation

$$\hat{H} = \sum_{i=1}^{L} \epsilon_i^2 \left(\hat{S}_i^0 + \frac{1}{2} \right) + g\gamma\epsilon_i \hat{S}_i^\dagger - g\lambda\epsilon_i \hat{S}_i + g \sum_{\substack{i,k \\ k \neq i}}^{L} \epsilon_i \epsilon_k \hat{S}_i^\dagger \hat{S}_k. \tag{11}$$

This model is still integrable [6], so that we can again use the Bethe ansatz wavefunction (5), but now the generalized creation operator is given by [7]

$$\hat{S}_\alpha^\dagger = \lambda + \sum_{k=1}^{L} \frac{\epsilon_k}{\epsilon_k^2 - E_\alpha} \hat{S}_k^\dagger. \tag{12}$$

The Richardson-Gaudin equations expressed in terms of the eigenvalue-based variables are given by

$$g\epsilon_i \Lambda_i^2 = -\Lambda_i + g \sum_{j \neq i}^{L} \frac{\epsilon_i^2 \Lambda_i - \epsilon_j^2 \Lambda_j}{\epsilon_i^2 - \epsilon_j^2} - g\gamma\lambda. \tag{13}$$

This set of equations can be solved very efficiently for Λ_i.

It is possible to express the overlap of the eigenstate $|\{v_\alpha\}\rangle$ with a direct product state

$$|\{i_a\}\rangle = \prod_{k=1}^{N} \hat{S}_k^\dagger |\theta\rangle \tag{14}$$

in terms of the eigenvalues-based variables

$$\langle\{i_a\}|\{E_\alpha\}\rangle = \lambda^{L-N}\left(\prod_{j=1}^{N}\right)\epsilon_{j_a}\det J^{a\beta}, \quad (15)$$

with

$$J_{ij}^{a\beta} = \begin{cases} \Lambda_i^\beta - \sum_{j\neq i}^{N}\frac{1}{\epsilon_{ia}^2-\epsilon_{ja}^2} & \text{if } i=j \\ \frac{1}{\epsilon_{ia}^2-\epsilon_{ja}^2} & \text{if } i\neq j \end{cases} \quad (16)$$

Using these overlaps, we can compute the time-dependent expectation values $\langle\{i_a\}(t)|\hat{S}_i^\dagger|\{i_a\}(t)\rangle$and $\langle\{i_a\}(t)|\hat{S}_i^0|\{i_a\}(t)\rangle$. These expectation values reveal important information about the dynamics of the systems.

IV. Numerical results

The results in this section are for an eight-level system, $L = 8$, with $\epsilon_i^2 = i$ for $i = 1, ..., 8$.

I. Statics

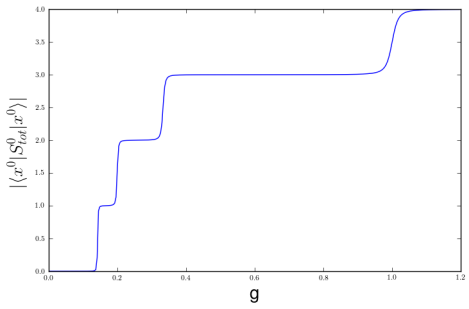

Figure 3: The occupation of the ground state as a function of the coupling strength at $\gamma = 10^{-3}$.

In Figure 3 we see how the number of pairs in the ground state changes strongly around $g = \frac{1}{7}$, $g = \frac{1}{5}$, $g = \frac{1}{3}$ and $g = 1$. Not surprisingly, these values correspond to the Read-Green points. We find that the transition is more abrupt as γ decreases. This is because for small γ the interaction between states with a different number of pairs will be very weak and hence the states involved in the transition will only interact in a very small interval around the Read-Green points.

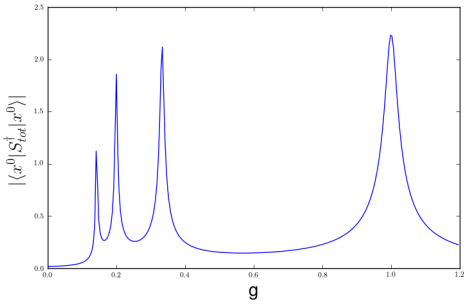

Figure 4: The expectation value of $\hat{S}_i^\dagger$ of the ground state as a function of the coupling strength at $\gamma = 10^{-3}$.

For the expectation value of $\hat{S}_{tot}^\dagger$ with respect to the ground state, shown in Figure 4, we find that for small γ there are only significant peaks around the Read-Green points, indicating that there is indeed a strong interaction between the ground state and the excited states at these points.

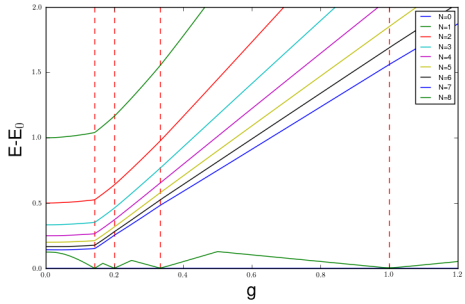

Figure 5: The eigenenergies of the first excitation sector with respect to the ground state energy at $\gamma = 10^{-3}$.

We see that at the Read-Green points, there is an avoided crossing between the ground state and the eigenstate of the first excitation sector with the lowest energy. The other states of the sector have no tendency to interact with the ground state and the difference between the ground state energy and the eigenenergy of these states increases monotonically with increasing coupling strength. The gap between the no-crossing states is proportional to γ, being of the order 10^{-2} for $\gamma = 10^{-4}$ and of the order 1 for $\gamma = 10^{-2}$. The unsmooth behavior of the eigenenergy of the lowest excited

state can be explained by looking at Figure 6. The lowest excited eigenstate also has avoided crossings with eigenstates from higher excitation sectors. In order not to overload the plot, we only show the eigenenergy of the most relevant eigenstate of each excitation sector. It is remarkable how the non-crossing only occur between the first excitation sector and higher order excitation sectors and not between the higher order excitation sectors mutually. For higher values of γ these avoided crossings are present. The absence of the no-crossing of the eigenstates for small values of γ is probably due to the limited numerical precision.

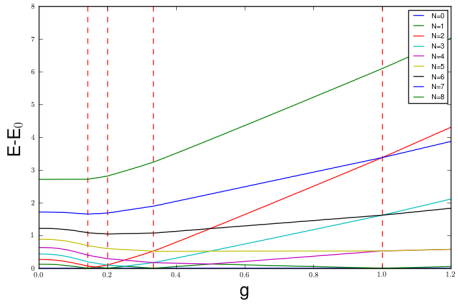

Figure 6: The eigenenergy of the eigenstate that, for each excitation sector, interacts most strongly with the vacuum state as a function of the coupling strength $\gamma = 10^{-3}$.

II. Dynamics

Figure 7 shows the expectation value of $\hat{S}^0_{tot}$ with respect to the vacuum state. There is a sharp peak at the Read-Green point $g = \frac{1}{7}$ for $\gamma = 10^{-3}$. The magnitude of this peak increases monotonously through time. For larger values of γ, the peak becomes broader and there also appear peaks at other Read-Green points. For instance, we find peaks both at $g = \frac{1}{7}$ and $g = \frac{1}{3}$ for $\gamma = 10^{-2}$. The presence of these peaks also seems to depend on the number of levels in the system. For a four-level system, there appeared a very small, large peak for $\frac{1}{2}$ that doesn't seem to have an equivalent in the eight-level system. In Figure 8 we see that for the expectation value of $\hat{S}^\dagger_{tot}$ with respect to the vacuum state there is also peak at $g = \frac{1}{3}$. The peak here is slightly broader than that of the occupancy. The time evolution is very similar to that of the occupancy.

V. Conclusion

We studied the dynamics of dissipation in quantum systems by considering two different models, the harmonic oscillator and the integrable $p + ip$ model. The interaction with the environment was included by breaking the particle-number conservation in the Hamiltonian. For the harmonic oscillator, we found that damping or amplification can be obtained by breaking the hermicity of the Hamiltonian. For the integrable $p + ip$ model, we found that there occurs avoided crossing at the Read-Green points. Based on the time-dependent expectation values $\langle\{i_a\}(t)|\hat{S}^\dagger_i|\{i_a\}(t)\rangle$and $\langle\{i_a\}(t)|\hat{S}^0_i|\{i_a\}(t)\rangle$, we found that the Read-Green points also play an important role in the dynamics of the model, which can be observed in sharp peaks.

References

[1] Bar-Gill, N. and Pham, L. M. and Jarmola, A. and Budker, D. and Walsworth, R. L. Solid-state electronic spin coherence time approaching one second *Nature Communications*, vol. 4 (2013)

[2] Tewari, S. and Das Sarma, S. and Nayak, C. and Zhang, C. and Zoller, P. Quantum Computation using Vortices and Majorana Zero Modes of a $p_x + ip_y$ Superfluid of Fermionic Cold Atoms *Phys. Rev. Lett.*, vol. 98 (2008)

[3] Rombouts, S. and Dukelsky, J. and Ortiz, G. Quantum phase diagram of the integrable $p_x + ip_y$ fermionic superfluid *Physical Review B*, vol. 82 (2010)

[4] Gaudin, M. and Caux, S. The Bethe Wavefunction *ISBN 9781107045859*, 2014

[5] Claeys, P. W. and De Baerdemacker, S. and Van Raemdonck, M. and Van Neck,

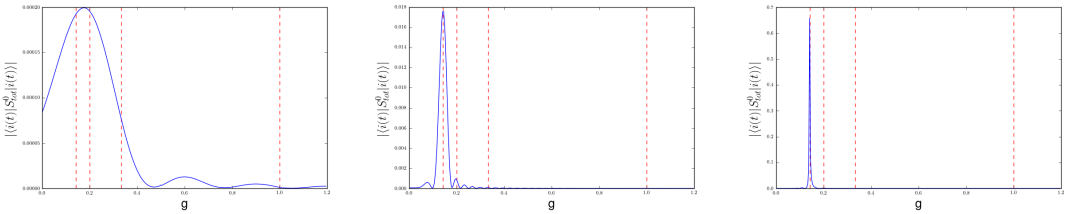

(a) $\gamma = 10^{-3}$ and $t = 100$ (b) $\gamma = 10^{-3}$ and $t = 1000$ (c) $\gamma = 10^{-3}$ and $t = 10000$

Figure 7: The occupation of the vacuum state as a function of the coupling strength and at several times.

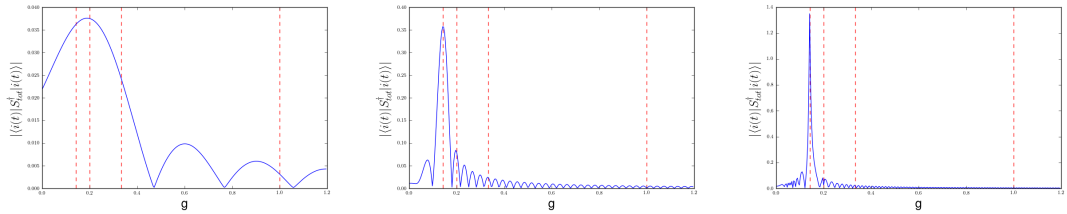

(a) $\gamma = 10^{-3}$ and $t = 100$ (b) $\gamma = 10^{-3}$ and $t = 1000$ (c) $\gamma = 10^{-3}$ and $t = 10000$

Figure 8: The expectation value of $\hat{S}^{\dagger}$ of the vacuum state as a function of the coupling strength and at several times.

D. Eigenvalue-based method and form-factor determinant representations for integrable XXZ Richardson-Gaudin models *Phys. Rev. B*, vol. 91 (2015)

[6] Lukyanenko, I. and Isaac, P. and Links, J. An integrable case of the $p + ip$ pairing Hamiltonian interacting with its environment *Journal of Physics A: Mathematical and Theoretical*, vol. 49 (2016)

[7] Claeys, P. W. and De Baerdemacker, S. and Van Raemdonck, M. and Van Neck, D. Eigenvalue-based determinants for scalar products and form factors in Richardson-Gaudin integrable models coupled to a bosonic mode *Journal of Physics A Mathematical General*, vol. 48 (2015)

Contents

Chapter 1

Introduction

In this thesis we aim to study the dissipation dynamics in (integrable) quantum systems. This subject is becoming increasingly more relevant, now that decoherence turns out to be one of the main challenges in quantum computation and spintronics[1] [1, 2].
In this chapter we will outline the structure of this thesis, briefly discuss some of the main concepts that will be used throughout this work and mention some of the applications.

1.1 Dynamics in quantum systems

In 1925 Schrödinger formulated his well-known equation [3]

$$i\hbar\frac{\partial}{\partial t}\left|\psi\right\rangle = \hat{H}\left|\psi\right\rangle \tag{1.1}$$

which describes the dynamics of a non-relativistic quantum system. This equation implies that given the Hamiltonian $\hat{H}$ of a system and an initial state, we know how the state will evolve through time. The Hamiltonian therefore contains the essential information on the dynamics of the system. If the Hamiltonian is time-independent, which will almost always be the case in this thesis, the equation can be formally solved to yield

$$\left|\psi(t)\right\rangle = e^{-\frac{i\hat{H}t}{\hbar}}\left|\psi(0)\right\rangle, \tag{1.2}$$

so that the time evolution operator is a unitary transformation if the Hamiltonian is hermitian. If one desires to further simplify the expression, one can expand $|\psi\rangle$ in terms of the eigenstates of the Hamiltonian, which can be determined by solving the corresponding eigenvalue equation. Thus, describing the dynamics of a quantum system boils down to

[1] For the relation between dissipation and decoherence, see section 1.2

solving an eigenvalue equation. Unfortunately, the dimension of the Hilbert space in which the eigenvalue equation has to be solved scales exponentially with the number of degrees of freedom in the system [4]. Therefore, one very seldom encounters a quantum system for which the dynamics can be described exactly. In this work we will focus on a special subclass of quantum models, for which we can still solve the eigenvalue equation exactly for many degrees of freedom. As we can thus obtain all the eigenstates, each possible state can be expanded in terms of the eigenstates and we can calculate how the state propagates in an exact manner. It is therefore possible to infer how the system will evolve after a sudden perturbation, also called a quantum quench [5].

1.2 Dissipation and decoherence

Under dissipation we understand the loss of (useful) energy in the system. From thermodynamics we know that dissipation can never occur in an isolated system. If we want to include dissipative effects, we will need interaction of the system with an external environment. Decoherence is the loss of interference, or the ordering of the phase angles, between the components in a system [6]. Decoherence relates to the loss of information, whereas dissipation refers to the loss of (useful) energy. In the context of quantum computing the typical timescale of decoherence is usually much smaller than that of dissipation. For an accessible discussion see [7]. In this work we will use the term dissipation, bearing in mind that the presented framework can also be used to describe decoherence.
The most general approach to include interaction with an environment is to split the Hamiltonian in three parts: one describing the system, one describing the environment and one describing the coupling between the system and the environment. As the environment usually contains a vast amount of degrees of freedom, the Hamiltonian describing the environment can be approximated or even neglected[2].

1.3 Quantum computing

In this section we will briefly describe a possible application. In quantum computing, one wants to make use of the entanglement in a quantum system to perform highly parallel computations. We will not discuss the underlying fundamentals, but we refer to [8] for an accessible overview of quantum computing. We here wish to focus on a possible method to create a quantum computer using spins and how the work presented here could be relevant

[2]We will discuss some methods to include damping in section 2.2.

in the modeling thereof.
In Figure 1.1a a nitrogen-vacancy impurity in diamond is depicted. The current state of technology allows to create this kind of impurities in synthetic diamond [9]. The impurity has energy levels in the band gap of diamond and from Figure 1.1b it is clear that for instance the $|^3A_2, +1\rangle$ and the $|^3A_2, 0\rangle$ state behave as a two state system, which can be used as a qubit[3] for quantum computation. This setup is appealing to many quantum computing researchers, because it conserves entanglement well at room temperature[4], thus offering the long term prospective of a quantum computer at room temperature [10].

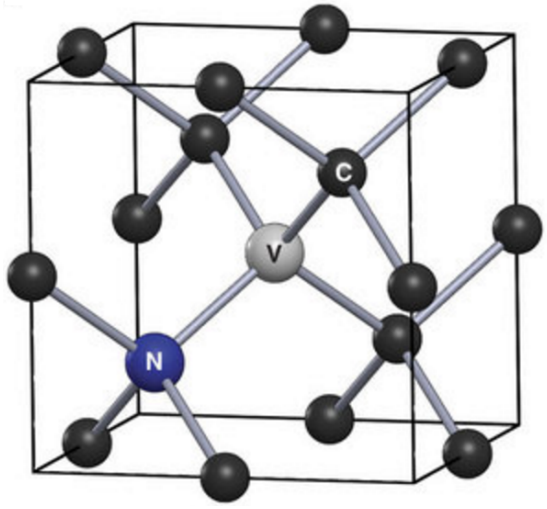

(a) A graphical illustration of a N-V impurity in diamond [11].

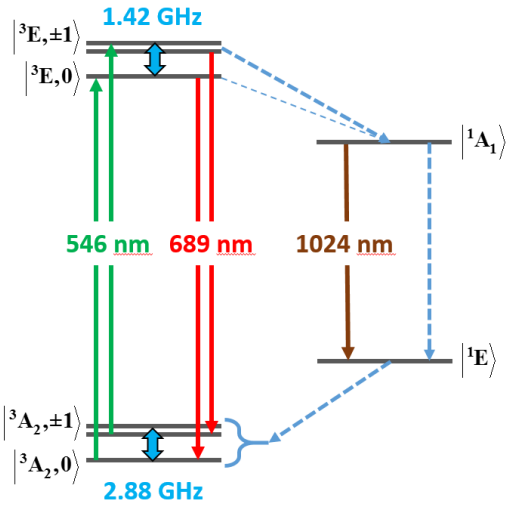

(b) The spin dynamics diagram [12]. There are two triplet states, $|^3E\rangle$ and $|^3A_2\rangle$, and two intermediate singlet states,$|^1E\rangle$ and $|^1A_1\rangle$ [13].

However, there are still many challenges ahead and a better understanding of spin decoherence is one of those. In [14] the model we discuss in chapter 5 is used to describe decoherence in such a spin system. The model used has the disadvantage that the environment has to be modeled as well. This drawback can be remedied by the model we introduce in chapter 6.

[3] A qubit is in fact the quantum information terminology for any two state system.
[4] In the reference a decoherence time of about 1 millisecond is mentioned. This should be enough to perform about 100,000 operations.

1.4 Outline

The aim of this thesis is to discuss the dissipation in integrable systems as set out in chapter 6. In order to better understand this kind of interaction with an environment, we study the same kind of dissipation in the harmonic oscillator, see chapter 2. The connection to the classical case is made several times, because this facilitates the interpretation. In chapter 3 we introduce integrable models and propose an ansatz for the eigenstates. We find that the eigenstates can be obtained by solving a set of algebraic equations that scales linearly with the system size. We note several analogies between the harmonic oscillator and the integrable models. In chapter 4 we discuss how these equations can be solved efficiently. In chapter 5 we introduce an isolated integrable system that exhibits an interesting phase diagram and to which we will add dissipation in chapter 6. We discuss how we can numerically compute the relevant physical properties of the model. In chapter 7 we proceed to numerically analyze both the statics and the dynamics of the model. In chapter 8 we give the conclusion and the outlook.

Chapter 2

Dissipation dynamics in the harmonic oscillator

The harmonic oscillator will be the starting point for our study of the dissipation dynamics in quantum integrable models, because for this system closed-form solutions can be obtained, facilitating the interpretation of the underlying physics. We will start by considering the regular harmonic oscillator and search for a state that mimics the dynamics of the classical harmonic oscillator. More specifically, we wish to construct a quantum equivalent of the damped classical pendulum. The connection to classical physics is made, because we thus hope to better understand the nature of damping in the quantum case. Next we will show that the discussion of the single oscillator can straightforwardly be extended to a set of coupled oscillators.

2.1 The single harmonic oscillator

In this section we will to find a wavefunction that gives the same time evolution of the displacement as in the classical case. The results for the classical case are derived in Appendix A. We summarize the most important results. The classical Hamiltonian of a a particle with a mass m in a harmonic oscillator potential with spring constant $m\omega^2$ is given by

$$H = \frac{p^2}{2m} + \frac{m\omega^2 x^2}{2}, \tag{2.1}$$

from which the well-known equation of motion can be derived

$$\frac{d^2x}{dt^2} = -\omega^2 x, \tag{2.2}$$

the general solution of which is given by

$$x(t) = A\cos(\omega t + \phi), \tag{2.3}$$

with A, ω and ϕ real. We are hence looking for a wavefunction $\psi(t)$ so that

$$\langle\psi(t)|\hat{X}|\psi(t)\rangle = A\cos(\omega t + \phi). \tag{2.4}$$

2.1.1 The harmonic oscillator without damping

The undamped quantum harmonic oscillator is described by the following Hamiltonian

$$\hat{H} = \frac{\hat{P}^2}{2m} + \frac{m\omega^2\hat{X}^2}{2}, \tag{2.5}$$

where the hat symbol indicates an operator. This Hamiltonian is the same as in the classical case, but in the quantum case the canonical coordinates are replaced by operators. By using the Dirac recipe

$$\{,\} \to i\hbar[,], \tag{2.6}$$

with $\{,\}$ the Poisson bracket and $[,]$ the commutator, we find the quantum equivalent of equation (A.4)

$$[\hat{X}, \hat{P}] = i\hbar. \tag{2.7}$$

In coordinate space, these operators have the well known representation

$$\hat{X} \to x \tag{2.8}$$

$$\hat{P} \to -i\hbar\frac{\partial}{\partial x}, \tag{2.9}$$

which clearly satisfies equation (2.7). By considering the eigenvalue equation of the Hamiltonian

$$\hat{H}\,|\psi_n\rangle = E_n\,|\psi_n\rangle \tag{2.10}$$

in coordinate space

$$-\frac{\hbar^2}{2m}\frac{\partial^2\psi_n}{\partial x^2} + \frac{m\omega^2x^2}{2}\psi_n = E_n\psi_n, \tag{2.11}$$

we obtain a differential equation that can straightforwardly be solved. The eigenenergies are then given by

$$E_n = \hbar\omega(n + \frac{1}{2}), \quad n \in \mathbb{N}. \tag{2.12}$$

As depicted in Figure 2.1, the spectrum of the harmonic oscillator is equidistant and the ground state has an energy different from zero, which is called the zero-point energy. The corresponding eigenfunctions are given by

$$\psi_n(x) = \frac{1}{\sqrt{2^n n!}}(\frac{m\omega}{\pi\hbar})^{1/4} e^{-\frac{m\omega x^2}{2\hbar}} H_n(\sqrt{\frac{m\omega}{\hbar}}x). \tag{2.13}$$

Here, H_n is the nth-order Hermite polynomial and n is the excitation level. It is convenient to write the normalized eigenfunction in terms of dimensionless variables

$$\psi_n(\zeta) = \frac{1}{\sqrt{2^n n!}}(\frac{1}{\pi})^{1/4} e^{-\frac{\zeta^2}{2}} H_n(\zeta), \tag{2.14}$$

with $\zeta = \sqrt{\frac{m\omega}{\hbar}}x$.
The ground state is given by

$$\psi_0(\zeta) = (\frac{1}{\pi})^{1/4} e^{-\frac{\zeta^2}{2}}, \tag{2.15}$$

which is a Gaussian function centered around zero. This can be seen as the quantum mechanical equivalent of a classical particle at rest. The non-zero variance in the position, $\sigma_x^2 = \frac{\hbar}{m\omega}$, is necessary to comply with the Heisenberg uncertainty principle. In the limit of large excitations, $n \to \infty$, we obtain a particle density that is very similar to the classical

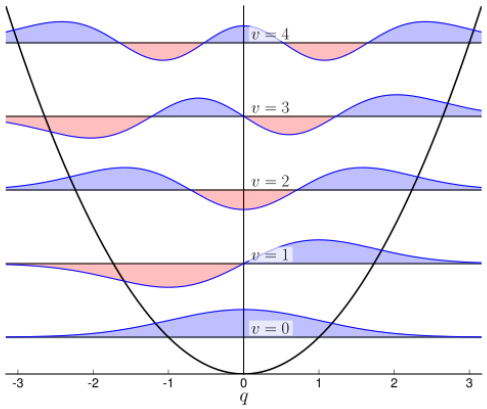

Figure 2.1: The eigenfunctions of harmonic oscillator Hamiltonian and their spectrum [15].

case, as shown in Figure 2.2. This is conform the correspondence principle, that stipulates that for large quantum numbers one should be able to reproduce classical results. We see that the particle is most likely to be found at the "walls" of the potential. It is easy to see that the expectation value of $\hat{X}$ with respect to an eigenstate is zero at each moment. This is clearly different from what we find in the classical case. Therefore, the correspondence principle won't help us to find a wavefunction that satisfies equation (2.4). For the lower excited states, no exact analogy can be made with the classical case, as due to presence of the Hermite polynomials, the particle will be less likely found at the "walls" of the harmonic potential than in the classical case, as can be seen in Figure 2.1.

It is customary to introduce the creation and annihilation operators

$$\hat{a} = \sqrt{\frac{m\omega}{2\hbar}}(\hat{X} + \frac{i}{m\omega}\hat{P}), \tag{2.16}$$

$$\hat{a}^\dagger = \sqrt{\frac{m\omega}{2\hbar}}(\hat{X} - \frac{i}{m\omega}\hat{P}). \tag{2.17}$$

These operators satisfy

$$[\hat{a}, \hat{a}^\dagger] = 1, \quad [\hat{N}, \hat{a}^\dagger] = \hat{a}^\dagger, \quad [\hat{N}, \hat{a}] = -\hat{a}, \tag{2.18}$$

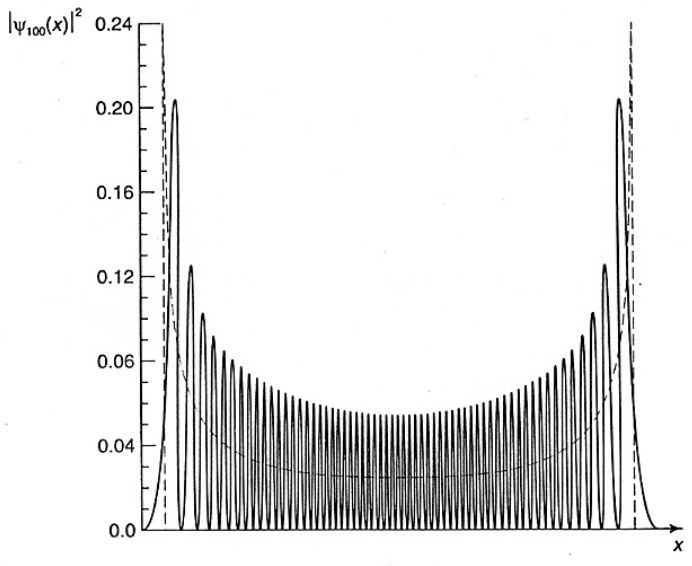

Figure 2.2: Comparison of the classical density (dashed curve) and the density of the wavefunction $|\psi_{n=100}(x)|^2$ [16].

where we have introduced the number operator, $\hat{N} \triangleq \hat{a}^\dagger \hat{a}$. We can write the original operators in terms of the new ones

$$\hat{X} = \sqrt{\frac{\hbar}{2m\omega}}(\hat{a} + \hat{a}^\dagger), \quad \hat{P} = i\sqrt{\frac{m\omega\hbar}{2}}(\hat{a} - \hat{a}^\dagger), \tag{2.19}$$

$$\hat{H} = \hbar\omega(\hat{N} + \frac{1}{2}), \tag{2.20}$$

The $\hat{a}^\dagger$ can be considered as an operator that creates an energy quantum with an energy of $\hbar\omega$ and similarly $\hat{a}$ annihilates such a quantum. The total energy in the system then equals the number of energy quanta times $\hbar\omega$ plus the zero-point energy. This is precisely what the Hamiltonian expresses. Written in terms of the creation operator, the normalized eigenstates of the Hamiltonian are

$$\psi_n = \frac{(\hat{a}^\dagger)^n}{\sqrt{n!}} \left|0\right\rangle, \tag{2.21}$$

with $|0\rangle$ the vacuum state. Each of the eigenstates has a distinct number of energy quanta. Because commutator relations are involved, the energy quanta behave as bosons [4]. We wonder whether it is possible to find a superposition of eigenstates for which the dynamical analogy, as in equation (2.4), does hold. In literature, states that have dynamics strongly resembling the classical case are called coherent states or Glauber states and are frequently used in quantum optics [17, 18, 19]. These states satisfy

$$\hat{a} \left|\alpha\right\rangle = \alpha \left|\alpha\right\rangle. \tag{2.22}$$

As Glauber states are the right eigenstates, as opposed to a left eigenstate, of the annihilation operator, we see that coherent states don't have a well defined number of energy quanta. Taking the hermitian conjugate of this definition, we find that

$$\left\langle\alpha\right| \hat{a}^\dagger = \left\langle\alpha\right| \alpha^*, \tag{2.23}$$

showing that the corresponding bra is a left eigenstate of the creation operator. Also note that, since $\hat{a} \left|0\right\rangle = 0$, the ground state is also a Glauber state with $\alpha = 0$.
The Glauber states can be expanded in terms of the eigenstates of the Hamiltonian as

$$\left|\alpha\right\rangle = C \sum_{n=0}^{\infty} \frac{(\alpha\hat{a}^\dagger)^n}{n!} \left|0\right\rangle = C e^{\alpha\hat{a^\dagger}} \left|0\right\rangle, \tag{2.24}$$

with C a normalization constant. To determine C we first introduce the displacement operator

$$\hat{D}(\alpha) = e^{\alpha\hat{a}^\dagger - \alpha^*\hat{a}}, \tag{2.25}$$

which is clearly a unitary operator, since the operator in the exponent is antihermitian. Using the Baker-Campbell-Hausdorff formula, examined in Appendix B, we can rewrite this as

$$\hat{D}(\alpha) = e^{-\frac{|\alpha|^2}{2}} e^{\alpha \hat{a}^\dagger} e^{-\alpha^* \hat{a}}. \tag{2.26}$$

Again using the Baker-Campbell-Hausdorff formula, we can prove that

$$\hat{D}^\dagger(\alpha) \hat{a} \hat{D}(\alpha) = \hat{a} - [\alpha^* \hat{a} - \alpha \hat{a}^\dagger, \hat{a}] = \hat{a} + \alpha. \tag{2.27}$$

Using this, it is straightforward to see that a Glauber state can also be written as

$$|\alpha\rangle = \hat{D}(a) |0\rangle . \tag{2.28}$$

This can be most easily shown by considering

$$\begin{aligned} \hat{a}\hat{D}(\alpha) |0\rangle &= \hat{D}(\alpha)\hat{D}^\dagger(\alpha)\hat{a}\hat{D}(\alpha) |0\rangle \\ &= \hat{D}(\alpha)(\hat{a} + \alpha) |0\rangle \\ &= \alpha \hat{D}(\alpha) |0\rangle \end{aligned} \tag{2.29}$$

We can now determine the normalization constant. First note that C is also the overlap with the ground state, $C = \langle 0|\alpha\rangle$. Writing $|\alpha\rangle$ in terms of the displacement operator, we get

$$C = \langle 0|\alpha\rangle = \langle 0|\hat{D}(\alpha)|0\rangle = e^{-\frac{|\alpha|^2}{2}} \langle 0| e^{\alpha \hat{a}^\dagger} e^{-\alpha^* \hat{a}} |0\rangle . \tag{2.30}$$

If we now expand the exponentials in the braket, we immediately see that only the zeroth order in $(\alpha^* \hat{a})$ is retained, so that we finally obtain

$$C = e^{-\frac{|\alpha|^2}{2}}. \tag{2.31}$$

The overlap of a coherent state $|\alpha\rangle$ with the eigenfunctions of the harmonic oscillator are hence given by

$$\langle n|\alpha\rangle = \frac{\alpha^n e^{-\frac{\alpha^2}{2}}}{\sqrt{n!}}. \tag{2.32}$$

The squared modulus of these coefficients is thus a Poisson distribution.
Being able to expand $|\alpha\rangle$ in terms of eigenstates of the Hamiltonian, we can determine its time evolution $|\alpha(t)\rangle$ as

$$|\alpha(t)\rangle = e^{-\frac{iHt}{\hbar}} |\alpha\rangle = \sum_{n=0}^{\infty} \langle n|\alpha\rangle \, e^{-i(n+\frac{1}{2})\omega t} |n\rangle = e^{-\frac{|\alpha|^2}{2}} e^{\frac{-i\omega t}{2}} \sum_{n=0}^{\infty} \frac{(\alpha e^{-i\omega t})^n}{\sqrt{n!}} |n\rangle , \tag{2.33}$$

which is, up to a phase factor $e^{\frac{-i\omega t}{2}}$, again a Glauber state with the time-dependent eigenvalue $\alpha e^{-i\omega t}$.

To obtain more insight in the behavior of Glauber states, we can derive their representation in coordinate space. Using the definition of a Glauber state, see equation 2.22, we find

$$\hat{a}\,|\alpha\rangle = \sqrt{\frac{m\omega}{2\hbar}}(\hat{X} + \frac{i}{m\omega}\hat{P})\,|\alpha\rangle = \alpha\,|\alpha\rangle\,, \tag{2.34}$$

so that in coordinate space

$$\sqrt{\frac{m\omega}{2\hbar}}(x + \frac{\hbar}{m\omega}\frac{d}{dx})\,\langle x|\alpha\rangle = \alpha\,\langle x|\alpha\rangle\,. \tag{2.35}$$

The solution of this linear differential equation is

$$\langle x|\alpha\rangle = \left(\frac{m\omega}{\pi\hbar}\right)^{1/4} e^{-\frac{\left(\sqrt{\frac{m\omega}{\hbar}}x - \sqrt{2}\alpha\right)^2}{2}} = \left(\frac{1}{\pi}\right)^{1/4} e^{-\frac{(\zeta - \sqrt{2}\alpha)^2}{2}}. \tag{2.36}$$

This is clearly the (dimensionless) ground state shifted to the right by $\sqrt{2}\alpha$. Hence, the particle is no longer at rest in the bottom of the harmonic potential, but ζ has an expectation value of $\sqrt{2}\alpha$. This clearly corresponds to a classical pendulum moved away from equilibrium and hence "excited". We've thus succeeded in finding the quantum mechanical equivalent of a classical oscillator, as depicted in Figure 2.3. In order to derive an expression for the expectation value of $\hat{X}$ with respect to a Glauber state $|\alpha\rangle$, we start by using the completeness relation of the eigenstates

$$\langle\alpha(t)|\hat{X}|\alpha(t)\rangle = \sum_{n,m} \langle\alpha(t)|n\rangle\,\langle n|\hat{X}|m\rangle\,\langle m|\alpha(t)\rangle\,. \tag{2.37}$$

The overlaps $\langle\alpha(t)|n\rangle$ are already determined in equation (2.32), but we still have to find an expression for $\langle n|\hat{X}|m\rangle$. We start by noting that these elements are symmetric, so that we can restrict ourselves to $n \leq m$, or since all diagonal elements will be zero due to the odd parity, $n < m$. As the Hermite polynomials are complete and orthogonal, only $m = n - 1$ will yield non-zero results. We can use the recursion relation

$$H_{n+1}(x) = 2xH_n(x) - 2nH_{n-1}(x) \tag{2.38}$$

to obtain

$$\langle n|\hat{\hat{X}}|n-1\rangle = \sqrt{\frac{\hbar n}{2m\omega}}. \tag{2.39}$$

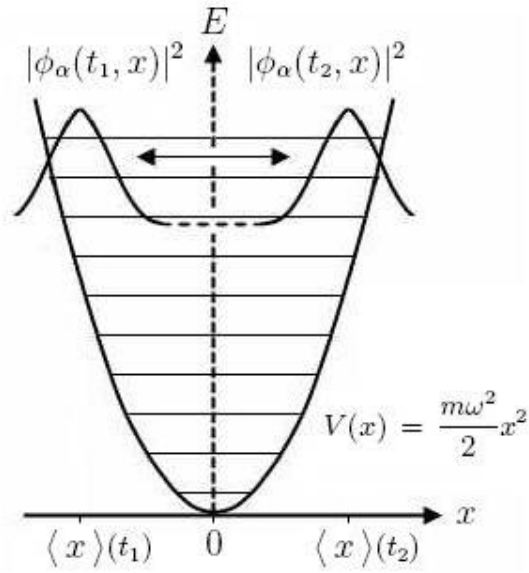

Figure 2.3: A graphical representation of the Glauber states in coordinate space. [16]

Hence, no integrals need to be computed in order to calculate the expectation value of $\hat{X}$. For the time evolution, we can now compare the quantum Glauber state with the classical case. We consider a classical harmonic oscillator that has no initial speed

$$x(t) = A\cos(\omega t). \tag{2.40}$$

For the Glauber state, we have that

$$\begin{aligned}
\langle\alpha|\hat{X}|\alpha\rangle &= \sum_{n,m}^{\infty} \langle\alpha(t)|\psi_n\rangle \langle\psi_n|\hat{X}|\psi_m\rangle \langle\psi_m|\alpha(t)\rangle \\
&= \sum_{n=0}^{\infty} (e^{i\omega t} \langle\alpha|\psi_n\rangle \langle\psi_n|\hat{X}|\psi_{n+1}\rangle \langle\psi_{n+1}|\alpha\rangle + e^{-i\omega t} \langle\alpha|\psi_{n+1}\rangle \langle\psi_{n+1}|\hat{X}|\psi_n\rangle \langle\psi_n|\alpha\rangle) \\
&= 2\cos(\omega t) \sum_{n=0}^{\infty} \langle n|\alpha\rangle \langle n+1|\alpha\rangle \langle n|\hat{X}|n+1\rangle \\
&= 2\cos(\omega t)\sqrt{\frac{\hbar}{m\omega}} \sum_{n=0}^{\infty} \frac{|\alpha|^n e^{-|\frac{\alpha|^2}{2}}}{\sqrt{n!}} \frac{|\alpha|^{n+1} e^{-\frac{|\alpha|^2}{2}}}{\sqrt{n+1!}} \sqrt{\frac{n+1}{2}} \\
&= 2\cos(\omega t)\sqrt{\frac{\hbar}{m\omega}} \frac{|\alpha|}{\sqrt{2}} \sum_{n=0}^{\infty} \frac{|\alpha|^n e^{-|\alpha|^2}}{n!} \\
&= \sqrt{\frac{2\hbar}{m\omega}} |\alpha| \cos(\omega t).
\end{aligned} \tag{2.41}$$

We obtain the classical result if we put $A = \sqrt{\frac{2\hbar}{m\omega}}|\alpha|$.
In what follows, we will also need the expectation value of $\hat{X}^2$. We therefore perform the

calculation here. Based on the recursion formula of Hermite polynomials, we find that

$$2x^2 H_n(x) = \frac{1}{2}H_{n+2}(x) + (2n+1)H_n(x) + n(n-1)H_{n-2}(x). \tag{2.42}$$

We can use this formula to obtain

$$\begin{aligned}
\langle\alpha|\hat{X}^2|\alpha\rangle &= \sum_{i=0}^{N}(e^{2i\omega t}\langle\alpha|i\rangle\langle i+2|\alpha\rangle\langle i|\hat{X}^2|i+2\rangle \\
&\qquad + e^{-2i\omega t}\langle\alpha|i+2\rangle\langle i|\alpha\rangle\langle i+2|\hat{X}^2|i\rangle + \langle\alpha|i\rangle\langle i|\alpha\rangle\langle i|\hat{X}^2|i\rangle) \\
&= 2\cos(2\omega t)\frac{\hbar}{m\omega}\sum_{i=0}^{N}\frac{|\alpha|^i e^{-|\frac{\alpha|^2}{2}}}{\sqrt{i!}}\frac{|\alpha|^{i+2}e^{-|\frac{\alpha|^2}{2}}}{\sqrt{i+2!}}\frac{1}{2}\sqrt{(i+1)(i+2)} \\
&\qquad + \frac{\hbar}{m\omega}\sum_{i=0}^{N}\frac{|\alpha|^i e^{-|\frac{\alpha|^2}{2}}}{\sqrt{i!}}\frac{|\alpha|^i e^{-|\frac{\alpha|^2}{2}}}{\sqrt{i!}}\frac{2i+1}{2} \\
&= \frac{2\hbar}{m\omega}\cos^2(\omega t)|\alpha|^2 + \frac{\hbar}{2m\omega}.
\end{aligned} \tag{2.43}$$

We see that the expectation value contains both a static and a dynamic contribution. The dynamic contribution is exactly what we would expect in the classical case. The static contribution accounts for the fact that we are considering a Gaussian wavepacket rather than a classical pendulum. Note that the variance is exactly the variance of the ground state, $\frac{\hbar}{2m\omega}$ and that it is time-independent. This explains the name coherent state: the wavepacket doesn't spread out as time is evolving. It is customary to make the displacement dimensionless by rescaling it with $\sqrt{\frac{m\omega}{\hbar}}$. We then find that the dimensionless standard deviation on the position is given by $\sigma_\zeta = \frac{1}{\sqrt{2}}$. Proceeding analogously for the momentum, we find that

$$\langle\alpha(t)|\hat{P}|\alpha(t)\rangle = \sqrt{2m\hbar\omega}|\alpha|\sin(\omega t) \tag{2.44}$$

$$\langle\alpha(t)|\hat{P}^2|\alpha(t)\rangle = 2m\hbar\omega|\alpha|^2\sin^2(\omega t) + \frac{m\omega\hbar}{2}. \tag{2.45}$$

The variance is hence given by $\frac{m\omega\hbar}{2}$, which is again time-independent. Rescaling the momentum with $\sqrt{\frac{1}{m\omega\hbar}}$, we find that the rescaled standard deviation of the momentum is the same as for the position, $\frac{1}{\sqrt{2}}$. This is also an important feature of the coherent states: the standard deviation of the dimensionless displacement is the same as the standard deviation of the dimensionless momentum. Multiplying standard deviation of the displacement with that of the momentum, we find

$$\sigma_x\sigma_p = \frac{\hbar}{2}, \tag{2.46}$$

so that coherent states exactly satisfy the Heisenberg uncertainty principle. States that do satisfy the Heisenberg principle, but that don't have an equal variance in the dimensionless momentum and the dimensionless displacement such as our coherent state are called squeezed states [20].

We now repeat the above calculation using the creation and annihilation operators. Considering again the Glauber state

$$\hat{a}\,|\alpha\rangle = \alpha\,|\alpha\rangle\,, \tag{2.47}$$

we can, as argued before, obtain the correct description of the time evolution when calculating expectation values by replacing α with $\alpha(t) = \alpha e^{-i\omega t}$, because the extra phase factor $e^{-i\omega t}$ drops out. Writing $\alpha = |\alpha|e^{i\phi}$, we obtain immediately

$$\langle\alpha(t)|\hat{X}|\alpha(t)\rangle = \sqrt{\frac{\hbar}{2m\omega}}(\alpha^*(t) + \alpha(t)) = \sqrt{\frac{2\hbar}{m\omega}}|\alpha|\cos(\omega t - \phi) \tag{2.48}$$

$$\langle\alpha(t)|\hat{P}|\alpha(t)\rangle = i\sqrt{\frac{\hbar m\omega}{2}}(\alpha^*(t) - \alpha(t)) = \sqrt{2\hbar m\omega}|\alpha|\sin(\omega t - \phi). \tag{2.49}$$

The latter result could have immediately obtained if we had used the Ehrenfest theorem. For $\hat{X}^2$ we find

$$\begin{aligned}\langle\alpha(t)|\hat{X}^2|\alpha(t)\rangle &= \frac{\hbar}{2m\omega}(\alpha^{*2}(t) + \alpha^2(t) + 2\alpha^*(t)\alpha(t) + 1)\\ &= \frac{\hbar}{2m\omega}((\alpha^*(t) + \alpha(t))^2 + 1)\\ &= \frac{2\hbar}{m\omega}|\alpha|^2\cos^2(\omega t - \phi) + \frac{\hbar}{2m\omega}.\end{aligned} \tag{2.50}$$

From the above it becomes clear that working with the annihilation and creation operators rather than working in coordinate space usually makes the calculations more compact and elegant. Therefore, we will mainly use the ladder operator formalism throughout the rest of this chapter.

2.1.2 Consequences of a non-hermitian Hamiltonian

In the next subsection we will examine systems with a non-hermitian Hamiltonian. This has a few important consequences which we will briefly discuss here.

1. For a hermitian operator, one has that the eigenvalues have to be real. For non-hermitian operators this is no longer the case. This implies that the eigenenergies can become complex, which can lead to dissipation or amplification.

2. The eigenfunctions of a hermitian operator are mutually orthogonal and they form a complete set. When the operator is non-hermitian, this is no longer guaranteed. This implies that we may lose the possibility to expand every wavefunction in terms of the eigenfunctions of the Hamiltonian.
3. When $\hat{H}$ is non-hermitian, the time evolution operator $e^{\frac{i\hat{H}t}{\hbar}}$ will no longer be unitary. This causes the norm of the wavefunctions to change through time. The norm of the wavefunction will hence no longer be one at each time.
4. When $\hat{H}$ is hermitian, we have that $(\hat{H}\left|\psi\right\rangle)^\dagger = \left\langle\psi\right|\hat{H}$, implying that the left and right eigenstate are the same. In the non-hermitian case this will not hold anymore and we will have to make a distinction between the left and the right eigenstates.

2.1.3 Single oscillator with dissipation

In the previous subsection we looked at the textbook quantum harmonic oscillator and made a connection to classical physics. In this subsection, we would like to include damping into the model. Damping can be seen as an energy transfer from the system to an environment, a "bath" to use the thermodynamical jargon. In order to have damping we must thus allow for the exchange of particles carrying energy between the system and the bath. This will have to be taken into account when constructing a suitable Hamiltonian. We should point out, however, that it is in generally very difficult to introduce damping in the Hamilton-Lagrange formalism, because it is by definition a non-conservative force and these cannot be described with said formalism. In the classical case, damping can easily be introduced within the Newton formalism. It suffices to add an extra term to the equation of motion that is proportional to the velocity

$$m\frac{d^2x}{dt^2} = -kx - \gamma\frac{dx}{dt}, \tag{2.51}$$

with $\gamma > 0$.This differential equation can easily be solved to give solutions of the form:

$$x(t) = e^{-\frac{\gamma t}{2}}\cos\left(\omega_{eff}t\right), \tag{2.52}$$

with $\omega_{eff} = \sqrt{\omega^2 - (\frac{\gamma}{2})^2}$.
In the quantum mechanical case, we can introduce the following Hamiltonian

$$\hat{H} = \frac{\hat{P}^2}{2m} + \frac{m\omega^2\hat{X}^2}{2} + \beta\hat{a}^\dagger + \gamma\hat{a} = \hbar\omega(\hat{a}^\dagger\hat{a} + \frac{1}{2}) + \beta\hat{a}^\dagger + \gamma\hat{a}. \tag{2.53}$$

With, as before:

$$\hat{a} = \sqrt{\frac{m\omega}{2\hbar}}(\hat{X} + \frac{i}{m\omega}\hat{P})\hat{a}^\dagger = \sqrt{\frac{m\omega}{2\hbar}}(\hat{X} - \frac{i}{m\omega}\hat{P}). \tag{2.54}$$

The two added terms will allow to exchange particles with the environment. Already, we can predict that there will be a competition between β and γ to determine whether there will be a net influx or outflux of particles.
Note that the above Hamiltonian will only be hermitian when $\gamma = \beta^*$. We purposely choose not to impose this condition right away, in order to be able to analyze the influence of γ and β separately.
To get an idea of how the eigenfunctions change due to the presence of the two extra terms, we will solve the eigenvalue equation in coordinate space. The Hamiltonian in coordinate space is given by

$$\hat{H} = -\frac{\hbar^2}{2m}\frac{\partial^2}{\partial x^2} + \frac{m\omega^2 x^2}{2} + (\gamma+\beta)\sqrt{\frac{m\omega}{2\hbar}}x + (\gamma-\beta)\sqrt{\frac{\hbar}{2m\omega}}\frac{\partial}{\partial x}. \tag{2.55}$$

We now consider the eigenvalue equation

$$\hat{H}\phi = -\frac{\hbar^2}{2m}\frac{\partial^2}{\partial x^2}\phi + \frac{m\omega^2 x^2}{2}\phi + (\gamma+\beta)\sqrt{\frac{m\omega}{2\hbar}}x\phi + (\gamma-\beta)\sqrt{\frac{\hbar}{2m\omega}}\frac{\partial}{\partial x}\phi = E\phi. \tag{2.56}$$

We define $A = \frac{(\gamma+\beta)}{\omega}\sqrt{\frac{1}{2\hbar m\omega}}$ and write

$$\frac{\hbar^2}{2m}(-\frac{\partial^2}{\partial x^2}\phi + 2(\frac{\gamma-\beta}{\hbar})\sqrt{\frac{m}{2\omega\hbar}}\frac{\partial}{\partial x}\phi) + \frac{m\omega^2(x+A)^2}{2}\phi = (E + \frac{m\omega^2A^2}{2})\phi. \tag{2.57}$$

We define $B = \frac{(\gamma-\beta)}{\hbar}\sqrt{\frac{m}{2\omega\hbar}}$ and write

$$-\frac{\hbar^2}{2m}(\frac{\partial^2}{\partial x^2}\phi - 2B\frac{\partial}{\partial x}\phi + B^2\phi) + \frac{m\omega^2(x+A)^2}{2}\phi = (E + \frac{m\omega^2A^2}{2} - \frac{\hbar^2B^2}{2m})\phi. \tag{2.58}$$

Defining $\psi = \phi e^{-Bx}$, we obtain, after multiplying each side with e^{-Bx}, the eigenvalue equation

$$-\frac{\hbar^2}{2m}\frac{\partial^2}{\partial x'^2}\psi + \frac{m\omega^2(x')^2}{2}\psi = (E + \frac{m\omega^2A^2}{2} - \frac{\hbar^2B^2}{2m})\psi. \tag{2.59}$$

We have put $x' = x + A$. Formally we have again obtained the single harmonic oscillator equation, of which the solution was thoroughly discussed before. A few changes have taken place:
1. The coordinate is shifted by A to the left.
2. The wave function is changed by a factor e^{-Bx}.
3. The energy is changed by $\frac{m\omega^2A^2}{2} - \frac{B^2}{2m} = \frac{\gamma\beta}{\hbar\omega}$.

This change can be interpreted as a shift in vacuum energy. To find the expression for the

new creation and annihilation operators it suffices to note that the new coordinates were obtained by making the following substitutions

$$x \to x + A, p \to p + i\hbar B, \tag{2.60}$$

so that we can write

$$\begin{aligned}\hat{a}' = \sqrt{\frac{m\omega}{2\hbar}}(\hat{X}' + \frac{i}{m\omega}\hat{P}') &= \sqrt{\frac{m\omega}{2\hbar}}(\hat{X}' + \frac{i}{m\omega}\hat{P} + A - \frac{\hbar}{m\omega}B) \\ &= \sqrt{\frac{m\omega}{2\hbar}}(\hat{X}' + \frac{i}{m\omega}\hat{P} + \frac{\beta}{\omega}\sqrt{\frac{2}{\hbar m\omega}}) = a + \frac{\beta}{\hbar\omega} \qquad (2.61)\\ \hat{a}^{\dagger'} = \sqrt{\frac{m\omega}{2\hbar}}(\hat{X}' - \frac{i}{m\omega}\hat{P}') &= \sqrt{\frac{m\omega}{2\hbar}}(\hat{X}' - \frac{i}{m\omega}\hat{P} + A + \frac{\hbar}{m\omega}B) \\ &= \sqrt{\frac{m\omega}{2\hbar}}(\hat{X}' + \frac{i}{m\omega}\hat{P} + \frac{\gamma}{\omega}\sqrt{\frac{2}{\hbar m\omega}}) = a^\dagger + \frac{\gamma}{\hbar\omega}. \qquad (2.62)\end{aligned}$$

In order to keep the notation as simple as possible we introduce the following definition

$$\hat{a}^{\dagger'} = \hat{a}^\dagger + \frac{\gamma}{\hbar\omega} = \hat{a}^\dagger_\gamma \tag{2.63}$$

$$\hat{a}' = \hat{a} + \frac{\beta}{\hbar\omega} = \hat{a}^\dagger_\beta. \tag{2.64}$$

We note that the commutation relations are preserved

$$[\hat{a}_\beta, \hat{a}^\dagger_\gamma] = 1 \tag{2.65}$$

$$[\hat{a}_\beta, \hat{a}_\gamma] = [\hat{a}^\dagger_\beta, \hat{a}^\dagger_\gamma] = 0 \tag{2.66}$$

We also have that

$$(\hat{a}_\beta)^\dagger = \hat{a}^\dagger_{\beta^*} \tag{2.67}$$

$$(\hat{a}^\dagger_\gamma)^\dagger = \hat{a}_{\gamma^*} \tag{2.68}$$

$$\hat{a}^\dagger_\beta = \hat{a}^\dagger_\gamma + \frac{\beta - \gamma}{\hbar\omega} \tag{2.69}$$

The Hamiltonian can thus be written as

$$\hat{H} = \hbar\omega(\hat{a}^\dagger_\gamma\hat{a}_\beta + \frac{1}{2} - \frac{\gamma\beta}{\hbar^2\omega^2}) \triangleq \hbar\omega\hat{a}^\dagger_\gamma\hat{a}_\beta + E_{vac}, \tag{2.70}$$

where we have defined $E_{vac} \triangleq \frac{\hbar\omega}{2} - \frac{\gamma\beta}{\hbar\omega}$ as the new vacuum energy. We will consider the most general case with $\beta \neq \gamma^*$ and $\hat{H}$ is not hermitian. As pointed out before, we are then no longer sure that the eigenstates will be orthogonal, nor that the right and left eigenfunction

will be the same. We will therefore calculate the overlap matrix of the eigenfunctions. A right eigenstate can be written as

$$|R_n\rangle = \frac{(\hat{a}_\gamma^\dagger)^n}{\sqrt{n!}} |0_\beta^r\rangle \,, \tag{2.71}$$

where $|0_\beta^r\rangle$ is the right vacuum that is annihilated by a_β

$$\hat{a}_\beta |0_\beta^r\rangle = 0. \tag{2.72}$$

From this it is immediately clear that the new right vacuum is a Glauber state with eigenvalue $-\frac{\beta}{\hbar\omega}$ of the system discussed in previous section

$$\hat{a} |0_\beta^r\rangle = -\frac{\beta}{\hbar\omega} |0_\beta^r\rangle \,. \tag{2.73}$$

Similarly, we find that a left eigenstate is given by

$$\langle L_n| = \langle 0_\gamma^l| \frac{(\hat{a}_\beta)^n}{\sqrt{n!}}, \tag{2.74}$$

where $\langle 0_\gamma^l|$ is the vacuum that is annihilated by a_γ

$$\langle 0_\gamma^l| \hat{a}_\gamma^\dagger = 0. \tag{2.75}$$

We now proceed to compute $\langle R_m|R_n\rangle$. We first consider the case where $m \leq n$

$$\begin{aligned}
\langle R_m|R_n\rangle =& \frac{1}{\sqrt{m!n!}} \langle 0_\beta^r| a_{\gamma^*}^m (a_\gamma^\dagger)^n |0_\beta^r\rangle \\
=& \frac{1}{\sqrt{m!n!}} \langle 0_\beta^r| (a_\beta + \frac{\gamma^* - \beta}{\hbar\omega})^m (a_\gamma^\dagger)^n |0_\beta^r\rangle \\
=& \frac{1}{\sqrt{m!n!}} \sum_{k=0}^{m} \binom{m}{k} (\frac{\gamma^* - \beta}{\hbar\omega})^{m-k} \langle 0_\beta^r| (a_\beta)^k (a_\gamma^\dagger)^n |0_\beta^r\rangle \\
=& \frac{1}{\sqrt{m!n!}} \sum_{k=0}^{m} \binom{m}{k} (\frac{\gamma^* - \beta}{\hbar\omega})^{m-k} \frac{n!}{(n-k)!} \langle 0_\beta^r| (a_\gamma^\dagger)^{n-k} |0_\beta^r\rangle \\
=& \frac{1}{\sqrt{m!n!}} \sum_{k=0}^{m} \binom{m}{k} (\frac{\gamma^* - \beta}{\hbar\omega})^{m-k} \frac{n!}{(n-k)!} \langle 0_\beta^r| (a_{\beta^*}^\dagger - \frac{\beta^* - \gamma}{\hbar\omega})^{n-k} |0_\beta^r\rangle \\
=& \frac{1}{\sqrt{m!n!}} \sum_{k=0}^{m} \binom{m}{k} (\frac{\gamma^* - \beta}{\hbar\omega})^{m-k} \frac{n!}{(n-k)!} (\frac{\gamma - \beta^*}{\hbar\omega})^{n-k} \\
=& \sqrt{m!n!} \sum_{k=0}^{m} \frac{1}{k!(m-k)!(n-k)!} (\frac{\gamma^* - \beta}{\hbar\omega})^{m-k} (\frac{\gamma - \beta^*}{\hbar\omega})^{n-k}
\end{aligned} \tag{2.76}$$

If $n \leq m$, we find analogously

$$\langle R_m|R_n\rangle = \sqrt{m!n!}\sum_{k=0}^{n}\frac{1}{k!(m-k)!(n-k)!}(\frac{\gamma^*-\beta}{\hbar\omega})^{m-k}(\frac{\gamma-\beta^*}{\hbar\omega})^{n-k}, \tag{2.77}$$

so that we can summarize the results as

$$\langle R_m|R_n\rangle = \sqrt{m!n!}\sum_{k=0}^{\min(m,n)}\frac{1}{k!(m-k)!(n-k)!}(\frac{\gamma^*-\beta}{\hbar\omega})^{m-k}(\frac{\gamma-\beta^*}{\hbar\omega})^{n-k} = \langle R_n|R_m\rangle^* . \tag{2.78}$$

We see that for $\gamma \neq \beta^*$, the eigenstates indeed aren't orthogonal.
We again define the Glauber state as

$$\hat{a}_\beta\,|\alpha'\rangle = \alpha'\,|\alpha'\rangle\,. \tag{2.79}$$

For the old annihilation operator we find

$$\hat{a}\,|\alpha'\rangle = (\alpha' - \frac{\beta}{\hbar\omega})\,|\alpha'\rangle\,, \tag{2.80}$$

so that the index represents the value over which the eigenvalue of the Glauber state is translated. For the creation operator, we find analogously

$$\langle\alpha'|\,\hat{a}^\dagger_\gamma = \langle\alpha|\,(\alpha^* + \frac{\gamma-\beta^*}{\hbar\omega}). \tag{2.81}$$

It is interesting to wonder whether the new eigenstates still form a complete set. By construction, we still have that

$$|\alpha'\rangle = N_{\alpha'}\sum_{n=0}^{\infty}(\alpha'\hat{a}^\dagger_\gamma)^n\,|0^r_\beta\rangle\,, \tag{2.82}$$

with $N_{\alpha'}$ a normalization constant that will be determined in the next subsection, satisfies the definition of a Glauber state, see equation (2.79). As the Glauber states with respect to the new annihilation operator are just translated versions of the original Glauber states, we find that the set of new Glauber states is still complete. Since we can construct a set of complete eigenstates with the new eigenstates, they form a complete set.

2.1.4 Time evolution in the damped single harmonic oscillator

We proceed to check the time dependency

$$\begin{aligned}\langle\alpha^{'}(t)|\hat{X}|\alpha^{'}(t)\rangle &= \langle\alpha^{'}|e^{\frac{iH^{\dagger}t}{\hbar}}\hat{X}e^{-\frac{iHt}{\hbar}}|\alpha^{'}\rangle \\ &= \sqrt{\frac{\hbar}{2m\omega}}\,\langle\alpha^{'}|e^{i\omega(\hat{a}^{\dagger}_{\beta^*}\hat{a}_{\gamma^*}+\frac{1}{2}-\frac{\gamma^*\beta^*}{\hbar^2\omega^2})t}(\hat{a}+\hat{a}^{\dagger})e^{-i\omega(\hat{a}^{\dagger}_{\gamma}\hat{a}_{\beta}+\frac{1}{2}-\frac{\gamma\beta}{\hbar^2\omega^2})t}|\alpha^{'}\rangle \\ &= \sqrt{\frac{\hbar}{2m\omega}}\,\langle\alpha^{'}|e^{i\omega(\hat{a}^{\dagger}_{\beta^*}\hat{a}_{\gamma^*}+\frac{1}{2}-\frac{\gamma^*\beta^*}{\hbar^2\omega^2})t}(\hat{a}_{\beta}+\hat{a}^{\dagger}_{\beta^*}-\frac{\beta+\beta^*}{\hbar\omega})e^{-i\omega(\hat{a}^{\dagger}_{\gamma}\hat{a}_{\beta}+\frac{1}{2}-\frac{\gamma\beta}{\hbar^2\omega^2})t}|\alpha^{'}\rangle\end{aligned} \tag{2.83}$$

For the first term, we can use the formula $Ae^{BA} = e^{AB}A$, with here $A = \hat{a}_{\beta}$ and $B = \hat{a}^{\dagger}_{\gamma}$ to pull the annihilation operator through the time evolution operator. For the second term we can proceed similarly, resulting in

$$\begin{aligned}= \sqrt{\frac{\hbar}{2m\omega}}\Big[&\langle\alpha^{'}|e^{i\omega(\hat{a}^{\dagger}_{\beta^*}\hat{a}_{\gamma^*}+\frac{1}{2}-\frac{\gamma^*\beta^*}{\hbar^2\omega^2})t}e^{-i\omega(\hat{a}_{\beta}\hat{a}^{\dagger}_{\gamma}+\frac{1}{2}-\frac{\gamma\beta}{\hbar^2\omega^2})t}\hat{a}_{\beta} \\ &+\hat{a}^{\dagger}_{\beta^*}e^{i\omega(\hat{a}^{\dagger}_{\beta^*}\hat{a}_{\gamma^*}+\frac{1}{2}-\frac{\gamma^*\beta^*}{\hbar^2\omega^2})t}e^{-i\omega(\hat{a}_{\beta}\hat{a}^{\dagger}_{\gamma}+\frac{1}{2}-\frac{\gamma\beta}{\hbar^2\omega^2})t}|\alpha^{'}\rangle - \frac{\beta+\beta^*}{\hbar\omega}\,\langle\alpha^{'}(t)|\alpha^{'}(t)\rangle\Big].\end{aligned} \tag{2.84}$$

We now use the fact that $[\hat{a}_{\beta}, \hat{a}^{\dagger}_{\gamma}] = 1$ to rewrite the exponentials and obtain

$$= \sqrt{\frac{\hbar}{2m\omega}}(\alpha^{'*}e^{i\omega t} + \alpha^{'}e^{-i\omega t} - \frac{\beta+\beta^*}{\hbar\omega})\,\langle\alpha^{'}(t)|\alpha^{'}(t)\rangle \tag{2.85}$$

To further simplify this expression, we need to know how the Glauber state propagates through time. To do this, we expand the Glauber states in terms of the new eigenfunctions

$$|\alpha^{'}\rangle = N_{\alpha^{'}}\sum_{n=0}^{\infty}(\alpha^{'}\hat{a}^{\dagger}_{\gamma})^n\,|0^r_{\beta}\rangle\,, \tag{2.86}$$

with $N_{\alpha'}$ a normalization constant, since this satisfies the definition of the Glauber state (2.79). We first determine $N_{\alpha'}$:

$$\begin{aligned}
&\langle\alpha'|\alpha'\rangle \\
&= |N_{\alpha'}|^2 \sum_{m=0}^{\infty}\sum_{n=0}^{\infty}(\frac{\alpha'^{*})^m(\alpha')^n}{\sqrt{m!n!}}\langle R_m|R_n\rangle \\
&= |N_{\alpha'}|^2 \sum_{m=0}^{\infty}\sum_{n=0}^{\infty}(\alpha'^{*})^m(\alpha')^n \sum_{k=0}^{min(m,n)}\frac{1}{k!(m-k)!(n-k)!}(\frac{\gamma^*-\beta}{\hbar\omega})^{m-k}(\frac{\gamma-\beta^*}{\hbar\omega})^{n-k} \\
&= |N_{\alpha'}|^2 \sum_{m=0}^{\infty}\sum_{n=0}^{\infty}(\frac{\alpha'^{*}\gamma^*-\alpha'^{*}\beta}{\hbar\omega})^m(\frac{\alpha'\gamma-\alpha'\beta^*}{\hbar\omega})^n \sum_{k=0}^{min(m,n)}\frac{1}{k!(m-k)!(n-k)!}|\frac{\gamma^*-\beta}{\hbar\omega}|^{-2k} \\
&= |N_{\alpha'}|^2 \sum_{k=0}^{\infty}\frac{1}{k!}|\frac{\gamma^*-\beta}{\hbar\omega}|^{-2k}(\sum_{m=k}^{\infty}\frac{1}{(m-k)!}(\frac{\alpha'^{*}\gamma^*-\alpha'^{*}\beta}{\hbar\omega})^m)(\sum_{m=k}^{\infty}(\frac{1}{(n-k)!}\frac{\alpha'\gamma-\alpha'\beta^*}{\hbar\omega})^n) \\
&= |N_{\alpha'}|^2 \sum_{k=0}^{\infty}\frac{1}{k!}|\frac{\gamma^*-\beta}{\hbar\omega}|^{-2k}(\frac{\alpha'^{*}\gamma^*-\alpha'^{*}\beta}{\hbar\omega})^k e^{\frac{\alpha'^{*}\gamma^*-\alpha'^{*}\beta}{\hbar\omega}}(\frac{\alpha'\gamma-\alpha'\beta^*}{\hbar\omega})^k e^{\frac{\alpha'\gamma-\alpha'\beta^*}{\hbar\omega}} \\
&= |N_{\alpha'}|^2 e^{\frac{\alpha'^{*}\gamma^*-\alpha'^{*}\beta}{\hbar\omega}} e^{\frac{\alpha'\gamma-\alpha'\beta^*}{\hbar\omega}} e^{|\alpha'|^2}.
\end{aligned} \tag{2.87}$$

Demanding that the norm be one, we thus find for $|N_\alpha|^2$:

$$|N_\alpha|^2 = e^{-\frac{\alpha'^{*}\gamma^*-\alpha'^{*}\beta}{\hbar\omega}} e^{-\frac{\alpha'\gamma-\alpha'\beta^*}{\hbar\omega}} e^{-|\alpha'|^2}. \tag{2.88}$$

The time evolution of the state is given by

$$\begin{aligned}
|\alpha(t)\rangle &= N_{\alpha'} e^{-\frac{i\hat{H}t}{\hbar}} \sum_{n=0}^{\infty}(\alpha'\hat{a}_\gamma^\dagger)^n |0'\rangle \\
&= N_{\alpha'} e^{-\frac{iE_{vac}t}{\hbar}} \sum_{n=0}^{\infty}(\alpha'\hat{a}_\gamma^\dagger e^{-i\omega t})^n |0'\rangle .
\end{aligned} \tag{2.89}$$

Using this and equation (2.88), we immediately find for the norm

$$\langle\alpha'(t)|\alpha'(t)\rangle = e^{4|\alpha'||\frac{\gamma-\beta^*}{\hbar\omega}|\sin(\frac{\omega t}{2}-\phi)\sin\frac{\omega t}{2}} e^{i\frac{\gamma\beta-\gamma^*\beta^*}{\hbar^2\omega^2}\omega t}. \tag{2.90}$$

The two exponentials have a very different behavior. The first one is causing the norm to oscillate, but doesn't contribute to damping or oscillating on the long term. This is the case for the latter factor, which clearly causes an exponential damping as $\frac{\gamma\beta-\gamma^*\beta^*}{\hbar^2\omega^2}$ is imaginary. When we want to mimic the classical damping, only the second factor is desirable.
The expectation value of $\hat{X}$ now becomes

$$\langle\alpha'(t)|\hat{X}|\alpha'(t)\rangle = \sqrt{\frac{\hbar}{2m\omega}}(\alpha'^{*}e^{i\omega t} + \alpha' e^{-i\omega t} - \frac{\beta+\beta^*}{\hbar\omega}) e^{4|\alpha'||\frac{\gamma-\beta^*}{\hbar\omega}|\sin(\frac{\omega t}{2}-\phi)\sin\frac{\omega t}{2}} e^{i\frac{\gamma\beta-\gamma^*\beta^*}{\hbar^2\omega^2}\omega t}. \tag{2.91}$$

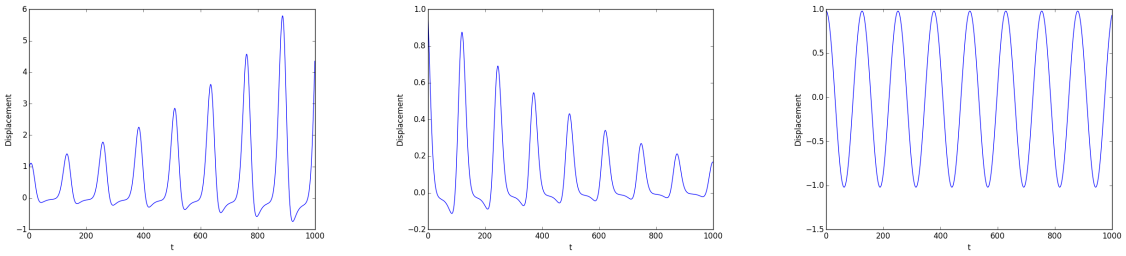

(a) $\beta = 9 - 4i, \quad \gamma = 5 - 3i$ (b) $\beta = 9 + 4i, \quad \gamma = 5 + 3i$ (c) $\beta = 5 + 3i, \quad \gamma = 5 - 3i$

Figure 2.4: The three different types of time evolution of the displacement: amplification, damping and oscillation. For all figures the following values were chosen $\omega = 50$, $\alpha = 5$ and $m = 1$.

The evolution of the expectation value of the displacement in time is shown in Figure 2.4 for a few well chosen values of γ and β. We see that the displacement will either be damped, amplified or oscillating. The latter is the case when $\hat{H}$ is hermitian. Note that the function is slightly shifted to below due to the presence of the linear terms in $\hat{a}$ and $\hat{a}^\dagger$, which can also be see by the extra term $-\frac{\beta+\beta^*}{\hbar\omega}$ in equation (2.91). For the other two regimes, we note that we indeed managed to introduce both damping and amplification. However, due to the extra oscillating behavior of the norm, the evolution of the displacement is different from the classical case.
For the expectation value of $\hat{X}^2$ we find

$$\begin{aligned}
\langle\alpha'(t)|\hat{X}^2|\alpha'(t)\rangle &= \frac{\hbar}{2m\omega}\langle\alpha'(t)|(\hat{a}_\beta + \hat{a}_\beta^\dagger - \frac{\beta+\beta^*}{\hbar\omega})^2|\alpha'(t)\rangle \\
&= \frac{\hbar}{2m\omega}\langle\alpha'(t)|(\hat{a}_\beta + \hat{a}_\beta^\dagger)^2 - 2\frac{\beta+\beta^*}{\hbar\omega}(\hat{a}_\beta + \hat{a}_\beta^\dagger) + (\frac{\beta+\beta^*}{\hbar\omega})^2|\alpha'(t)\rangle \\
&= \frac{\hbar}{2m\omega}\langle\alpha'(t)|\hat{a}_\beta^2 + 1 + 2\hat{a}_\beta^\dagger\hat{a}_\beta + \hat{a}_\beta^{\dagger 2} - 2\frac{\beta+\beta*}{\hbar\omega}(\hat{a}_\beta + \hat{a}_\beta^\dagger) + (\frac{\beta+\beta^*}{\hbar\omega})^2|\alpha'(t)\rangle \\
&= \frac{\hbar}{2m\omega}((\alpha')^2 e^{2i\omega t} + 1 + 2(\alpha')(\alpha'^*) \\
&\quad + (\alpha'^*)^2 e^{-2i\omega t} - 2\frac{\beta+\beta*}{\hbar\omega}((\alpha')e^{-i\omega t} + (\alpha'^*)e^{i\omega t}) + (\frac{\beta+\beta^*}{\hbar\omega})^2)\langle\alpha'(t)|\alpha'(t)\rangle \\
&= \frac{\hbar}{2m\omega}(1 + ((\alpha')e^{-i\omega t} + (\alpha'^*)e^{i\omega t})^2 + (\frac{\beta+\beta^*}{\hbar\omega})^2 \\
&\quad - 2\frac{\beta+\beta*}{\hbar\omega}((\alpha')e^{-i\omega t} + (\alpha'^*)e^{i\omega t}))\langle\alpha'(t)|\alpha'(t)\rangle \\
&= \langle\alpha'(t)|\hat{X}|\alpha'(t)\rangle^2 + \frac{\hbar}{2m\omega}\langle\alpha'(t)|\alpha'(t)\rangle \qquad (2.92)
\end{aligned}$$

We see that the variance in the displacement is a constant. A similar calculation for the momentum gives

$$\langle\alpha'(t)|\hat{P}^2|\alpha'(t)\rangle = \langle\alpha'(t)|\hat{P}|\alpha'(t)\rangle^2 + \frac{\hbar m\omega}{2}\langle\alpha'(t)|\alpha'(t)\rangle\,, \tag{2.93}$$

so that we still have that the equality in the uncertainty principle is respected[1]: $\sigma_p\sigma_x = \frac{\hbar}{2}$. We can also compute the expectation value of the number of quanta in the original HO system

$$\begin{aligned}
\langle\alpha'(t)|\hat{a}^\dagger\hat{a}|\alpha'(t)\rangle &= \langle\alpha'(t)|(\hat{a}^\dagger_{\beta^*} - \frac{\beta^*}{\hbar\omega})(\hat{a}_\beta - \frac{\beta}{\hbar\omega})|\alpha'(t)\rangle \\
&= \langle\alpha'(t)|\hat{a}^\dagger_{\beta^*}\hat{a}_\beta - \frac{\beta^*}{\hbar\omega}\hat{a}_\beta - \frac{\beta}{\hbar\omega}\hat{a}^\dagger_{\beta^*} + \frac{|\beta|^2}{\hbar^2\omega^2}|\alpha'(t)\rangle \\
&= (|\alpha'|^2 - \frac{\beta^*\alpha}{\hbar\omega}e^{-i\omega t} - \frac{\beta\alpha^*}{\hbar\omega}e^{i\omega t} + \frac{|\beta|^2}{\hbar^2\omega^2})\langle\alpha'(t)|\alpha'(t)\rangle \\
&= (|\alpha'|^2 - \frac{2|\alpha'\beta|}{\hbar\omega}\cos(\omega t - \phi_{\alpha'\beta^*}) + \frac{|\beta|^2}{\hbar^2\omega^2})\langle\alpha'(t)|\alpha'(t)\rangle \\
&= (|\alpha'|^2 - \frac{2|\alpha'\beta|}{\hbar\omega}\cos(\omega t - \phi_{\alpha'\beta^*}) + \frac{|\beta|^2}{\hbar^2\omega^2})e^{4|\alpha'||\frac{\gamma-\beta^*}{\hbar\omega}|\sin(\frac{\omega t}{2}-\phi)\sin\frac{\omega t}{2}}e^{i\frac{\gamma\beta-\gamma^*\beta^*}{\hbar^2\omega^2}\omega t},
\end{aligned} \tag{2.94}$$

with $\phi_{\alpha^*\beta}$ the phase of $\alpha^*\beta$. This expectation value is formally identical to the expectation value of the displacement: a cosine that is shifted upwards and damped due to the change in norm of the Glauber state. Therefore, the discussion is completely analogous to that of the displacement. We can also look at the time evolution of the original HO-orbitals:

$$\begin{aligned}
\langle n(t)|m(t)\rangle =& \frac{1}{\sqrt{n!m!}}\langle 0|\hat{a}^n e^{\frac{i\hat{H}^\dagger t}{\hbar}}e^{\frac{-i\hat{H}t}{\hbar}}(\hat{a}^\dagger)^m|0\rangle \\
=& \frac{1}{\sqrt{n!m!}}\langle 0|(\hat{a}^*_\gamma - \frac{\gamma^*}{\hbar\omega})^n e^{\frac{i\hat{H}^\dagger t}{\hbar}}e^{\frac{-i\hat{H}t}{\hbar}}(\hat{a}^\dagger_\gamma - \frac{\gamma}{\hbar\omega})^m|0\rangle \\
=& \frac{1}{\sqrt{n!m!}}\langle 0|e^{\frac{i\hat{H}^\dagger t}{\hbar}}(\hat{a}_{\gamma^*}e^{i\omega t} - \frac{\gamma^*}{\hbar\omega})^n(\hat{a}^\dagger_\gamma e^{-i\omega t} - \frac{\gamma}{\hbar\omega})^m e^{\frac{-i\hat{H}t}{\hbar}}|0\rangle\,.
\end{aligned} \tag{2.95}$$

Consider the case where $n \leq m$. We use the following formula

$$\hat{A}^n(\hat{B})^m = \sum_{l=0}^{n}\frac{n!m!}{(n-l)!(m-l)!l!}\hat{B}^{m-l}\hat{A}^{n-l}, \tag{2.96}$$

[1]Because the Heisenberg uncertainty relation is only valid for wavefunctions normalized to one, the factor $\langle\alpha'(t)|\alpha'(t)\rangle$ drops out.

with $[\hat{A}, \hat{B}] = 1$. This formula can easily be proven by induction. The overlap of the eigenstates of the undamped oscillator then becomes

$$\begin{aligned}
&\langle n(t)|m(t)\rangle \\
&= \sqrt{n!m!}\sum_{l=0}^{n}\frac{1}{(n-l)!(m-l)!l!}\,\langle 0|e^{\frac{i\hat{H}^\dagger t}{\hbar}}(\hat{a}^\dagger_\gamma e^{-i\omega t}-\frac{\gamma}{\hbar\omega})^{m-l}(\hat{a}_{\gamma^*}e^{i\omega t}-\frac{\gamma^*}{\hbar\omega})^{n-l}e^{\frac{-i\hat{H}t}{\hbar}}|0\rangle \\
&= \sqrt{n!m!}\sum_{l=0}^{n}\frac{1}{(n-l)!(m-l)!l!} \\
&\qquad\qquad \langle 0|e^{\frac{i\hat{H}^\dagger t}{\hbar}}((\hat{a}^\dagger_{\gamma^*}+\frac{\gamma-\beta^*}{\hbar\omega})e^{-i\omega t}-\frac{\gamma}{\hbar\omega})^{m-l}((\hat{a}_\beta+\frac{\gamma^*-\beta}{\hbar\omega})e^{i\omega t}-\frac{\gamma^*}{\hbar\omega})^{n-l}e^{\frac{-i\hat{H}t}{\hbar}}|0\rangle \\
&= \sqrt{n!m!}\sum_{l=0}^{n}\frac{1}{(n-l)!(m-l)!l!} \qquad (2.97)\\
&\qquad \langle 0|((\hat{a}^\dagger_{\beta^*}e^{i\omega t}+\frac{\gamma-\beta^*}{\hbar\omega})e^{-i\omega t}-\frac{\gamma}{\hbar\omega})^{m-l}e^{\frac{i\hat{H}^\dagger t}{\hbar}}e^{\frac{-i\hat{H}t}{\hbar}}((\hat{a}_\beta e^{-i\omega t}+\frac{\gamma^*-\beta}{\hbar\omega})e^{i\omega t}-\frac{\gamma^*}{\hbar\omega})^{n-l}|0\rangle\,.
\end{aligned}$$

In the last line we used the same trick as before to pull the creation and annihilation operators through the time evolution operator. We now write the new creation and annihilation operators in terms of the old ones and apply them to their vacuum state $|0\rangle$

$$\begin{aligned}
&\langle n(t)|m(t)\rangle \\
&= \sqrt{n!m!}\sum_{l=0}^{n}\frac{1}{(n-l)!(m-l)!l!}((\frac{\gamma-\beta^*}{\hbar\omega})e^{-i\omega t}+\frac{\beta^*-\gamma}{\hbar\omega})^{m-l}((\frac{\gamma^*-\beta}{\hbar\omega})e^{i\omega t}+\frac{\beta-\gamma^*}{\hbar\omega})^{n-l} \\
&\qquad\qquad \langle 0|e^{\frac{i\hat{H}^\dagger t}{\hbar}}e^{\frac{-i\hat{H}t}{\hbar}}|0\rangle \\
&= \sqrt{n!m!}\sum_{l=0}^{n}\frac{1}{(n-l)!(m-l)!l!}((\frac{\gamma-\beta^*}{\hbar\omega})e^{-i\omega t}+\frac{\beta^*-\gamma}{\hbar\omega})^{m-l}((\frac{\gamma^*-\beta}{\hbar\omega})e^{i\omega t}+\frac{\beta-\gamma^*}{\hbar\omega})^{n-l} \\
&\qquad\qquad \langle\frac{\beta}{\hbar\omega}(t)|\frac{\beta}{\hbar\omega}(t)\rangle\,. \qquad (2.98)
\end{aligned}$$

In the last line we used that $|0\rangle$ is a Glauber state with eigenvalue $\frac{\beta}{\hbar\omega}$. This is a useful observation, because we already know how the norm of such a state changes through time, see equation (2.90). As the expression is again proportional to the norm of a Glauber state, the same conclusions with regard to damping and amplification apply. The case $n > m$ can be treated analogously. The time dependency in the overlap of the undamped harmonic oscillator eigenstates is thus completely determined by the shift of the vacuum state, $\frac{\beta}{\hbar\omega}$. The overlap $|\,\langle n = 3(t)|n = 4(t)\rangle\,|$ is shown in Figure 2.5.

2.1.5 A set of coupled harmonic oscillators

Coupled oscillators play an important role in many physical models. An example is spectroscopy, where the molecular Hamiltonian can usually be well approximated by a set of

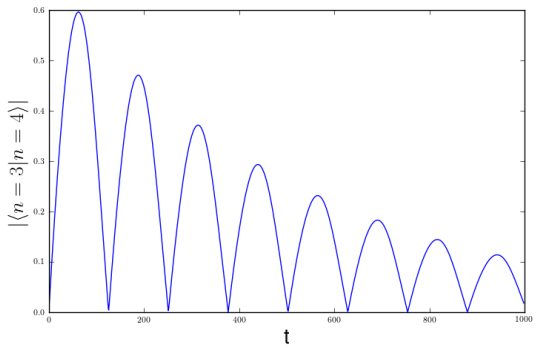

Figure 2.5: The overlap $|\langle n=3|n=4\rangle|$ as a function of time. The used values are $\beta = 9+4i$, $\gamma = 5+3i$ and $\omega = 50$.

coupled oscillators. The vibrational motion of the atoms can be decomposed into a set of normal modes, which are harmonic oscillations at a fixed frequency. It is the symmetry of these modes that will determine the infrared spectrum of the molecules. The normal modes of CO_2 are shown in Figure 2.6. The Hamiltonian of N coupled harmonic oscillators in coordinate space is given by

$$\hat{H} = \sum_i^N \frac{\hat{P}_i^2}{2m_i} + \frac{1}{2}\sum_{i,j}^N K_{ij}\hat{X}_i\hat{X}_j = -\sum_i^N \frac{\hbar^2}{2m_i}\frac{\partial^2}{\partial x_i^2} + \frac{1}{2}\sum_{i,j}^N K_{ij}x_i x_j. \tag{2.99}$$

To find the eigenstates of the Hamiltonian, we introduce new coordinates

$$q_i = \sqrt{m_i}x_i \tag{2.100}$$

and define the new K-matrix

$$K_{ij}^{'} = \frac{1}{\sqrt{m_i}}K_{ij}\frac{1}{\sqrt{m_j}}. \tag{2.101}$$

Written out in these new coordinates, the Hamiltonian becomes

$$H = -\sum_i^N \frac{\hbar^2}{2}\frac{\partial^2}{\partial q_i^2} + \frac{1}{2}\sum_{i,j}^N K_{ij}^{'}q_i q_j. \tag{2.102}$$

As K_{ij} and hence $K_{ij}^{'}$ is symmetric, we can diagonalize it in order to uncouple the oscillators. We define the normal coordinates as

$$Q_i = \sum_{j=1}^N V_{ij}q_j, \tag{2.103}$$

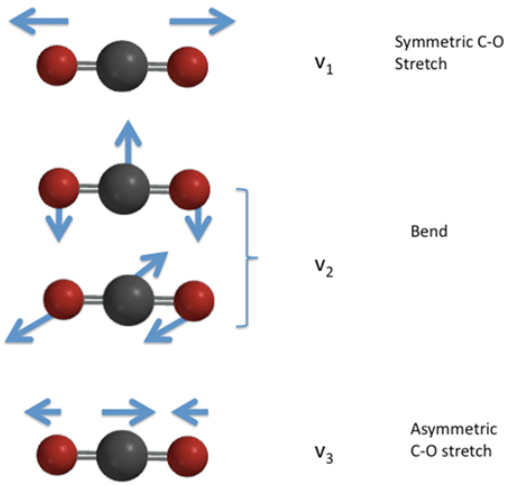

Figure 2.6: The normal modes of CO_2. [21]

with V an orthogonal matrix that diagonalizes K'_{ij}, so that

$$H = -\sum_i^N \frac{\hbar^2}{2}\frac{\partial^2}{\partial Q_i^2} + \frac{1}{2}\sum_i^N \omega_i^2 Q_i^2, \tag{2.104}$$

with ω^2 the eigenvalues of K'_{ij}. By introducing the notation ω^2, we have assumed K to be positive definite. We have obtained a sum of single harmonic oscillator Hamiltonians, which correspond to the normal modes. The total energy is simply the sum of the individual energies

$$E_{tot} = \hbar\sum_{i=1}^N \omega_i(n_i + \frac{1}{2}). \tag{2.105}$$

The total wavefunction can now be written in terms of the normal coordinates as

$$\Psi_{n_1,\ldots,n_N} = \prod_{i=1}^N \psi_{n_i} = \prod_{i=1}^N \frac{1}{\sqrt{2^{n_i} n_i!}}(\frac{\omega_i}{\pi\hbar})^{1/4} e^{-\frac{\omega_i Q_i^2}{2\hbar}} H_{n_i}(\sqrt{\frac{\omega_i}{\hbar}}Q_i) = \prod_{i=1}^N \frac{1}{\sqrt{2^{n_i} n_i!}}(\frac{1}{\pi})^{1/4} e^{-\frac{\xi_i^2}{2}} H_{n_i}(\xi_i), \tag{2.106}$$

with again $\xi_i = \sqrt{\frac{\omega_i}{\hbar}}Q_i$.

We will now try to find a state that mimics the classical case, where only one of the pendulums has an initial displacement and all pendulums have zero velocity. Writing the new, dimensionless variables in terms of the old ones, we have that

$$\xi_i = \sum_{j=1}^N V_{ij}\sqrt{\frac{\omega_i m_j}{\hbar}}x_j, \tag{2.107}$$

and by inverting this also

$$x_j = \sum_{i=1}^{N} V_{ij} \sqrt{\frac{\hbar}{\omega_i m_j}} \xi_i. \tag{2.108}$$

Based on the single oscillator case, we pick one original coordinate x_0 and shift it to the right by A: $x_0^{'} = x_0 - A$. It is easy to see that this will lead to

$$\xi_j^{'} = \xi_j - V_{j0} \sqrt{\frac{\omega_j m_0}{\hbar}} A. \tag{2.109}$$

the index 0 refers to the oscillator that gets an initial displacement. Hence, we see that each of the normal ground states becomes a Glauber state with $|\alpha_j| = V_{j0} \sqrt{\frac{\omega_j m_0}{\hbar}} \frac{A}{\sqrt{2}}$ and we write formally

$$|\Psi_{\alpha_1,\ldots,\alpha_N}\rangle = \otimes_{i=1}^{N} |\alpha_i\rangle \,. \tag{2.110}$$

We now compute the expectation value of $\hat{X}_k$

$$\begin{aligned} \langle \hat{X}_k \rangle &= \langle \Psi_{\alpha_1,\ldots,\alpha_N} | \hat{X}_k | \Psi_{\alpha_1,\ldots,\alpha_N} \rangle \\ &= \sum_{i=1}^{N} \frac{V_{ik}}{\sqrt{m_k}} \langle \alpha_i | \hat{Q}_i | \alpha_i \rangle \\ &= \sum_{i=1}^{N} V_{ik} \sqrt{\frac{2\hbar}{m_k \omega_i}} |\alpha_i| \cos(\omega_i t) \\ &= \sqrt{\frac{m_l}{m_k}} A \sum_{i=1}^{N} V_{ik} V_{i0} \cos(\omega_i t). \end{aligned} \tag{2.111}$$

The time evolution of $\langle \hat{X}_0 \rangle$ is shown in Figure 2.7. The parameters used in the plot are

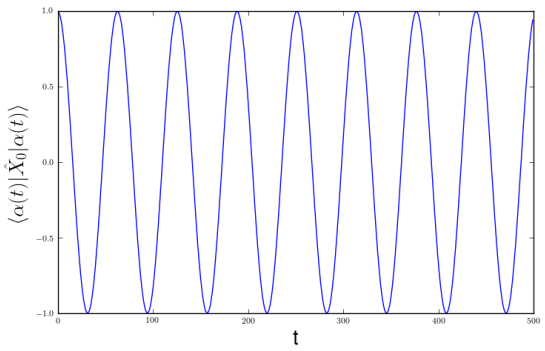

Figure 2.7: The displacement of the oscillator with index 0.

$N = 4$ and

$$K_{ij} = \begin{cases} i & \text{if } i = j \\ \sqrt{N-i} & \text{if } j = 1 \\ \sqrt{N-j} & \text{if } i = 1 \end{cases} \tag{2.112}$$

for $i, j = 1, .., N$. These parameters will be used in all plots in this section. We used the result from the single oscillator to evaluate the matrix element. At $t = 0$, we get

$$\langle \hat{X}_k \rangle = \delta_{k0} A. \tag{2.113}$$

By comparing the quantum solution to the classical one, we see that both solutions are completely the same. We have thus succeeded in finding a wavefunction that completely mimics the dynamics of the classical harmonic oscillator.

We are also interested in correlations between the expectation values of the original coordinates. We obtain

$$\begin{aligned} \langle \Psi_{\alpha_1,...,\alpha_N} | \hat{X}_k \hat{X}_p | \Psi_{\alpha_1,...,\alpha_N} \rangle &= \sum_{\substack{i,j=1 \\ i \neq j}}^{N} \frac{V_{ik}}{\sqrt{m_k}} \frac{V_{jp}}{\sqrt{m_p}} \langle \alpha_i | \hat{Q}_i | \alpha_i \rangle \langle \alpha_j | \hat{Q}_j | \alpha_j \rangle \\ &\quad + \sum_{i=1}^{N} \frac{V_{ik} V_{ip}}{\sqrt{m_k m_p}} \langle \alpha_i | \hat{Q}_i{}^2 | \alpha_i \rangle \\ &= \frac{m_l}{\sqrt{m_k m_p}} A^2 \sum_{i=1}^{N} V_{ik} V_{i0} \cos(\omega_i t) \sum_{i=1}^{N} V_{jp} V_{j0} \cos(\omega_j t) \\ &\quad + \frac{\hbar}{2\sqrt{m_k m_p}} \sum_{i=1}^{N} \frac{V_{ik} V_{ip}}{\omega_i}. \end{aligned} \tag{2.114}$$

We again obtain a result that is very close to the classical one, but there is an extra term necessary to comply with the uncertainty principle. In the limit $\hbar \to 0$ we get the exact correspondence.

2.1.6 Damped coupled oscillators

Similarly to the single damped oscillator case, we will consider a Hamiltonian of the form

$$\hat{H} = \sum_{i}^{N} \frac{\hat{P}_i^2}{2m_i} + \frac{1}{2} \sum_{i,j}^{N} K_{ij} \hat{X}_i \hat{X}_j + \sum_{l=1}^{N} \left(A_l \hat{X}_l + B_l \hat{P}_l \right). \tag{2.115}$$

Here we have added linear terms in $\hat{X}_l$ and $\hat{P}_l$, because we can only introduce creation and annihilation operators after having decomposed the system in normal modes. As $\hat{X}$ and

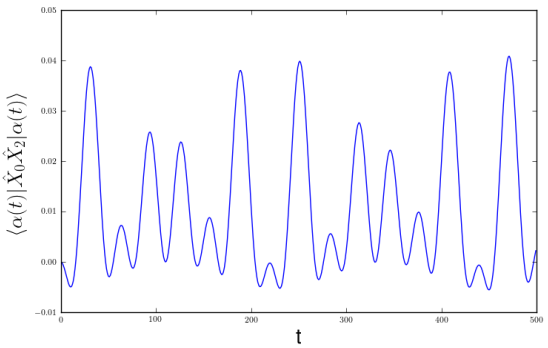

Figure 2.8: The correlation of the displacement the oscillator with index 0 and an oscillator without initial displacement as a function of time.

$\hat{P}$ are linear combinations of the creation and annihilation operator in the single oscillator case, we presume that we will eventually obtain the same kind of damping as for the single oscillator. To diagonalize the Hamiltonian, we transform to normal coordinates

$$\xi_i = \sum_{j=1}^{N} V_{ij} \sqrt{\frac{\omega_i m_j}{\hbar}} x_j, \tag{2.116}$$

where ω_i^2 is a labeled eigenvalue of K_{ij}. Inverting the above coordinate transformation, we find the original coordinates in terms of the normal ones

$$x_j = \sum_{i=1}^{N} V_{ij} \sqrt{\frac{\hbar}{\omega_i m_j}} \xi_i. \tag{2.117}$$

We can now write the Hamiltonian in normal coordinates as

$$\begin{aligned} H &= \sum_i^N \hbar\omega_i \left(\hat{a}_i^\dagger \hat{a}_i + \frac{1}{2}\right) + \sum_l^N A_l V_{il} \sqrt{\frac{\hbar}{\omega_i m_l}} \xi_i - i B_l V_{il} \sqrt{\hbar\omega_i m_l} \frac{\partial}{\partial \xi_i} \\ &= \sum_i^N \hbar\omega_i \left(\hat{a}_i^\dagger \hat{a}_i + \frac{1}{2}\right) + \sum_l^N A_l V_{il} \sqrt{\frac{\hbar}{2\omega_i m_l}} \left(a_i + a_i^\dagger\right) + B_l V_{il} \sqrt{\frac{\hbar\omega_i m_l}{2}} \left(a_i - a_i^\dagger\right) \\ &= \sum_i^N \hbar\omega_i \left(\hat{a}_i^\dagger \hat{a}_i + \frac{1}{2}\right) + \sum_l^N \left(A_l V_{il} \sqrt{\frac{\hbar}{2\omega_i m_l}} + B_l V_{il} \sqrt{\frac{\hbar\omega_i m_l}{2}}\right) a_i \\ &\qquad + \sum_l^N \left(A_l V_{il} \sqrt{\frac{\hbar}{2\omega_i m_l}} - B_l V_{il} \sqrt{\frac{\hbar\omega_i m_l}{2}}\right) a_i^\dagger. \end{aligned} \tag{2.118}$$

We formally retrieve the uncoupled equations. If we put

$$\gamma_i = \sum_l^N \left(\frac{A_l V_{il}}{\omega_i} \sqrt{\frac{1}{2\hbar\omega_i m_l}} + B_l V_{il} \sqrt{\frac{m_l}{2\hbar\omega_i}}\right) \tag{2.119}$$

$$\beta_i = \sum_l^N \left(\frac{A_l V_{il}}{\omega_i} \sqrt{\frac{1}{2\hbar\omega_i m_l}} - B_l V_{il} \sqrt{\frac{m_l}{2\hbar\omega_i}} \right), \tag{2.120}$$

we can simplify the notation to

$$\hat{H} = \sum_{i=1}^N \hbar\omega_i \left(\hat{a}_i^\dagger \hat{a}_i + \frac{1}{2} + \beta_i \hat{a}_i^\dagger + \gamma_i \hat{a}_i \right). \tag{2.121}$$

We now proceed to compute the time-dependent expectation value of the displacement using Glauber states in the normal coordinates. We impose the initial condition

$$x_j(t=0) = C\delta_{j0}, \tag{2.122}$$

so only the oscillator labeled with index 0 has an initial displacement of C. The other oscillators have zero displacement. Using the same reasoning as we did for the undamped oscillator, we find for the eigenvalue α_i of the Glauber state in the i-th normal coordinate that

$$|\alpha_i| = V_{i0} \sqrt{\frac{\omega_i m_0}{\hbar}} C. \tag{2.123}$$

Using the results from the previous section, we can obtain an expression for the expectation value of $\hat{X}$

$$\begin{aligned}
\langle \hat{X}_k \rangle &= \langle \Psi_{\alpha_1,\ldots,\alpha_N}(t) | \hat{X}_k | \Psi_{\alpha_1,\ldots,\alpha_N}(t) \rangle \\
&= \sum_{i=1}^N \frac{V_{ik}}{\sqrt{m_k}} \langle \alpha_i(t) | \hat{Q}_i | \alpha_i(t) \rangle \prod_{j \neq i} \langle \alpha_j(t) | \alpha_j(t) \rangle \\
&= \sum_{i=1}^N \frac{V_{ik}}{\sqrt{m_k}} \sqrt{\frac{\hbar}{2\omega_i}} \left[\left(\alpha_i^* + \frac{\beta_i^*}{\hbar\omega_i} \right) e^{i\omega_i t} + \left(\alpha_i + \frac{\beta_i}{\hbar\omega_i} \right) e^{-i\omega_i t} - \frac{\beta_i + \beta_i^*}{\hbar\omega_i} \right] \prod_{j=1}^N \langle \alpha_j(t) | \alpha_j(t) \rangle .
\end{aligned} \tag{2.124}$$

We see that the expectation value of the position is proportional to $\prod_{j=1}^N \langle \alpha_j(t) | \alpha_j(t) \rangle$, which will be responsible for the damping or amplification of the displacement. This factor is independent of the index k, which indicates the harmonic oscillator for which we calculate the expectation value of the displacement. Therefore, each of the oscillators will be damped in the same way. This conclusion is not restricted to the displacement, since all expectation values will be proportional to this factor. If we demand that $\hat{H}$ be hermitian, we have that $\beta_i = \gamma_i^*$. Using this and the fact that the norm of the Glauber state remains one throughout time, we can greatly simplify the formula to

$$\begin{aligned}
= \sum_{i=1}^N \frac{V_{ik}}{\sqrt{m_k}} \sqrt{\frac{\hbar}{\omega_i}} \Bigg[V_{il} \sqrt{\frac{\omega_i m_l}{\hbar}} \frac{A}{\sqrt{2}} + \sum_{l=1}^N \left(\frac{A_l V_{il}}{\omega_i} \sqrt{\frac{1}{2\hbar\omega_i m_l}} - B_o V_{il} \sqrt{\frac{m_l}{2\hbar\omega_i}} \right) \cos\omega_i t \\
- \sum_{l=1}^N \left(\frac{A_l V_{il}}{\omega_i} \sqrt{\frac{1}{2\hbar\omega_i m_l}} - B_l V_{il} \sqrt{\frac{m_l}{2\hbar\omega_i}} \right) \Bigg],
\end{aligned} \tag{2.125}$$

where $l^{'}$ is the fixed coordinate with the initial value equal to C. In Figure 2.9 we show an example. As we are interested in the correlations, we also compute

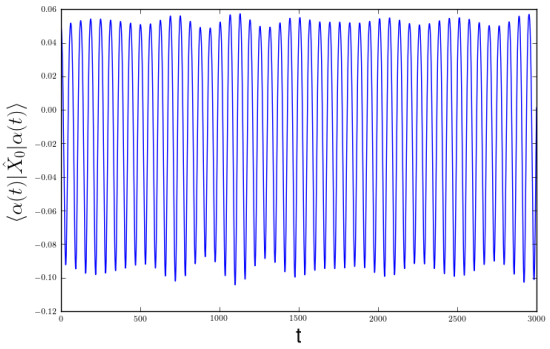

Figure 2.9: The displacement of the oscillator with index 0 as a function of time.

$$\begin{aligned}
&\langle\Psi_{\alpha_1,\ldots,\alpha_N}|\hat{X}_k\hat{X}_p|\Psi_{\alpha_1,\ldots,\alpha_N}\rangle \\
&= \sum_{\substack{i,j=1 \\ i\neq j}}^{N} \frac{V_{ik}}{\sqrt{m_k}}\frac{V_{jp}}{\sqrt{m_p}} \langle\alpha_i(t)|\hat{Q}_i|\alpha_i(t)\rangle \langle\alpha_j(t)|\hat{Q}_j|\alpha_j(t)\rangle + \sum_{i=1}^{N} \frac{V_{ik}V_{ip}}{\sqrt{m_k m_p}} \langle\alpha_i(t)|\hat{Q}_i{}^2|\alpha_i(t)\rangle \\
&= \sum_{i,j=1}^{N} \frac{V_{ik}}{\sqrt{m_k}}\frac{V_{jp}}{\sqrt{m_p}} \langle\alpha_i(t)|\hat{Q}_i|\alpha_i(t)\rangle \langle\alpha_j(t)|\hat{Q}_j|\alpha_j(t)\rangle + \sum_{i=1}^{N} \frac{V_{ik}V_{ip}}{\sqrt{m_k m_p}} \frac{\hbar}{2\omega_i}
\end{aligned} \tag{2.126}$$

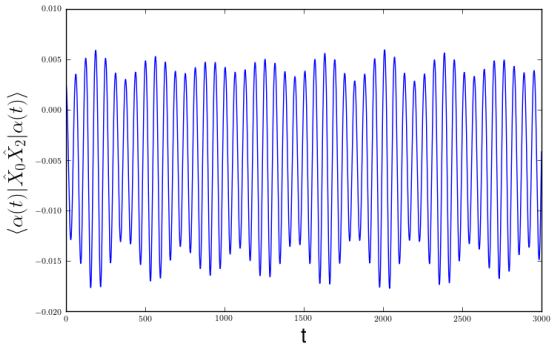

Figure 2.10: The correlation of the displacement the oscillator with index 0 and an oscillator without initial displacement as a function of time.

2.1.7 Conclusion

In the previous section we found that by breaking the hermiticity of the Hamiltonian $\hat{H}$, the norm of the states changes through time. This should not be surprising, since the time evolution operator $e^{\frac{-i\hat{H}t}{\hbar}}$ is then no longer unitary. It is, however, questionable whether we can interpret the change in norm as damping or amplification. This is because according to the Copenhagen interpretation of quantum mechanics, the norm should represent a probability and should therefore be normalized to one at all time. In the results we present above this is clearly not the case. An approach to solve this is by renormalizing each state at each time. However, is it clear that we then lose the damping and amplification effects we encountered above, since these were solely attributable to the change of the norm of the states through time.
Another interpretation is that the reduction or increase of the norm can be seen as bosonic particles respectively leaving or entering the system, thus effectively causing damping or amplification. In this case, one has to arbitrarily choose a initial moment t_0 and set the norm at that moment equal to one. The norm, and hence the number of particles, are then referred to with respect to the norm at the initial time. This interpretation implies that it is possible to describe damping of a quantum system within the Hamilton formalism.
It may be clear that the way damping was introduced in this section is straightforward, yet unconventional. In the following section we will briefly discuss some other methods to introduce damping in a harmonic oscillator.

2.2 Others methods of introducing damping

2.2.1 Quadratic terms

An obvious extension to the use of linear terms in creation and annihilation operators in order to introduce damping would be to add quadratic terms to the Hamiltonian. We will consider a Hamiltonian of the following form

$$\hat{H} = \frac{\hbar\omega}{2}(\hat{a}^\dagger\hat{a} + \hat{a}\hat{a}^\dagger) + \frac{iV\hbar}{2}(\hat{a}\hat{a} - \hat{a}^\dagger\hat{a}^\dagger), \tag{2.127}$$

with ω positive and V real. In our discussion we will make a distinction between the cases $V^2 < \omega^2$,$V^2 > \omega^2$ and $V^2 = \omega^2$. We won't aim for completeness or mathematical rigor in this subsection and refer the interested reader to [22]. We will determine the time evolution of the displacement with respect to a Glauber state. To do this, we will use a quasi-particle

transformation as put forward by Bogoliubov and Valentin in 1958 [23, 24] to simplify the Hamiltonian.

The case $V^2 < \omega^2$

Here the term $\frac{iV\hbar}{2}(\hat{a}\hat{a} - \hat{a}^\dagger\hat{a}^\dagger)$ in the Hamiltonian can be seen as a perturbation to the harmonic oscillator. We can now try to formally retrieve the original harmonic oscillator Hamiltonian by performing a linear transformation of the annihilation and creation operators. In order to preserve the commutation relations, the transformation should have a determinant of one. Therefore, we put forward following transformation

$$\hat{a} = \cosh\theta\hat{c} + i\sinh\theta\hat{c}^\dagger \tag{2.128}$$

$$\hat{a}^\dagger = -i\sinh\theta\hat{c} + \cosh\theta\hat{c}^\dagger. \tag{2.129}$$

We obtain the desired form if

$$\tanh(2\theta) = \frac{V}{\omega}. \tag{2.130}$$

The transformation will hence only yield the correct result if $V^2 < \omega^2$, because otherwise the transformations (2.131) and (2.132) will no longer be each others complex conjugate. Written in terms of the new creation and annihilation operators, the Hamiltonian becomes

$$\hat{H} = \hbar\omega^{'}(\hat{c}^\dagger\hat{c} + \frac{1}{2}) - \frac{\hbar\omega^{'}\sinh^2\theta}{2}. \tag{2.131}$$

Here $\omega^{'}$ is given by

$$\omega^{'} = \frac{\omega}{\cosh 2\theta} = \sqrt{1 - \frac{V^2}{\omega^2}}\omega. \tag{2.132}$$

We again define the Glauber state as

$$\hat{a}\left|\alpha\right\rangle = \alpha\left|\alpha\right\rangle. \tag{2.133}$$

Next, we proceed to compute the expectation value of $\hat{X}$

$$\langle\alpha(t)|\hat{X}|\alpha(t)\rangle = \langle\alpha|e^{\frac{i\hat{H}t}{\hbar}}\hat{X}e^{-\frac{i\hat{H}t}{\hbar}}|\alpha\rangle \tag{2.134}$$

$$= \sqrt{\frac{\hbar}{2m\omega}}((1 - i\sinh 2\theta)\alpha e^{-i\omega^{'}t} + (1 + i\sinh 2\theta)\alpha^* e^{i\omega^{'}t}). \tag{2.135}$$

If we now define $\alpha^{'} = (1 + i\sinh 2\theta)\alpha$, we can write this as

$$\langle\alpha(t)|\hat{X}|\alpha(t)\rangle = \sqrt{\frac{\hbar}{2m\omega}}(\alpha^{'}e^{-i\omega^{'}t} + \alpha^{'*}e^{i\omega^{'}t}), \tag{2.136}$$

so that compared to the regular harmonic oscillator, we only get a change of frequency and a change in α, which can be interpreted as the initial displacement.

The case $V^2 = \omega^2$

If we define

$$\hat{c} = \hat{a} - i\hat{a}^\dagger \tag{2.137}$$

$$\hat{c}^\dagger = i\hat{a} + \hat{a}^\dagger = i\hat{c}, \tag{2.138}$$

We formally retrieve the regular harmonic oscillator Hamiltonian

$$\hat{H} = \frac{\hbar\omega}{2}\hat{c}^\dagger\hat{c}, \tag{2.139}$$

but in this case we have that the creation operator is proportional to the annihilation operator and hence that $[\hat{c}^\dagger, \hat{c}] = 0$. We also note that the transformation (2.140) isn't invertible, so that we cannot express operators such as $\hat{X}$ in terms of the new operators. Therefore, we will need a different approach if we want to compute the time evolution of the expectation value of $\hat{X}$. We would like to use following formula, which is based on the Baker-Hausdorff-Campbell formula

$$e^{\frac{i\hat{H}t}{\hbar}}\hat{X}e^{-\frac{i\hat{H}t}{\hbar}} = \hat{X} + [\hat{H}, \hat{X}]\frac{it}{\hbar} - [\hat{H}, [\hat{H}, \hat{X}]]\frac{t^2}{2\hbar^2} + \cdots . \tag{2.140}$$

We have that

$$[\hat{H}, \hat{X}] = i\hat{c}\sqrt{\frac{2\hbar}{m\omega}}[\hat{a} - i\hat{a}^\dagger, \hat{a} + \hat{a}^\dagger] = \sqrt{\frac{2\hbar}{m\omega}}(i-1)\hat{c}. \tag{2.141}$$

From this, it is easy to see that $[\hat{H}, [\hat{H}, \hat{X}]] = 0$ and so we only retain the first two terms in the expansion. We thus find

$$e^{\frac{i\hat{H}t}{\hbar}}\hat{X}e^{-\frac{i\hat{H}t}{\hbar}} = \hat{X} - \sqrt{\frac{2}{m\hbar\omega}}(1+i)t\hat{c} \tag{2.142}$$

$$= \sqrt{\frac{\hbar}{2m\omega}}(\hat{a} + \hat{a}^\dagger) - \sqrt{\frac{2}{m\hbar\omega}}(1+i)t(\hat{a} - i\hat{a}^\dagger). \tag{2.143}$$

In the last step, we have expressed everything in terms of the original creation and annihilation operators, so that we can easily evaluate

$$\langle\alpha(t)|\hat{X}|\alpha(t)\rangle = \sqrt{\frac{2\hbar}{m\omega}}(\alpha e^{-i\omega t} + \alpha^* e^{i\omega t}) - \sqrt{\frac{2}{m\hbar\omega}}((1+i)\alpha e^{-i\omega t} + (1-i)\alpha^* e^{i\omega t})t \tag{2.144}$$

The spectrum of the Hamiltonian is the positive real axis and it is doubly degenerate. The proof of this can be found in [22].

The case $V^2 > \omega^2$

We can find a transformation so that the Hamiltonian becomes

$$\hat{H} = \frac{iV'}{2}(\hat{c}\hat{c} - \hat{c}^\dagger\hat{c}^\dagger), \tag{2.145}$$

where V' is real. If we use the same transformations as before, see equations (2.131) and (2.132), we find that θ is given by

$$\tanh(2\theta) = \frac{\omega}{V}. \tag{2.146}$$

To determine the expectation value of the displacement, we first define the squeeze operator

$$\hat{S}(\xi) = e^{\frac{\xi^*\hat{a}}{2} - \frac{\xi^*\hat{a}^\dagger}{2}}, \tag{2.147}$$

where $\xi = re^{i\theta}$ is a complex number ($r > 0$ and $0 < \theta < 2\pi$). Note that the squeeze operator is unitary, as the exponent is antihermitian.
Next, we use the following operator identity

$$\hat{S}(\xi)^\dagger\hat{a}\hat{S}(\xi) = \hat{a}\cosh r - e^{i\theta}\hat{a}^\dagger\sinh r, \tag{2.148}$$

which can be quickly verified by writing down the series expansion in $\hat{a}$ and $\hat{a}^\dagger$. If we now realize that the Hamiltonian in the new coordinates is in fact the squeeze operator with $\xi = V't$, we can use this formula to obtain

$$\begin{aligned}\langle\alpha(t)|\hat{X}|\alpha(t)\rangle &= \sqrt{\frac{\hbar}{2m\omega}}\,\langle\alpha|e^{\frac{iHt}{\hbar}}(\hat{a}^\dagger + \hat{a})e^{-\frac{iHt}{\hbar}}|\alpha\rangle \\ &= \sqrt{\frac{\hbar}{2m\omega}}e^{-V't}\,\langle\alpha|\hat{a} + \hat{a}^\dagger|\alpha\rangle \\ &= \sqrt{\frac{\hbar}{2m\omega}}e^{-V't}(\alpha^* + \alpha)\end{aligned} \tag{2.149}$$

We conclude that there are three completely different regimes and that the nature of the system is completely determined by $\omega^2 - V^2$. In the first case we obtain the typical oscillating behavior of the harmonic oscillator. In the second case, we obtain a damped or driven exponential for the displacement. The third transition regime exhibits a linearly decreasing displacement upon which an oscillating behavior is superposed. The spectrum of the Hamiltonian is the entire real axis and it is doubly degenerate. The proof of this can be found in [22].

2.2.2 Time-dependent Hamiltonian

A different approach in achieving classical damping in the harmonic oscillator model is taken in [25]. Here, the authors start from a general Hamiltonian of the form

$$\hat{H}(q,p,t) = [A(t)p^2 + B(t)(pq+qp) + C(t)q^2] + D(t)q + E(t)p + F(t) \tag{2.150}$$

and impose that the equation of motion should be the same as in the classical, damped case

$$\frac{\partial^2 q}{\partial t^2} + \gamma\frac{\partial q}{\partial t} + \omega^2 q = 0. \tag{2.151}$$

Thus the correspondence with damping in the classical case is imposed at operator level. It is found that there is a rather broad class of Hamiltonians that yields the desired equation of motion. One of the simpler solutions is

$$\hat{H} = e^{-\gamma t}\frac{\hat{P}^2}{2} + e^{-\gamma t}\hat{P} + e^{\gamma t}\frac{\omega^2\hat{Q}^2}{2}. \tag{2.152}$$

To introduce a Glauber state, we will an approach similar as in [26]. We can define creation and annihilation operators by

$$\hat{a} = \sqrt{\frac{e^{-\gamma t}}{2\hbar\omega}}(e^{\gamma t}(\omega + i\frac{\gamma}{2})\hat{Q} + i\hat{P} + i) \tag{2.153}$$

$$\hat{a}^\dagger = \sqrt{\frac{e^{-\gamma t}}{2\hbar\omega}}(e^{\gamma t}(\omega - i\frac{\gamma}{2})\hat{Q} - i\hat{P} - i). \tag{2.154}$$

Writing $\hat{Q}$ in terms of these operators, we find

$$\hat{Q} = \sqrt{\frac{\hbar}{2\omega}}e^{-\frac{\gamma t}{2}}(\hat{a}^\dagger + \hat{a}). \tag{2.155}$$

The problem with this approach is that the Glauber state itself becomes time dependent, so that the state is not stable through time. It is a very difficult task to find a stable Glauber state for a given time-dependent Hamiltonian. In the next subsection we illustrate a case where it is possible to do this in a relatively simple manner.

2.2.3 Time-dependent interaction with a bath

In [26] a Hamiltonian of the following kind is considered

$$\hat{H} = \hbar\left(\omega\hat{a}^\dagger\hat{a} + \beta^*(t)\hat{a} + \beta(t)\hat{a}^\dagger + b(t)\right). \tag{2.156}$$

Here $\beta(t)$ is a possibly complex function of time and $b(t)$ is a real function. The interaction with the environment is thus time-dependent, but $\hat{H}$ is hermitian at all time. Usually, time dependent problems are very difficult to solve, because we can no longer use the formal solution, see equation (1.2), of the Schrödinger equation. However, in [26] a different approach is used. Instead of solving the Schrödinger equation, an invariant $\hat{I}$ is constructed. This invariant satisfies

$$\frac{d\hat{I}}{dt} = \frac{\partial \hat{I}}{\partial t} + \frac{1}{i\hbar}[\hat{I}, \hat{H}] = 0 \tag{2.157}$$

and is hence time-independent. This implies that the eigenvalues will also be time-independent. All time-dependence is hence found in the eigenstates, which we can denote by $|\lambda, t)$. It can be checked that the wavefunction

$$|\lambda, t\rangle = e^{i\Phi_\lambda t}|\lambda, t) \tag{2.158}$$

satisfies the Schrödinger equation, provided that

$$\frac{d\Phi_\lambda}{dt} = (\lambda, t|i\hbar\frac{\partial}{\partial t} - \hat{H}|\lambda, t). \tag{2.159}$$

For the Hamiltonian in equation 2.159, it is found that $\hat{I}$ is given by

$$\hat{I} = \left(\hat{a}^\dagger\hat{a} + \theta(t)\hat{a} + \theta^*(t)\hat{a}^\dagger + \delta(t)\right), \tag{2.160}$$

with

$$\frac{d\theta(t)}{dt} = \omega\theta + \beta, \tag{2.161}$$

$$i\frac{d\delta(t)}{dt} = \theta^*\beta - \theta\beta^*. \tag{2.162}$$

Introducing the new creation and annihilation operators

$$\hat{a}^\dagger_{-\theta^*} = \hat{a}^\dagger - \theta^*, \tag{2.163}$$

$$\hat{a}_{-\theta} = \hat{a}^\dagger - \theta, \tag{2.164}$$

the invariant $\hat{I}$ can be rewritten as

$$\hat{I} = \hat{a}^\dagger_{-\theta^*}\hat{a}_{-\theta} + \left(\chi - |\beta|^2\right). \tag{2.165}$$

From this it is clear that $\hat{I}$ has the same structure as the Hamiltonian harmonic oscillator. Its eigenstates can therefore be constructed in the same way. We are especially interested in its vacuum state $|0\rangle$, for which we have that

$$\hat{a}_{-\theta}\,|0\rangle = 0 \quad \text{or} \quad \hat{a}\,|0\rangle = \theta\,|0\rangle\,. \tag{2.166}$$

The vacuum state of the invariant is hence a stable Glauber state. The Φ_λ in the extra phase factor $e^{i\Phi_\lambda t}$ necessary to satisfy the Schrödinger equation will be equal to zero when

$$b(t) = -\Re(\beta^*\theta). \tag{2.167}$$

We can wonder whether it is possible to find a $\gamma(t)$ and $b(t)$, so that we obtain classical damping for the expectation value of the displacement. The displacement with respect to the stable Glauber state is given by

$$\langle\theta(t)|\hat{X}|\theta(t)\rangle = \sqrt{\frac{\hbar}{2m\omega}}\,\langle\theta(t)|\hat{a}+\hat{a}^\dagger|\theta(t)\rangle \tag{2.168}$$

$$= \sqrt{\frac{\hbar}{2m\omega}}\,(\theta^*(t)+\theta(t))\,, \tag{2.169}$$

so that we obtain the desired outcome if $\theta(t) = e^{-(i\omega+\gamma)t}$, with γ real. Based on equation (2.164), we find for $\beta(t)$

$$\beta(t) = i\gamma e^{-(i\omega+\gamma)t} \tag{2.170}$$

if we impose the initial value $\beta(t=0) = i\gamma$. Using equation (2.170), we find for $b(t)$

$$b(t) = 0. \tag{2.171}$$

The Hamiltonian is given by

$$\hat{H} = \hbar\left(\omega\hat{a}^\dagger\hat{a} - i\gamma e^{(i\omega-\gamma)t}\hat{a} + i\gamma e^{-(i\omega+\gamma)t}\hat{a}^\dagger\right), \tag{2.172}$$

and for its eigenvalue spectrum we find

$$E_n = n\hbar\left(\omega - \frac{\gamma^2 e^{-2\gamma t}}{\omega}\right) \tag{2.173}$$

2.2.4 Bath of harmonic oscillators

An often encountered method in literature, see *e.g.* [27] and the references therein, to include damping within a quantum system, is by coupling the system to a bath of harmonic oscillators. The Hamiltonian can then be written as follows

$$\hat{H} = \hat{H}_S + \hat{H}_B + \hat{H}_I, \tag{2.174}$$

where $\hat{H}_S$ is the Hamiltonian of the system under consideration, $\hat{H}_B$ is the Hamiltonian of the bath and $\hat{H}_I$ describes the coupling of the system with the bath. In our case, both the system and the bath are a system of coupled oscillators.

$$\hat{H}_S = \frac{p^2}{2M} + \frac{M\omega^2 q^2}{2} \tag{2.175}$$

$$\hat{H}_B = \sum_{i=1}^{N} (\frac{p_i^2}{2m_i} + \frac{m_i \omega_i^2 x_i^2}{2}) \tag{2.176}$$

The coupling Hamiltonian is chosen to be bilinear, which is justified by the assumption of weak coupling, and is given by

$$\hat{H}_I = -q \sum_{i=1}^{N} c_i x_i. \tag{2.177}$$

This type of model is known in literature as the Caldeira-Legett model [27], although in that model an extra term is usually included to ensure that the effective potential of the system doesn't change. If we know consider the entire Hamiltonian, we see that we get exactly the same Hamiltonian as discussed in paragraph 2.1.5. It should be pointed out, however, that due to the oscillating behavior, we will get a state that is very similar to the initial state, after a sufficiently long time span, which is called the Poincaré recurrence time. This phenomenon is known in literature as quantum revival and is of course undesired in a damped model as the dissipated energy is eventually fed back into the system. This is mainly due to the finite number N of oscillators in the bath. However, it turns out that already for a small number of oscillators the Poincaré recurrence time can become practically infinite.

We have thus managed to introduce damping in the system. Still, there are a few remarks to be made. Firstly, the damping is approximative as an infinite amount of oscillators in the bath is needed to really make the Poincaré recurrence time infinite. Secondly, for the system to be ergodic, it should be possible for the system and the bath to exchange an infinitesimal amount of energy. Otherwise, depending on the initial state, the equilibrium state might never be reachable. We would thus need a continuum of oscillators with

circular frequencies starting from zero. There are closed form solutions at hand for this continuum of oscillators, but we won't discuss them here. We refer to [27] for a more extensive discussion.

2.2.5 Damping in the density operator formalism

Perhaps the most conventional method of introducing damping is by using the density operator formalism to embed the system in an environment. See for example [28] or [29] for an accessible introduction. We start by deriving the time evolution equation for the density operator $\hat{\rho} = |\psi(t)\rangle \langle\psi(t)|$ of the harmonic oscillator. Starting from the Schrödinger equation

$$i\hbar \frac{\partial}{\partial t} |\psi\rangle = \hat{H} |\psi(t)\rangle , \tag{2.178}$$

we immediately derive the time evolution equation for the density operator

$$i\hbar \frac{\partial \hat{\rho}}{\partial t} = [\hat{H}, \hat{\rho}], \tag{2.179}$$

which can be rewritten as

$$\frac{\partial \hat{\rho}}{\partial t} = -i[\omega \hat{N}, \hat{\rho}]. \tag{2.180}$$

Damping is now introduced by adding extra terms to this equation

$$\frac{\partial \hat{\rho}}{\partial t} = -i[\omega \hat{N}, \hat{\rho}] - \frac{\gamma}{2}(\hat{\rho}\hat{a}^\dagger \hat{a} + \hat{a}^\dagger \hat{a}\hat{\rho} - 2\hat{a}\hat{\rho}\hat{a}^\dagger), \tag{2.181}$$

with γ a positive constant. This equation is called the Lindblad equation and plays an important role in quantum optics [29]. We will not give the derivation of the equation here. We point out, however, that several approximations were made in deriving the equation. An important assumption, of which the validity is hard to check in practice, is that the evolution of the density operator only depends on the actual state of the system. In statistics, a system that changes states based on a transition rule that only depends on the current state of the system is called a Markov process. The Lindblad equation is therefore called a Markovian type of master equation.
If we start from an initial state $|\alpha_0\rangle$ and therefore $\hat{\rho}_0 = |\alpha_0\rangle \langle\alpha_0|$, it is straightforward to check that the solution to this equation is given by

$$\hat{\rho} = |\alpha_t\rangle \langle\alpha_t| , \tag{2.182}$$

with $\alpha_t = \alpha_0 \exp^{-i\omega t - \frac{\gamma}{2}t}$. The eigenvalue of the Glauber state will go to zero for t going to infinity, thus reaching the ground state. When we calculate the expectation value of the position, $\hat{X}$, we get

$$\langle \alpha_t | \hat{X} | \alpha_t \rangle = e^{-\gamma t} \langle \alpha_0 | \hat{X} | \alpha_0 \rangle , \tag{2.183}$$

which is what we would expect in the classical case. We have thus managed to find an equivalent to classical damping. It is interesting to wonder whether we can obtain the same result within the Hamilton formalism. From formula (2.182), it is clear that the extra terms added to the time evolution equation are impossible to add to include in the Hamilton formalism, as they cannot be written as commutators of $\hat{\rho}$ with some Hamiltonian.

2.3 Relation to integrable models

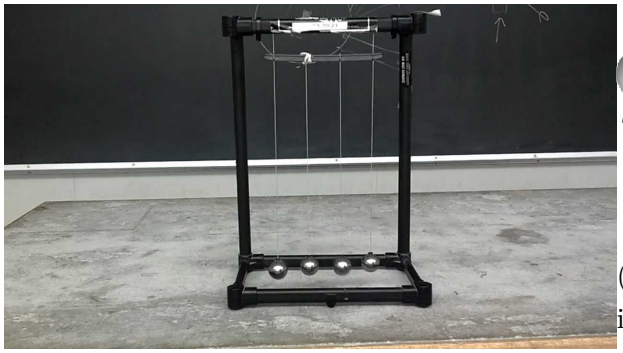

(a) The coupled pendulums experiment.

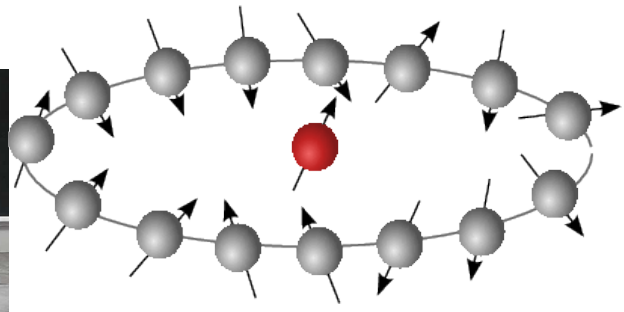

(b) The central spin model as an example of an integrable. The red ball in the center has a spin that interacts with the spins of the gray balls. The spins of the gray balls don't interact mutually.

Figure 2.11: The similarties between a coupled harmonic oscillator system and an integrable model.

In Figure 2.11a an experimental setup of the coupled pendulums experiment is shown. All pendulums are connected by a rod, which we assume to also behave as a harmonic oscillator. The pendulums move in and out of the plane of the picture. The rod connecting the pendulums is also considered to be a harmonic oscillator. For this experimental setup

shown, we can presume that K has the following form

$$K = \begin{bmatrix} * & 0 & 0 & 0 & * \\ 0 & * & 0 & 0 & * \\ 0 & 0 & * & 0 & * \\ 0 & 0 & 0 & * & * \\ * & * & * & * & * \end{bmatrix}, \tag{2.184}$$

which expresses that each of the pendulums is coupled only to the bar and not directly to the other pendulums. Matrices of this type are suggestively called arrowhead matrices. If we write

$$K = \begin{bmatrix} D & z \\ z^T & \delta \end{bmatrix}, \tag{2.185}$$

with $D = \mathrm{diag}(d_1, d_2, \ldots, d_{n-1})$, $z = \begin{bmatrix} \zeta_1 & \zeta_2 & \cdots & \zeta_{n-1} \end{bmatrix}^T$ and δ a real scalar, we find the following eigenvalue equation

$$\gamma - \lambda - z^T (D - \lambda I)^{-1} z \equiv \gamma - \omega^2 - \sum_{i=1}^{n-1} \frac{\zeta_i^2}{d_i - \omega^2} = 0. \tag{2.186}$$

This set of equations is then to be solved for ω^2, which are the eigenvalues of K. This equation will also be encountered in the following chapter on integrable systems, indicating the intricate link between these models. This link can be appreciated by considering Figure 2.11. Both figures depict a system, the rod or the central spin, that is coupled to a set of non-interacting oscillators or spin, which can be considered as non-interacting baths.

Chapter 3

Richardson-Gaudin models

In physics, one rarely encounters a nontrivial model that can be solved exactly. This is mainly due to the exponential scaling of the Hilbert space, which makes exact diagonalization usually impossible. In most of the cases, one has to use approximative and/or numerical methods in order to obtain some insight in the model. However, these approximative solutions might overlook some of the essential features. Therefore, it is interesting to look at models that *can* be solved exactly. Especially for systems with strongly-correlated particles, where typical quantum phenomena appear, the existence of exactly solvable models is essential for the understanding of these systems.
An important class of exactly solvable models are the Richardson-Gaudin models. These models are extremely well-suited to describe pairing phenomena in strongly correlated systems. Richardson-Gaudin models play an important role in describing superconductivity and superfluidity [30]. The models also have a great potential for quantum computation [31, 32].
In this chapter we introduce the Richardson-Gaudin models and discuss how they can be exactly solved. As an example, we will examine the BCS Hamiltonian, which is historically very important.

3.1 Integrable models

Integrable models are special in the sense that (i) they can be exactly solved and (ii) they possess a number of conservation laws scaling with the system size. However, the notion of quantum integrability is not so well defined as its classical analogue [33]. In the following integrable models are defined as models for which one can construct a set of L non-trivial, mutually commuting operators that commute with the Hamiltonian, resulting a in set of

L conserved charges, with L the degrees of freedom in the system [34]. It is usually a very difficult or even impossible task to find such a set of operators for a given Hamiltonian. Therefore, a possible method of constructing integrable Hamiltonians is by starting from a given set of mutually commuting operators and by taking suitable linear combinations of these operators. As all the operators of the set commute mutually and by construction with the Hamiltonian, the system is by definition integrable and there is a common basis of eigenstates. It suffices thus to know the eigenstate of one of the operators in order to know the eigenstates of the Hamiltonian. The difficulty in this approach is to give a physical sense to the constructed Hamiltonian.

3.2 The pairing problem

Due to the importance of the Richardson-Gaudin integrability in the description of pairing phenomena, we will discuss a general framework for describing pairing of fermions in physical systems in this section. The Hamiltonian will be defined in second quantization using creation and annihilation operators. The operator $\hat{a}_\alpha$ is called the annihilation operator and annihilates a fermion in the state with label α. α does not necessarily represent one quantum number, but can also refer to a set of quantum numbers. The operator $\hat{a}^\dagger_\alpha$ is called the creation operator and creates a fermion in the state with label α. The creation and annihilation operators introduced here are very similar to the ladder operators encountered in the harmonic oscillator system, where the particles represent quanta of energy. The main advantage of using these operators is that one automatically obtains the correct particle symmetry by imposing the correct commutation relations. For example, fermions should be antisymmetric upon exchange of two particles and it should be impossible to have two particles with the same quantum numbers. To express this in second quantization, we introduce the following anti-commutation relations

$$\{\hat{a}_\alpha, \hat{a}^\dagger_{\alpha'}\} = \delta_{\alpha\alpha'}, \quad \{\hat{a}^\dagger_\alpha, \hat{a}^\dagger_{\alpha'}\} = 0, \quad \{\hat{a}_\alpha, \hat{a}_{\alpha'}\} = 0, \tag{3.1}$$

with δ_{ij} the Kronecker delta symbol and $\{\}$ the anti-commutator, $\{\hat{A}, \hat{B}\} = \hat{A}\hat{B} + \hat{B}\hat{A}$. The equations (3.1) indeed express the impossibility of finding two particles in the same quantum state

$$\{\hat{a}^\dagger_\alpha, \hat{a}^\dagger_\alpha\} = 2\hat{a}^\dagger_\alpha \hat{a}^\dagger_\alpha = 0. \tag{3.2}$$

We see that the use of the anti-commutator is necessary to get this result. If one would use the commutator, equation (3.2) would automatically be zero and no restriction on the

amount of particles in the same state could be imposed. For bosons there is no such restriction and therefore commutation relations are used for their creation and annihilation operators. Indeed, recall that for the ladder operators in the harmonic oscillator commutation relations are imposed. This is because the energy quanta are bosons.
We are now set to discuss the pairing problem. To keep the discussion as general as possible, we will consider the framework used for the description of nuclear superfluidity [35]. When pairing is present, fermions of the opposite spins will have the tendency to occupy identical spatial orbitals. In order to have pairing in a system it should hence be energetically favorable for the fermions of opposite spins to occupy the same spatial orbitals. We can therefore describe pairing by introducing the following Hamiltonian

$$\hat{H} = \sum_{jm} \epsilon_j \hat{a}^\dagger_{jm} \hat{a}_{jm} + \frac{1}{4} \sum_{jj'mm'} V_{jj'} (-1)^{j+j'+m+m'} \hat{a}^\dagger_{jm} \hat{a}^\dagger_{j-m} \hat{a}_{j'm'} \hat{a}_{j'-m'}, \tag{3.3}$$

with ϵ_j the energy of the single particle state with quantum number j and $V_{jj'}$ a real, symmetric matrix. It is this part of the Hamiltonian that will induce pairing. The operators $\hat{a}_{jm}$ and $\hat{a}^\dagger_{jm}$ annihilate, respectively create, a particle in the state labeled with indices j and m. The quantum number j is the total angular momentum of the fermion, arising from the coupling between the spatial angular momentum and the spin. The quantum number m is the projection of this total angular momentum and can therefore take values $m = -j, -j+1, ..., j-1, j$. Throughout the remainder of this discussion we will assume that these two quantum numbers are sufficient to completely specify a state. The degeneracy Ω_j of a state with quantum number j is $\Omega_j = 2j + 1$. The first term of the Hamiltonian is reminiscent of the harmonic oscillator and represents the single-particle energies. The second term of the Hamiltonian is the one responsible for the pairing of the particles. For suitable values of $V_{jj'}$ it will be energetically favorable for the particles to doubly occupy the same orbital and hence to form pairs. The extra phase factor $(-1)^{j+j'+m+m'}$ ensures that the Hamiltonian has time-reversal symmetry. This can be made more explicitly by introducing following notations

$$\hat{a}_{j,\bar{m}} = (-)^{j+m} \hat{a}_{j,-m}, \qquad \hat{a}^\dagger_{j,\bar{m}} = (-)^{j+m} \hat{a}^\dagger_{j,-m}, \tag{3.4}$$

so that $(j, \bar{m})$ is the time-reversed state of (j, m). Using this notation, the time reversal symmetry becomes apparent

$$\hat{H} = \sum_{jm} \epsilon_j \hat{a}^\dagger_{j,m} \hat{a}_{j,m} + \frac{1}{4} \sum_{jj'mm'} V_{jj'} \hat{a}^\dagger_{j,m} \hat{a}^\dagger_{j,\bar{m}} \hat{a}_{j',m'} \hat{a}_{j',\bar{m}'}. \tag{3.5}$$

The form of the Hamiltonian suggests the introduction of a new set of operators

$$\hat{S}_j^\dagger = \sum_m \frac{1}{2}(\hat{a}_{j,m}^\dagger \hat{a}_{j,\bar{m}}^\dagger), \tag{3.6}$$

$$\hat{S}_j = (\hat{S}_j^\dagger)^\dagger = \sum_m \frac{1}{2}(\hat{a}_{j,m}\hat{a}_{j,\bar{m}}), \tag{3.7}$$

$$\hat{S}_j^0 = \frac{1}{2}\sum_m \hat{a}_{j,m}^\dagger \hat{a}_{j,m} - \frac{1}{4}\Omega_j = \frac{1}{2}\hat{n}_j - \frac{1}{4}\Omega_j, \tag{3.8}$$

where we have introduced the number operator $\hat{n}_j \triangleq \sum_m \hat{a}_{j,m}^\dagger \hat{a}_{j,m}$, which counts the number of particles in level j. $\hat{S}_j^\dagger$ creates a pair of fermions in level j, $\hat{S}_j$ annihilates one and $\hat{S}^0$ contains the information on the occupation of the level. These operators are called the quasi-spin operators[35]. The following commutations relations hold

$$[\hat{S}_i^0, \hat{S}_j^\dagger] = \delta_{ij} S_i^\dagger, \qquad [\hat{S}_i^0, \hat{S}_j] = -\delta_{ij} S_i, \qquad [\hat{S}_i^\dagger, \hat{S}_j] = 2\delta_{ij} S_i^0, \tag{3.9}$$

so that these operators close an $su(2)$ algebra. We can rewrite the Hamiltonian in terms of the new operators as

$$\hat{H} = \sum_j \epsilon_j (2\hat{S}_j^0 + \frac{1}{2}\Omega_j) + \sum_{jj'} V_{jj'} \hat{S}_j^\dagger \hat{S}_{j'}. \tag{3.10}$$

The new algebra (3.9) is the same as the angular momentum and the spin algebra, thus motivating the denoting of a "quasi-spin" algebra. For the spin vector $\hat{\vec{S}} = (\hat{S}_1, \hat{S}_2, \hat{S}_3)$ with the familiar commutation relations

$$[\hat{S}_l, \hat{S}_m] = i \sum_{n=1}^{3} \varepsilon_{lmn} \hat{S}_n \tag{3.11}$$

we can define

$$\hat{S}^+ = \hat{S}^x + i\hat{S}^y, \quad \hat{S}^- = \hat{S}^x - i\hat{S}^y, \quad \hat{S}^0 = \hat{S}^z, \tag{3.12}$$

which indeed satisfy the same commutation relations as respectively $\hat{S}^\dagger, \hat{S}, \hat{S}^0$. Quasispin states $|d_i, \mu_i\rangle$ can now be constructed in the same way as for the spin

$$\hat{S}_i^\dagger |d_i, \mu_i\rangle = \sqrt{(d_i - \mu_i)(s_i + mu_i + 1)}\, |d_i, \mu_i + 1\rangle \tag{3.13}$$

$$\hat{S}_i |d_i, \mu_i\rangle = \sqrt{(d_i + \mu_i)(s_i - mu_i + 1)}\, |d_i, \mu_i - 1\rangle \tag{3.14}$$

$$\hat{S}_i^0 |d_i, \mu_i\rangle = \mu_i |d_i, \mu_i\rangle, \tag{3.15}$$

where μ_i ranges from $-d_i$ to d_i. We thus have found a representation for the quasi-spin states. The physical interpretation of the newly introduced quantum numbers d_i and μ_i

can be deduced by elaborating on the analogy with the spin case. When using the usual operators $\hat{S}^2$ and $\hat{S}^z$ to label spin states, we see that the quantum number associated with $\hat{S}^2$ determines the maximum (absolute) value that the projection of the spin can take. The quantum number d_i can therefore be given an analogous interpretation as the maximum allowable number of pairs in level i. Just like in the spin case, it is the quantum number associated with the Casimir operator, which for the quasi-spin algebra is given by

$$\hat{\mathscr{C}}\left[su(2)_i\right] = \frac{1}{2}(\hat{S}_i^\dagger \hat{S}_i + \hat{S}_i \hat{S}_i^\dagger) + (\hat{S}_i^0)^2. \tag{3.16}$$

Casimir operators of an algebra are special operators, since they commute with all other operators. This maximum amount of pairs in the level is given by $\frac{\Omega_i}{2} = j_i + \frac{1}{2}$. Besides pairs it is also possible to have unpaired fermions occupying a state at level i. The presence of each such a fermion prevents a pair to occupy an orbital in level i. This is called the blocking effect [35]. Denoting v_i as the number of unpaired fermions in the level, also called the seniority of level i, the maximum amount of pairs allowed at the level is given by $\frac{\Omega_i}{2} - v_i = j_i - \frac{v_i}{2}$. The eigenstates of $\hat{S}_i^0$ with the lowest eigenvalue is $|d_i, -d_i\rangle$ and is destroyed by $\hat{S}_i$. The state $|d_i, -d_i\rangle$ therefore has no pairs in level i. Bearing in mind all this and the definition of $\hat{S}^0$, we find that

$$d_i = \frac{\Omega_i}{2} - \frac{v_i}{2} \tag{3.17}$$

$$\mu_i = \frac{n_i}{2} - \frac{\Omega_i}{2}, \tag{3.18}$$

where n_i is the total number of fermions in level i. For a given seniority, we can now define the vacuum $|\theta\rangle$ as

$$|\theta\rangle = |d_1, -d_1\rangle \otimes ... \otimes |d_i, -d_i\rangle ... \tag{3.19}$$

From the above discussion it should be clear that there is no difference between spin and quasi-spin systems on the mathematical level. In what follows, we will not make a clear distinction between spin and quasi-spin systems in the notation. For instance, a direct product state is denoted as $|\uparrow \cdots \downarrow\rangle$. The uparrow may represent either a state filled with a pair or a $+\frac{1}{2}$ spin projection, whereas the downarrow can refer to either an empty state or a $+\frac{1}{2}$ spin projection.

3.3 Integrability conditions

In this section we aim to construct a set of L commuting operators, where L is the number of degree of freedom in the model. We can then construct an integrable Hamiltonian by

taking a linear combination of these operators. By construction the Hamiltonian will be integrable. As our pairing Hamiltonian is quadratic in the operators, we propose operators of the following form

$$R_i = \sum_{\alpha=1}^{3} A_i^\alpha \hat{S}^\alpha + g \sum_{k\neq i}^{n} \sum_{\alpha=1}^{3} X_{ik}^\alpha \hat{S}_i^\alpha S_k^\alpha, \tag{3.20}$$

with g a real number, representing the coupling strength. By imposing these operators to commute mutually, we retrieve after a calculation the following equations [36]

$$\epsilon_{\alpha\beta\gamma}\left(A_i^\alpha X_{ji}^\beta + A_j^\alpha X_{ij}^\gamma\right) = 0 \tag{3.21}$$

$$X_{ij}^\alpha + X_{ji}^\alpha = 0, \quad \forall\alpha = 1,2,3 \tag{3.22}$$

$$X_{ki}^1 X_{ij}^2 + X_{jk}^2 X_{ki}^3 + X_{ij}^3 X_{jk}^1 = 0. \tag{3.23}$$

From the pairing Hamiltonian, equation (3.10), it should be clear that $A_j^3 \neq 0$. Imposing this, we find

$$X_{ij} = \pm Y_{ij}, \tag{3.24}$$

where the notation $\{X^1, X^2, X^3\} = \{X, Y, Z\}$ was introduced and also that, dependent on the sign chosen in equation (3.24), $A_i^3 = \pm A_j^3$. Only retaining A_i^3 and putting $A_i^1 = A_1^2 = 0$ has the advantage that the operator conserves the number of particles, which is necessary for a closed system. Usually the plus sign is chosen and this gives rise to the XXZ integrable models. The operators become

$$\hat{R}_i = \hat{S}_i^0 + g \sum_{k\neq i} \frac{1}{2} X_{ik}\left(\hat{S}_i^\dagger \hat{S}_k + \hat{S}_i \hat{S}_k^\dagger\right) + Z_{ik}\hat{S}_i^0 \hat{S}_k^0 \tag{3.25}$$

and the Gaudin equations are given by

$$X_{ij} + X_{ji} = 0, \quad Z_{ij} + Z_{ji} = 0, \tag{3.26}$$

$$X_{ki}X_{ij} + X_{jk}Z_{ki} + Z_{ij}X_{jk} = 0. \tag{3.27}$$

Using these equations, it can be proven that [37]

$$X_{ij}^2 - Z_{ij}^2 = \Gamma, \quad \forall i, j. \tag{3.28}$$

The value of Γ can help us to make a distinction between the several classes of solutions. There are three main classes of solutions to this set of equations. As antisymmetry is required, it is useful to write the solutions as an odd function in terms of arbitrary parameters $\eta_i - \eta_j$, as shown in the following

1. The rational model ($\Gamma = 0$)

$$X_{ij} = Z_{ij} = \frac{1}{\eta_i - \eta_j} \tag{3.29}$$

2. The trigonometric model ($\Gamma > 0$)

$$X_{ij} = \frac{1}{\sin(\eta_i - \eta_j)}, \qquad Z_{ij} = \cot(\eta_i - \eta_j) \tag{3.30}$$

3. The hyperbolic model ($\Gamma < 0$)

$$X_{ij} = \frac{1}{\sinh(\eta_i - \eta_j)}, \qquad Z_{ij} = \coth(\eta_i - \eta_j) \tag{3.31}$$

The first model is also called the XXX model and the other two are called XXZ models. There do exist XYZ models, also called elliptic models [37], but we won't discuss them here.

3.4 Bethe ansatz wavefunction

Now that we have found a set of commuting operators, we still need to find the eigenstates of the operators. As all the operators commute, it suffices to find the eigenstate of one of a single operator $\hat{R}_i$.

To do this, we start by defining the following operators, based on the Gaudin algebra

$$\hat{S}^\dagger_\alpha = \sum_{i=1}^{L} X_{i\alpha} \hat{S}^\dagger_i \tag{3.32}$$

$$\hat{S}_\alpha = (\hat{S}^\dagger_{\alpha^*})^\dagger = \sum_{i=1}^{L} X_{i\alpha} \hat{S}_i \tag{3.33}$$

$$S^0_\alpha = \sum_{i=1}^{L} Z_{i\alpha} \hat{S}^0_i. \tag{3.34}$$

We use the notational convention that the greek indices are not referring to the (quasi-)spin copies, but merely label the newly defined operators. We put forward that $X_{i\alpha}$ and $Z_{i\alpha}$ still satisfy the Gaudin equations, so that we can parametrize them with the extra variables η_α in equations (3.29-3.31). The new, generalized operators are thus linear combinations of the old ones, with the coefficients satisfying the integrability conditions.

We use the following ansatz for the eigenstate

$$|\psi\rangle = \prod_{\alpha=1}^{N} \hat{S}_\alpha^\dagger |\theta\rangle \,, \tag{3.35}$$

with $|\theta\rangle$ the vacuum state and N the number of pair/quasi-spin excitations. A similar ansatz was first made by Hans Bethe in 1931 to find the exact eigenspectrum of the one-dimensional anti-ferromagnetic Heisenberg model [38]. We impose that this state is an eigenstate of the $\hat{R}_i$, so that

$$\hat{R}_i \prod_{\alpha=1}^{N} \hat{S}_\alpha^\dagger |\theta\rangle = r_i \prod_{\alpha=1}^{N} \hat{S}_\alpha^\dagger |\theta\rangle \,, \tag{3.36}$$

should hold. Making use of the following commutation relations

$$[\hat{R}_i, \hat{S}_\alpha^\dagger] = X_{i\alpha}\hat{S}_i^\dagger(1 - g\hat{S}_\alpha^0) - gZ_{\alpha i}\hat{S}_\alpha^\dagger \hat{S}_i^0 \tag{3.37}$$

$$[[\hat{R}_i, \hat{S}_\alpha^\dagger], \hat{S}_\beta^\dagger] = -g\hat{S}_i^\dagger Z_{\alpha\beta}(X_{i\beta}\hat{S}_\alpha^\dagger - X_{i\alpha}\hat{S}_\beta^\dagger) \tag{3.38}$$

and the action of $\hat{R}_i$ on the vacuum

$$\hat{R}_i |\theta\rangle = d_i(-1 + g\sum_{k\neq i} Z_{ik}d_k) |\theta\rangle \,, \tag{3.39}$$

we can pull R_i through the product state [54]

$$\begin{aligned}
\hat{R}_i \prod_{\alpha=1}^{N} \hat{S}_\alpha^\dagger |\theta\rangle = &\sum_{\alpha=1}^{N}\sum_{\beta=\alpha+1}^{N} \left(\prod_{\gamma\neq\alpha,\beta}^{N} \hat{S}_\gamma^\dagger\right) \left[\left[\hat{R}_i, \hat{S}_\alpha\right], \hat{S}_\beta^\dagger\right] |\theta\rangle + \sum_{\alpha=1}^{N} \left(\prod_{\beta\neq\alpha}^{N} \hat{S}_\beta^\dagger\right) \left[\hat{R}_i, \hat{S}_\alpha\right] |\theta\rangle \\
&+ \prod_{\alpha=1}^{N} \left(\hat{S}_\alpha^\dagger\right) \hat{R}_i |\theta\rangle \\
= &\sum_{\alpha=1}^{N} \left[X_{i\alpha}(1 + gd_\alpha) - g\sum_{\beta\neq\alpha}^{N} Z_{\beta\alpha}X_{i\alpha}\right] \hat{S}_i^\dagger \prod_{\gamma\neq\alpha}^{N} \hat{S}_\gamma^\dagger |\theta\rangle \\
&+ d_i \left[-1 + g\sum_{k\neq i} Z_{ik}d_k + g\sum_{\beta=1}^{N} Z_{\beta i}\right] \prod_{\alpha}^{N} \hat{S}_\alpha^\dagger |\theta\rangle \,,
\end{aligned} \tag{3.40}$$

with $d_\alpha = \sum_i^m Z_{i\alpha}d_i$. We find that $\prod_\alpha^N \hat{S}_\alpha^\dagger |\theta\rangle$ is an eigenstate with its eigenvalue given by

$$r_i = d_i \left(-1 + g\sum_{k\neq i} Z_{ik}d_k + g\sum_{\beta=1}^{N} Z_{\beta i}\right) , \tag{3.41}$$

with d_i is the spin degeneracy of orbital i, when the term that is not proportional to $\prod_\alpha^N \hat{S}_\alpha^\dagger |\theta\rangle$ disappears

$$1 + gd_\alpha - g \sum_{\beta \neq \alpha}^{N} Z_{\alpha\beta} = 0, \quad \forall \alpha. \tag{3.42}$$

These equation are called the Richardson-Gaudin equations. In order to find the wavefunction, we thus need to solve this set of equations that grows linearly in the number of particles. See section 3.6 for an example of how this is done. We have thus obtained a much more favorable scaling than the usual exponential one encountered in many-body problems. Besides, many powerful methods to solve these equations have been conceived, so that it is possible to model systems of the mesoscopic scale, see for instance [39]. In chapter 4 we discuss how to solve these equations.

3.5 Dual states

The wavefunction in equation (3.35) can alternatively be defined as

$$|\psi\rangle = \prod_{\mu=1}^{(L-N)} \hat{S}_\mu |\uparrow\uparrow\uparrow \cdots\rangle \,. \tag{3.43}$$

Instead of adding particles to the vacuum $|\theta\rangle = |\downarrow\downarrow\downarrow\downarrow\downarrow\downarrow\downarrow\downarrow\rangle$, particles are removed from the completely filled state. This can also be seen as creating holes. Clearly, each state can be defined both in terms of particles as in terms of holes. This implies that there is a duality between particles and holes and hence between creation and annihilation operators. The state in equation (3.43) is called a dual state. Expressions for the eigenvalues and the Richardson-Gaudin equation can be derived in a similar way as in the previous section. In the next section we will discuss the BCS hamiltonian as an example of an integrable model.

3.6 Example of an integrable system: The reduced BCS Hamiltonian

In 1957 Bardeen, Cooper and Schrieffer managed to successfully describe superconductivity at low temperatures in certain materials [40]. They proposed a Hamiltonian that was very similar to the pairing Hamiltonian we introduced in equation (3.10). Under the assumption

that the superconductivity is isotropic, the BCS Hamiltonian reduces to

$$\hat{H} = \sum_j \epsilon_j (2\hat{S}_j^0 + \frac{1}{2}\Omega_j) + g \sum_{jj'} \hat{S}_j^\dagger \hat{S}_{j'}, \tag{3.44}$$

which is just (3.10) with $V_{jj'} = g$. This kind of isotropic superconductivity is called s-wave superconductivity [41]. Bardeen, Cooper and Schrieffer had proposed a variational method to approximate the eigenstates of this Hamiltonian using following coherent state

$$|\psi\rangle \propto e^{\sum_\nu \frac{v_\nu}{u_\nu} \hat{a}_\nu^\dagger \hat{a}_{\bar{\nu}}^\dagger} |\theta\rangle \,. \tag{3.45}$$

The obtained solution had the right thermodynamical limit, but for smaller systems it gave the wrong results, because of large fluctuations in the particle number. In 1963 Richardson [42] solved the pairing problem exactly by proposing an ansatz of the form

$$|\psi\rangle = \prod_\alpha \hat{S}_\alpha^\dagger |\theta\rangle \,, \tag{3.46}$$

with

$$\hat{S}_\alpha^\dagger = \sum_i \frac{\hat{S}_i^\dagger}{2\epsilon_i - E_\alpha}. \tag{3.47}$$

This ansatz wavefunction was found to be the exact eigenstate of the Hamiltonian if E_α satisfies

$$1 + 2g \sum_j \frac{d_j}{2\epsilon_j - E_\alpha} + 2g \sum_{\beta \neq \alpha}^{N} \frac{1}{E_\beta - E_\alpha} = 0, \qquad \alpha = 1, ..., N. \tag{3.48}$$

These equations are called the Richardson equations. The energy of the system is given by

$$E = \sum_\alpha^N E_\alpha + \sum_j \epsilon_j v_j. \tag{3.49}$$

The first term is the contribution of the pairs to the energy and the second term is the contribution of the unpaired fermions and, for fixed seniority, this corresponds to the vacuum energy. E_α can hence be loosely interpreted as the energy of pair α and is also called a rapidity. Note that the solutions can be complex, but as pairs will always appear in complex conjugates, (3.49) will always be real.

As the BCS theory got the right thermodynamic limit little attention was paid to this exact solution. It was only in the late '90s that Richardson's solution came back into prominence, as it was realized that the BCS theory could not be applied to small systems such as ultrasmall superconducting grains. In 1997 Cambiaggio *et al.* [43] conceived a

framework making the connection between Richardson's solution and the Gaudin algebra. By taking a suitable linear combination of the operators $\hat{R}_i$, we can indeed obtain the reduced BCS Hamiltonian. We use the rational model, so that

$$X_{ij} = Z_{ij} = \frac{1}{\epsilon_i - \epsilon_j}. \tag{3.50}$$

The operators $\hat{R}_i$ become

$$\begin{aligned}\hat{R}_i &= \hat{S}_i^0 + g\sum_{j\neq i}\frac{1}{\epsilon_i-\epsilon_j}\left[\frac{1}{2}(\hat{S}_i^\dagger\hat{S}_j + \hat{S}_i\hat{S}_j^\dagger) + \hat{S}_i^0\hat{S}_j^0\right] \\ &= \hat{S}_i^0 + g\sum_{j\neq i}\frac{\hat{\vec{S}}_i\cdot\hat{\vec{S}}_j}{\epsilon_i-\epsilon_j}.\end{aligned} \tag{3.51}$$

The Hamiltonian can now be found as

$$\sum_i 2\epsilon_i\hat{R}_i = \hat{H}_{BCS} - g\sum_i \hat{\mathscr{C}}\left[su(2)_i\right] + g\left(\sum_i \hat{S}_i^0\right)\left(\sum_i \hat{S}_i^0 - 1\right), \tag{3.52}$$

where the last two terms commute with $\hat{H}_{BCS}$. It is indeed straightforward to see that the wavefunction (3.46) proposed by Richardson is the Bethe ansatz wavefunction in the rational model with the small, conventional difference that there is a $2\epsilon_i$ in the denominator instead of ϵ_i. From the previous it should be clear how the Gaudin algebra in combination with the Bethe ansatz wavefunction provide a more general framework for the ansatz (3.46) proposed by Richardson. Figures 3.1 and 3.2 show some exact results of an eight level system. In the next chapter we will discuss how these results can be obtained.

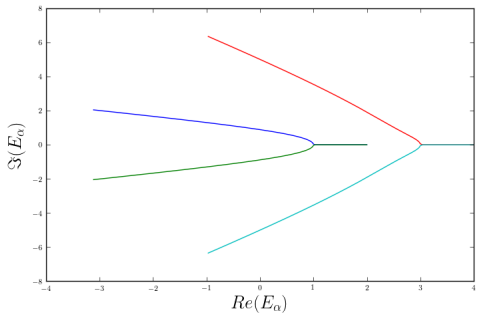

(a) The evolution of the rapidities in the complex plane for changing coupling strength.

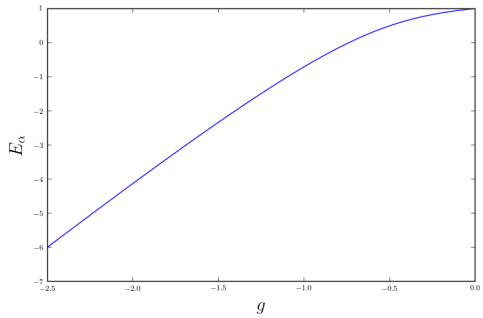

(b) The eigenenergy of the first excited eigenstate as a function of the coupling strength.

Figure 3.1: Numerical results of the reduced BCS Hamiltonian for an eight level system.

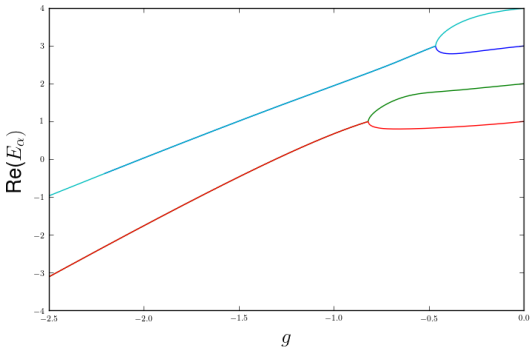

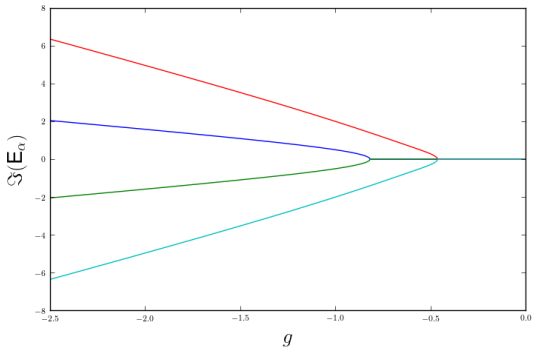

Figure 3.2: The real and imaginary part of the rapidities as a function of the coupling strength. At the single-particle energies 1 and 3, the rapidities become degenerate.

Chapter 4

Solving the Richardson-Gaudin equations

In this chapter we will discuss how to numerically solve the Richardson-Gaudin equations (3.42). Using the Richardson equation as an example, we will first demonstrate some of the obstacles encountered when straightforwardly solving the equations. Next, we will introduce the eigenvalue based variables and show how solving for these variables completely sidesteps the usual problems. We then demonstrate how the rapidities can be retrieved from the eigenvalue-based variables. Finally, we will give a short overview of other popular methods to solve the Richardson-Gaudin equations.

4.1 Difficulties in solving the Richardson-Gaudin equations

Consider as an example the Richardson equations we have encountered while discussing the reduced BCS Hamiltonian

$$1 + 2g \sum_{j}^{L} \frac{d_j}{2\epsilon_j - E_\alpha} + 2g \sum_{\beta \neq \alpha}^{N} \frac{1}{E_\beta - E_\alpha} = 0, \qquad \alpha = 1, ..., N. \tag{4.1}$$

The rapidities E_α can, for fixed values of the single particle energies, be seen as functions of the coupling strength g. As the coupling strength is changed the rapidities will also change. It turns out that for certain values of the coupling strength some of the rapidities might take the value of a single-particle energy, $E_\alpha = 2\epsilon_j$. This is shown in Figure 3.2. This implies that the denominator of a term in the first summation of equation (4.1) becomes zero and the term goes to infinity. This was already encountered by Richardson in his numerical

study [44] and has since then been thoroughly discussed in many papers, for example [45, 46, 47, 48]. The values of the coupling strength for which this happens are therefore called singular points. Still, the equality can remain satisfied if another rapidity also takes the value of the same single-particle energy, $E_\alpha = E_\beta$, such that the contributions of the second and third term cancel each other exactly. However, this poses serious computational problems, as the numerical methods cannot deal with the singularities. In the remainder of the chapter we will discuss a method to overcome these numerical difficulties.

4.2 The eigenvalue-based variables method

In this method we prefer not to solve directly for the rapidities, but rather to rewrite the Richardson-Gaudin equations in terms of variables that aren't plagued by singularities. Based on the expression for the eigenvalues, see equation (3.41) we define [49]

$$\Lambda_i = \sum_{\alpha=1}^{N} Z_{i\alpha}, \tag{4.2}$$

so that expressed in these new variables the eigenvalues become

$$r_i = d_i(-1 + g\sum_{k\neq i}^{L} Z_{ik}d_k - g\Lambda_i). \tag{4.3}$$

Therefore the eigenvalues r_i only depend on the rapidities through the variables Λ_i, explaining the name eigenvalue-based variables. We would like to rewrite the Richardson-Gaudin equations, see equation (3.42), in terms of these variables. To do so, we start by noting that

$$\Lambda_i^2 = \sum_{\alpha=1}^{N}\sum_{\beta=1}^{N} Z_{i\alpha}Z_{i\beta} = -\sum_{\alpha=1}^{N}\sum_{\beta\neq\alpha}^{N} Z_{\alpha i}Z_{i\beta} + \sum_{\alpha=1}^{N} Z_{i\alpha}^2. \tag{4.4}$$

We now use the relation

$$Z_{ki}Z_{ij} + Z_{jk}Z_{ki} + Z_{ij}Z_{jk} = \Gamma, \tag{4.5}$$

which can be derived directly from the Gaudin Equations (3.26) to obtain

$$\Lambda_i^2 = -N(N-1)\Gamma + 2\sum_{\alpha=1}^{N} Z_{\alpha i}\sum_{\beta\neq\alpha}^{N} Z_{\beta_\alpha} + \sum_{\alpha=1}^{N} Z_{i\alpha}^2. \tag{4.6}$$

So far, we have only made use of the Gaudin algebra to rewrite Λ_i^2. To make the connection with the Bethe ansatz we will use equation (3.42) to get rid of $\sum_{\beta\neq\alpha}^{N} Z_{\beta_\alpha}$

$$\Lambda_i^2 = -N(N-1)\Gamma + 2\sum_{\alpha=1}^{N} Z_{\alpha i}(\frac{1}{g} + \sum_{k=1}^{L} d_k Z_{k\alpha}) + \sum_{\alpha=1}^{N} Z_{i\alpha}^2. \tag{4.7}$$

If we now again use equation 4.5, we finally obtain

$$\Lambda_i^2 = N(\sum_{k\neq i}^{L} 2d_k - N + 1)\Gamma - \frac{2}{g}\Lambda_i + 2\sum_{k=1}^{L} d_k Z_{ki}(\Lambda_k - \Lambda_i) + (1-2d_i)\sum_{\alpha=1}^{N} Z_{i\alpha}^2. \tag{4.8}$$

This is in general not a closed set of equations in Λ_i, because of the $Z_{i\alpha}$ in the last term the expression still depends explicitly on the rapidities. Fortunately, for the case where all levels are doubly degenerate, $d_i = \frac{1}{2}$, the last term drops out and we obtain

$$\Lambda_i^2 = N(L-N)\Gamma - \frac{2}{g}\Lambda_i + \sum_{k=1}^{L} Z_{ki}(\Lambda_k - \Lambda_i). \tag{4.9}$$

This is the set of equations we have to solve numerically. In Appendix C we discuss a numerical method to solve this set of equations. To apply the method, we need a suitable initial guess and the Jacobian of this set of equations. We will now explain how these can be obtained.

4.2.1 A suitable initial guess

One possible solution method would be to start from a system for which the solution is explicitly known and to gradually deform this system until the desired model is obtained. At each step of this path, the solution of the previous step can be used as initial guess for the Newton-Raphson algorithm at the current step. Here, this will be done starting from the weak-coupling limit and gradually increasing the coupling strength. If we consider the weak coupling limit, we can propose a series expansion of the eigenvalue based variables to zeroth order

$$\Lambda_i = \frac{\lambda_i^{(-1)}}{g} + \lambda_i^{(0)} + O(g). \tag{4.10}$$

If we plug this expansion in (4.9), we find

$$\lambda_i^{(-1)} = 0 \quad \text{or} \quad -2 \tag{4.11}$$

$$\lambda_i^{(0)} = \frac{1}{\left(2\lambda_i^{(-1)} + 2\right)} \sum_{j\neq i}^{L} Z_{ji}(\lambda_j^{(-1)} - \lambda_i^{(-1)}). \tag{4.12}$$

If we are now interested in the eigenvalue based variables at very weak coupling strength we can use zero as an initial guess and solve this using the Newton-Raphson method. The obtained solution can then serve as an initial guess for the eigenvalue based variables at a slightly stronger coupling strength by taking

$$\Lambda_i|_{g+dg} \approx \Lambda_i|_g + \left.\frac{\partial \Lambda_i}{\partial g}\right|_g dg. \tag{4.13}$$

Repeating this procedure, we can obtain the eigenvalue based variables at any value of the coupling strength. The partial derivative $\frac{\partial \Lambda_i}{\partial g}$ can be obtained by taking the partial derivative to g of equation (4.9). After rewriting this equation, we find

$$(2\Lambda_i + \sum_{k=1}^{L} d_k Z_{ki} + \frac{2}{g})\frac{\partial \Lambda_i}{\partial g} - \sum_{k=1}^{L} d_k Z_{ki} \frac{\partial \Lambda_k}{\partial g} = \frac{2}{g^2}\Lambda_i, \tag{4.14}$$

which is a linear set of equations in $\frac{\partial \Lambda_i}{\partial g}$ and can as such be easily solved. Note that from equation (4.10) it becomes apparent that Λ_i might still exhibit singular behavior in the limit $g \to 0$. It is therefore numerically favorable to solve for the variables $g\Lambda_i$.

4.2.2 Determining the derivatives

From equation (C.4) it is clear that we need to know the Jacobian. This can be done by taking the partial derivatives obtained in equation (4.9). We find

$$J_{ik} = \begin{cases} 2\Lambda_i + \frac{2}{g} + \sum_{k\neq i}^{N} Z_{ki} & \text{if } i = k \\ -Z_{ki} & \text{if } i \neq k \end{cases} \tag{4.15}$$

The Jacobian can thus be easily computed.

4.3 Retrieving the rapidities

Although many physical properties can be computed by relying solely on the eigenvalue based variables [50, 49], it might be useful in certain cases to obtain the rapidities. In this section we discuss how the rapidities can be obtained from the eigenvalue-based values. We will assume that once $Z_{i\alpha}$ is found, x_α can be easily retrieved from this, so that we can focus on finding $Z_{i\alpha}$. We start from equation (4.5) and rewrite it to obtain

$$Z_{i\alpha} = \frac{\Gamma + Z_{ri} Z_{r\alpha}}{Z_{ri} - Z_{r\alpha}}, \tag{4.16}$$

here r refers to an auxiliary single-particle level or an additional rapidity ϵ_r. Once the expression for Z_{ij} is known, we can easily compute Z_{ri}, as we are free to choose ϵ_r. Making the summation over α on both sides, we find

$$\Lambda_i = \sum_{\alpha=1}^{N} Z_{i\alpha} = \sum_{\alpha=1}^{N} \frac{\Gamma - Z_{ri}Z_{r\alpha}}{Z_{ri} - Z_{r\alpha}} \tag{4.17}$$

$$= -NZ_{ri} + (\Gamma + Z_{ri}^2) \sum_{\alpha=1}^{N} \frac{1}{Z_{ri} - Z_{r\alpha}}. \tag{4.18}$$

Next, we define a polynomial with the full set of $Z_{i\alpha}$ ($\alpha = 1, .., N$) as its roots

$$P(z) = \prod_{\alpha=1}^{N} (z - Z_{r\alpha}) = \sum_{k=0}^{N} P_{N-k} z^k. \tag{4.19}$$

The idea is that if we can find the coefficients P_{N-k}, we only have to solve for the roots of a polynomial to obtain the $Z_{i\alpha}$'s. An expression for the coefficients P_{N-k} can be found by noting that

$$\frac{P'(z)}{P(z)} = \frac{\sum_{k=0}^{N} k P_{N-k} z^{k-1}}{\sum_{k=0}^{N} P_{N-k} z^k} = \sum_{\alpha=1}^{N} \frac{1}{z - Z_{r\alpha}} \tag{4.20}$$

so that for $z = Z_{ri}$, we get

$$\frac{P'(Z_{ri})}{P(Z_{ri})} = \frac{\Lambda_i + NZ_{ri}}{\Gamma + Z_{ri}^2}. \tag{4.21}$$

Writing the polynomials out in series expansion, we find the following m relations for the coefficients

$$\sum_{k=0}^{N-1} P_{N-k} \left[k\Gamma Z_{ri}^{k-1} - \Lambda Z_{ri}^k + (k-N) Z_{ri}^{k+1} \right] = \Lambda_i Z_{ri}^N - N\Gamma Z_{ri}^{N-1}. \tag{4.22}$$

From equation (4.17) it is clear that this set of equations is linearly dependent. As there are only $N < L$ variables to solve for, one should therefore select N of the above equations and solve these. Once the coefficients of the polynomial have been determined, we have to find the roots of this polynomial. Many efficient algorithms to do this have been conceived, for instance Laguerre's method or the Jenkins-Traub algorithm. As such, the rapidities can be determined from the set of eigenvalue-based variables.

Chapter 5

The p+ip model

5.1 Introduction

In this chapter we will examine the factorisable Richardson-Gaudin XXZ model. We will focus on the p-wave pairing that might be found in unconventional superconductors such as Sr_2RuO_4 [51], a material that has structures similar to the cuprates [52], which play a very important role in high temperature superconductivity. This model exhibits a rare third order phase transition [53].
We will start by introducing the $p_x + ip_y$ Hamiltonian and by examining the quantum phase diagram. We will note that at certain values of the coupling strength, called the Moore-Read points, the eigenstates of the system become degenerate. This degeneracy is related to the rapidities becoming zero. In section 5.3 we will derive an expression for the coupling strength to cause Moore-Read points.

5.2 The quantum phase diagram

The Hamiltonian of the system under consideration is given by

$$\hat{H}_{p+ip} = \sum_{k} \frac{|\boldsymbol{k}|^2}{2m} \hat{S}_k^0 + \frac{g}{4m} \sum_{\substack{\boldsymbol{k},\boldsymbol{k}' \\ \boldsymbol{k} \neq \pm \boldsymbol{k}'}}^{L} (k_x + ik_y)(k_x' - ik_y') \hat{S}_k^\dagger \hat{S}_{k'}. \tag{5.1}$$

This system is called the $p_x + ip_y$ model and can be interpreted as describing the coupling of spinless, two-dimensional fermions with momentum $\boldsymbol{k}$ and mass m. Note that this Hamiltonian is particle-number conserving. The quantum phase diagram of this system is shown in Figure 5.1. We see that there are three distinct regimes. The dashed line separates

the weak-coupling BCS regime with the quasi-molecular Bose-Einstein condensate (BEC) regime. There is no phase transition between both regimes, but rather a crossover. The dashed line is called the Moore-Read line. The full line represents the transition between BEC regime and the strong coupling regime. In [53] it is shown that this transition is a third order phase transition, meaning that the third derivative of the energy is discontinuous at this line. The full line is also called the Read-Green line. Note that we will use a different sign convention for the coupling constant, so that in our case the coupling constant would have to be negative in order to have the phase transition.

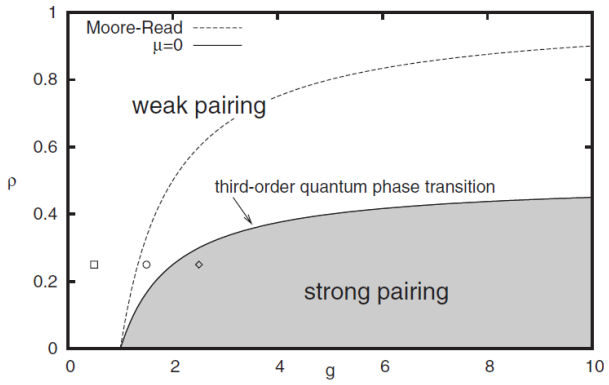

Figure 5.1: The quantum phase diagram of the $p_x + ip_y$ model [53].

5.3 Moore-Read points

Using the machinery outlined in chapter 3, we construct an integrable and factorisable Hamiltonian in subsection 5.3.1. Next, we take a look at what happens when the rapidity becomes zero.

5.3.1 A factorisable Hamiltonian

If we write $\boldsymbol{k} = |k|e^{i\phi}$, the Hamiltonian in equation (5.1) becomes

$$\hat{H}_{p+ip} = \sum_k \frac{|\boldsymbol{k}|^2}{2m}\hat{S}^0_k + \frac{g}{4m}\sum_{\substack{\boldsymbol{k},\boldsymbol{k}'\\ \boldsymbol{k}\neq\pm\boldsymbol{k}'}}^{L} |k|e^{i\phi}|k'|e^{-i\phi'}\hat{S}^\dagger_k\hat{S}_{k'}. \tag{5.2}$$

This suggests the introduction of a new set of operators

$$\tilde{S}^\dagger_i = e^{-i\phi}\hat{S}^\dagger_i, \quad \tilde{S}_i = e^{i\phi}\hat{S}_i, \quad \tilde{S}^0_i = \hat{S}^0_i, \tag{5.3}$$

closing the same quasi-spin algebra as the original set, see equation (3.9). The Hamiltonian becomes

$$\hat{H}_{p+ip} = \sum_k \frac{|\boldsymbol{k}|^2}{2m}\tilde{S}^0_k + \frac{g}{4m}\sum_{\substack{\boldsymbol{k},\boldsymbol{k}'\\ \boldsymbol{k}\neq\pm\boldsymbol{k}'}}^{L} |k||k'|\tilde{S}^\dagger_k\tilde{S}_{k'}. \tag{5.4}$$

This is formally identical to the integrable Hamiltonian

$$\hat{H}_{fact} = \sum_{i=1}^{L}\epsilon_i^2\hat{S}^0_i + g\sum_{\substack{i,k=1\\ k\neq i}}^{L}\epsilon_i\epsilon_k\hat{S}^\dagger_i\hat{S}_k, \tag{5.5}$$

implying that the $p+ip$ Hamiltonian is integrable. It is straightforward to check that the Hamiltonian in equation (5.5) is indeed integrable. Starting from the hyperbolic solutions of the Gaudin equations

$$X_{ij} = g\frac{\epsilon_i\epsilon_j}{\epsilon_i^2-\epsilon_j^2}, \qquad Z_{ij} = g\frac{1}{2}\frac{\epsilon_i^2+\epsilon_j^2}{\epsilon_i^2-\epsilon_j^2}, \tag{5.6}$$

which is a reparametrization of equation (3.31), we can define a set of operators $\hat{R}_i$, as given by equation (3.25). Using these operators we can construct the Hamiltonian

$$\hat{H} = \sum_{i=1}^{L}\epsilon_i^2\hat{R}_i = \sum_{i=1}^{L}\epsilon_i^2\hat{S}^0_i + g\sum_{i,k=1}^{L}\epsilon_i\epsilon_k\hat{S}^\dagger_i\hat{S}_k. \tag{5.7}$$

This is the general pairing Hamiltonian, see equation (3.10), with $V_{ij} = \epsilon_i\epsilon_j$, which explains why this model is called factorisable.

5.3.2 The complex Bethe ansatz wavefunction

If we would blindly use the wavefunction suggested by equation (3.35) and the complex X_{ij} from equation (5.6), we would find

$$|\psi\rangle = \prod_{\alpha=1}^{N}\sum_{i=1}^{L}X_{i\alpha}\hat{S}^\dagger_i|\theta\rangle = \prod_{\alpha=1}^{N}\sum_{i=1}^{L}\frac{\epsilon_i E_\alpha}{|\epsilon_i|^2-E_\alpha}\hat{S}^\dagger_i|\theta\rangle\,, \tag{5.8}$$

with N the number of excitations, which we will also call pairons. However, we are interested in the case where at least one of the rapidities E_α becomes zero. This implies that the ansatz wavefunction will also become zero. Fortunately, we can bring out a factor $(\prod_\alpha E_\alpha)$ and rescale the wavefunction so that said factor can be omitted. The ansatz wavefunction then becomes

$$|\psi\rangle = \prod_{\alpha=1}^{N}\hat{K}^\dagger_\alpha|\theta\rangle\,. \tag{5.9}$$

with

$$\hat{K}_\alpha^\dagger = \sum_{i=1}^{L} \frac{\epsilon_i}{|\epsilon_i|^2 - E_\alpha} \hat{S}_i^\dagger. \tag{5.10}$$

This is the generalized creation operator that will be used throughout this section. Similarly, we can define

$$\hat{K}_\alpha = \sum_{i=1}^{L} \frac{\epsilon_i^*}{|\epsilon_i|^2 - E_\alpha} \hat{S}_i, \qquad \hat{K}_\alpha^0 = \sum_{i=1}^{L} \frac{|\epsilon_i|^2}{|\epsilon_i|^2 - E_\alpha} \hat{S}_i^0. \tag{5.11}$$

Using these operators and proceeding in a similar fashion as outlined in chapter 3, we eventually find that the Richardson-Gaudin equation is given by

$$1 + 2g \sum_i \frac{|\epsilon_i|^2 d_i}{|\epsilon_i|^2 - E_\alpha} - 2g \sum_{\beta \neq \alpha} \frac{E_\beta}{E_\beta - E_\alpha} = 0 \tag{5.12}$$

and the eigenvalues of the Hamiltonian, see equation (5.5),

$$E = \sum_\alpha E_\alpha - \sum_k |\epsilon_k|^2 d_k. \tag{5.13}$$

Hence, we can again loosely interpret the rapidities as the energy of a single pair.

5.3.3 Zero-rapidity condensation

Having done all the preliminaries, we can now examine the circumstances under which at least one of the rapidities can becomes zero. We start by noting that when the rapidity is zero, the Gaudin algebra becomes

$$\hat{K}_0^\dagger = \sum_{i=1}^{L} \frac{\epsilon_i}{|\epsilon_i|^2} \hat{S}_i^\dagger, \quad \hat{K}_0 = \sum_{i=1}^{L} \frac{\epsilon_i^*}{|\epsilon_i|^2} \hat{S}_i, \quad \hat{K}_0^0 = \sum_{i=1}^{L} \frac{\epsilon_i^*}{|\epsilon_i|^2} \hat{S}_i. \tag{5.14}$$

To be as general as possible, we will propose an ansatz state with p zero rapidity pairs and q regular pairs [54]

$$|\psi\rangle = (\hat{K_0^\dagger})^p \prod_{\alpha=1}^{q} \hat{K}_\alpha^\dagger |\theta\rangle . \tag{5.15}$$

Using the same procedure as in section 3.4, we find eventually that the same Richardson-Gaudin equations have to hold as equations (5.12) and a supplementary constraint

$$\frac{1}{g} = 2q + p - 1 - 2\sum_{k=1}^{L} d_k - 1 = 2N - p - L - 1, \tag{5.16}$$

where we imposed $d_k = \frac{1}{2}\ \forall k$ as before. Note that the supplementary constraint is
There are two special cases:
1. $p = 1$, the Read-Green line. In this case there is one pairon with zero rapidity. In Figure 5.1 this corresponds to the full line. To see this, note that in the thermodynamic limit $L \to \infty$, $N/L \to \rho$ and $gL \to G$[1], so from equation (5.16) that we indeed obtain $\rho = \frac{1}{2G} + \frac{1}{2}$.
2. $p = N$, the Moore-Read line. All the pairons have zero rapidity. In Figure 5.1 this corresponds to the dashed line, as in the thermodynamic limit $\rho = \frac{1}{G} + 1$.
Based on equation (5.13), it is clear that when a rapidity becomes zero, two eigenstates will have the same energy, as the non-zero rapidities are the solutions of the same Richardson-Gaudin equations 5.12.

5.4 Dynamics within the p+ip model

In this section we will discuss some elementary insights in the dynamics of the p+ip models. As the Hamiltonian is particle-number conserving, the Hilbert space can be partitioned into subspaces with an equal amount of particles. Each of these subspaces has a different scaling. For instance, the vacuum state is the only state having no particles and therefore the dimension of this subspace will be one regardless of L. For the states with one particle, we have a linear scaling with L. In general for a states with N particles, we have a dimension of $\frac{L!}{N!(L-N)!}$. Especially for the low and high excitation numbers, the favorable scaling allows to investigate the behavior of the subspace for larger L.
If we define

$$\hat{S}^\dagger_{tot} = \sum_{j=1}^{L} \hat{S}^\dagger_j, \quad \hat{S}^0_{tot} = \sum_{j=1}^{L} \hat{S}^0_j, \tag{5.17}$$

we immediately find, due to the number of particles being conserved

$$\langle i(t)|\hat{S}^\dagger_{tot}|i(t)\rangle = 0, \quad \langle i(t)|\hat{S}^0_{tot}|i(t)\rangle = N - \frac{L}{2}. \tag{5.18}$$

The state $|i(t)\rangle$ denotes a time-evolved direct product state. For the single orbitals we still have that

$$\langle i(t)|\hat{S}^\dagger_j|i(t)\rangle = 0, \tag{5.19}$$

but the expectation value of $\hat{S}^0_j$ with respect to a direct product state is no longer trivial, except for the vacuum ($=\langle\downarrow\cdots\downarrow|\hat{S}^\dagger_j|\downarrow\cdots\downarrow\rangle - \frac{1}{2}$) and the completely filled state

[1]The g in the figure is our $-G$.

$(=\langle\uparrow\cdots\uparrow|\hat{S}_j^\dagger|\uparrow\cdots\uparrow\rangle = \frac{1}{2})$. In Figure 5.2 the behavior of $\langle i(t)|\hat{S}_{tot}^0|i(t)\rangle$ is shown for a direct product state with one excitation. In the next chapter, we will discuss a method to break the particle-number conservation of the model and show how this leads to much more complicated dynamics.

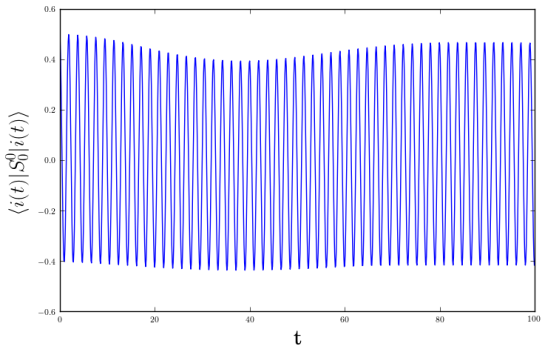

(a) $g = 1.2$

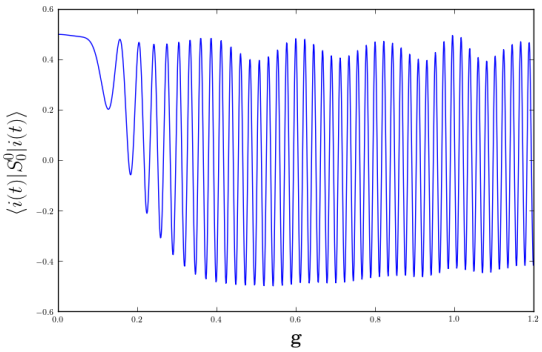

(b) $t = 100$

Figure 5.2: The expectation value of $\hat{S}_8^0$, with respect to $|\downarrow\downarrow\downarrow\downarrow\downarrow\downarrow\downarrow\downarrow\uparrow\rangle$ as a function of time and the coupling strength. The used parameters are $L = 8$ and $\epsilon_i = i$

Chapter 6

RG models interacting with a bath

In this chapter, we will introduce some recently discovered Richardson-Gaudin models for which the particle number is not conserved [55, 56]. This can be interpreted as a system exchanging particles with an environment, similar to the additional interactions we introduced in the harmonic oscillator. We will first introduce the model and derive some important formulas for the expectation values of relevant operators. Next, we will numerically investigate the time evolution of these expectation values. More concretely, we are interested in how the system evolves through time if we start from direct product state at $t = 0$. We thus perform a quantum quench from a non-interacting system to an interacting one. The kind of dissipation we will introduce is exactly the same as the one we have discussed for the harmonic oscillator in subsection 2.1.3.

6.1 Introducing interaction with a bath

In this section we wish to derive the integrability equations for an XXZ model interacting with a bath. The effect of the bath will be approximated by allowing particle exchange and as such we want to consider non-number conserving Hamiltonians. We will proceed in a similar fashion as we did for the regular Richardson-Gaudin models. Starting from the same set of operators

$$R_i = \sum_{\alpha=1}^{3} A_i^\alpha \hat{S}^\alpha + g \sum_{k\neq i}^{n} \sum_{\alpha=1}^{3} X_{ik}^\alpha \hat{S}_i^\alpha S_k^\alpha, \tag{6.1}$$

there are two important differences from the derivation given in section 3.3. Firstly, since we want interaction with an environment, we will would like to retain the terms that are linear in the creation and annihilation operators. This method of coupling the system to a

bath is completely analogous to what we have done for the harmonic oscillator. We have that at least one of the following equations should hold

$$A_i^2 \neq 0, \qquad A_i^1 \neq 0. \tag{6.2}$$

Secondly, we will restrict the discussion to spin $\frac{1}{2}$ particles. In this case, we can make use of the following relation

$$\hat{S}_i^\alpha \hat{S}_i^\beta = \frac{i}{2}\sum_\gamma \epsilon_{\alpha\beta\gamma}\hat{S}_i^\gamma + \frac{1}{4}\delta_{\alpha\beta} I, \tag{6.3}$$

with $\epsilon_{\alpha\beta\gamma}$ the Levi-Civita symbol. Demanding that all operators $\hat{R}_i$ commute mutually and making use of (6.3), we eventually find that following relations should hold [57]

$$A_i^\alpha X_{ji}^\beta + A_j^\alpha X_{ij}^\gamma = 0, \tag{6.4}$$

$$-X_{ik}^\gamma X_{ji}^\beta - X_{jk}^\gamma X_{ij}^\alpha + X_{ik}^\alpha X_{jk}^\beta = 0, \tag{6.5}$$

with $\alpha \neq \beta \neq \gamma$. This can be compared to the previous derivation, see section 3.3, where the restriction to spin $\frac{1}{2}$ relaxes the integrability conditions. As we are considering the XXZ model, we take $X_{ij}^1 = X_{ij}^2 = X_{ij}$ and $X_{ij}^3 = Z_{ij}$. Solving the equations (6.4), we find that by putting $A_i^3 = 1$ we have

$$A_i^1 = g^2\frac{(\gamma-\lambda)^2}{2}A_i, \quad A_i^2 = g^2\frac{(\lambda-\gamma)^2}{2}A_i. \tag{6.6}$$

From the equations (6.5), we then have

$$X_{ik} = \frac{A_i A_k}{\epsilon_i^2 - \epsilon_k^2}, \quad Z_{ik} = \frac{A_i^2}{\epsilon_i^2 - \epsilon_k^2}, \tag{6.7}$$

$$(A_i)^2 = c\epsilon_i^2 + d, \tag{6.8}$$

with λ, γ, c and d possibly complex numbers. In what follows, we set $d = 0$ and $c = 1$ to formally obtain the following set of operators

$$\hat{R}_i = \left(\hat{S}_i^0 + \frac{1}{2}\right) + g\gamma\epsilon_i\hat{S}_i^\dagger - g\lambda\epsilon_i\hat{S}_i + g\sum_{k\neq i}\left[\frac{\epsilon_i\epsilon_k}{\epsilon_i^2-\epsilon_k^2}(\hat{S}_i^\dagger\hat{S}_k + \hat{S}_i\hat{S}_k^\dagger) + \frac{2\epsilon_i^2}{\epsilon_i^2-\epsilon_k^2}(\hat{S}_i^0\hat{S}_k^0 - \frac{1}{4})\right], \tag{6.9}$$

where we have added an extra term $\frac{1}{2} - g\frac{1}{4}\sum_{k\neq i}\frac{2\epsilon_i^2}{\epsilon_i^2-\epsilon_k^2}$ for convenience. This set of operators was first introduced by Lukyanenko *etal.* [55], who proved the integrability through the boundary quantum inverse scattering matrix. Recalling the general form of a pairing

Hamiltonian, see equation (3.10), we would like to obtain a factorisable interaction of the kind $V_{ij} = z_i z_j$, with $z_i = \epsilon_i^{-1}$ We can construct such a Hamiltonian by taking a suitable linear combination

$$\begin{aligned}\hat{H} &= \sum_{i=1} z_i^2 \hat{R}_i \\ &= \sum_{i=1} z_i^2 \left(\hat{S}_i^0 + \frac{1}{2}\right) + g\gamma z_i \hat{S}_i^\dagger - g\lambda z_i \hat{S}_i + g \sum_{k\neq i} z_i z_k \hat{S}_i^\dagger \hat{S}_k. \end{aligned} \tag{6.10}$$

6.2 The Bethe Ansatz

We will use a wavefunction ansatz of the form

$$|\psi\rangle = \prod_{\alpha=1}^{L} \hat{S}_\alpha^\dagger \, |\downarrow \cdots \downarrow\rangle \,, \tag{6.11}$$

with the generalized creation operator given by [56].

$$\hat{S}_\alpha^\dagger = \lambda + \sum_{k=1}^{L} \frac{\epsilon_k}{\epsilon_k^2 - v_\alpha^2} \hat{S}_k^\dagger. \tag{6.12}$$

This can be compared to the non-hermitian harmonic oscillator, where the presence of the non-number conserving interaction terms also shifted the creation and annihilation operators by a constant (2.63). Note that equation (6.11) is different from equation (3.35), because the former contains L pairons instead of N. We now demand that $|\psi\rangle$ is an eigenfunction of $\hat{R}_i$ in a similar fashion as before. We find that this is the case if

$$(1+g) - g\sum_{j=1}^{L} \frac{v_\alpha^2}{v_\alpha^2 - \epsilon_j^2} + 2g \sum_{\beta\neq\alpha} \frac{v_\alpha^2}{v_\alpha^2 - v_\beta^2} = g\gamma\lambda \frac{\prod_{j=1}^{L}(v_\alpha^2 - \epsilon_j^2)}{\prod_{j=1}^{L}(v_\alpha^2 - v_\beta^2)}, \tag{6.13}$$

this expression was also obtained in [55]. The eigenvalues are then given by[1]

$$gr_i = -g \sum_{\alpha=1}^{L} \frac{\epsilon_i^2}{\epsilon_i^2 - v_\alpha^2}. \tag{6.14}$$

As we will also need the dual states, we give the necessary formulas here as well. We will denote dual states with the greek indices μ and κ. The generalized annihilation operator is given by

$$\hat{S}_\mu = \gamma + \sum_{k=1}^{L} \frac{\epsilon_k}{\epsilon_k^2 - v_\mu^2} \hat{S}_k \tag{6.15}$$

[1] We choose to define the eigenvalues as gr_i rather than r_i for notational convenience.

and the wavefunction ansatz is given by

$$\langle\psi| = \langle\uparrow\cdots\uparrow| \prod_{\mu=1} \hat{S}^{\dagger}_{\mu}. \tag{6.16}$$

The resulting eigenvalues become

$$r_i = \frac{1}{g} - \sum_{\mu=1}^{L} \frac{\epsilon_i^2}{\epsilon_i^2 - v_\mu^2} \tag{6.17}$$

if the dual Richardson-Gaudin equations are satisfied

$$(1-g) + g\sum_{j=1}^{L} \frac{v_\mu^2}{v_\mu^2 - \epsilon_j^2} - 2g \sum_{\kappa\neq\mu} \frac{v_\mu^2}{v_\mu^2 - v_\kappa^2} = -g\gamma\lambda \frac{\prod_{j=1}^{L}(v_\alpha^2 - \epsilon_j^2)}{\prod_{\kappa\neq\mu}^{L}(v_\mu^2 - v_\kappa^2)}. \tag{6.18}$$

As the dual state represents the same physical state, the eigenvalues should be the same. From this we immediately get that

$$\Lambda_i^{dual} = \Lambda_i + \frac{1}{g\epsilon_i^2}, \tag{6.19}$$

where we have again introduced the eigenvalue-based variables

$$\Lambda_i = \sum_{\alpha=1}^{L} \frac{1}{\epsilon_i^2 - v_\alpha^2} \quad \text{and} \quad \Lambda_i^{dual} = \sum_{\mu=1}^{L} \frac{1}{\epsilon_i^2 - v_\mu^2}. \tag{6.20}$$

Just as for the regular RG model it is possible to rewrite the Richardson-Gaudin equation as a closed set of equations in terms of these variables. After a rather long calculation, we get

$$g\epsilon_i\Lambda_i^2 = -\Lambda_i + g\sum_{j\neq i} \frac{\epsilon_i^2\Lambda_i - \epsilon_j^2\Lambda_j}{\epsilon_i^2 - \epsilon_j^2} - g\gamma\lambda. \tag{6.21}$$

6.3 Derivation of the expectation values

We would like to analyze the dynamics of the XXZ models introduced in previous section. To do this, we will look at the overlap of the eigenstate with much more familiar direct product states, denoted as $|\uparrow\cdots\downarrow\rangle$. Once we know this overlap, it is straightforward to compute the time evolution of matrix elements such as $\langle\uparrow\cdots\uparrow|\hat{S}_i^{\dagger}|\uparrow\cdots\uparrow\rangle$ and $\langle\uparrow\cdots\uparrow|\hat{S}_i^{0}|\uparrow\cdots\uparrow\rangle$. The first expectation value reveals important information on the interaction between states with a different number of excitations and the second expectation value tells about the occupancy of the state.

6.3.1 Overlap of the eigenstates with a direct product state

As presented before, an eigenstate of the system is given by

$$|\{v_\alpha\}\rangle = \prod_{\alpha=1}^{L}(\lambda + \sum_{k=1}^{L}\frac{\epsilon_k}{\epsilon_k^2 - v_\alpha^2}\hat{S}_k^\dagger)\,|\downarrow\cdots\downarrow\rangle\,, \tag{6.22}$$

whereas a direct product state with N excitations is labeled as

$$|\{i_a\}\rangle = \prod_{a=1}^{N}\hat{S}_{i_a}^\dagger\,|\downarrow\cdots\downarrow\rangle\,. \tag{6.23}$$

Where the excited states are labeled as $\{i_a\}$. We start by noting that, as the direct product states are orthogonal, only the terms in $|\{v_\alpha\}\rangle$ that are proportional to $|\{i_a\}\rangle$ will be non-zero. Therefore, it is easy to see that the overlap can be written as

$$\langle\{i_a\}|\{v_\alpha\}\rangle = \frac{\lambda^{L-N}}{(L-N)!}\mathrm{per}\begin{pmatrix} \lambda & \cdots & \lambda & \frac{\epsilon_{1_a}}{\epsilon_{1_a}^2 - v_1^2} & \cdots & \frac{\epsilon_{N_a}}{\epsilon_{N_a}^2 - v_1^2} \\ \lambda & \cdots & \lambda & \frac{\epsilon_{1_a}}{\epsilon_{1_a}^2 - v_2^2} & \cdots & \frac{\epsilon_{N_a}}{\epsilon_{N_a}^2 - v_2^2} \\ \vdots & \cdots & \vdots & \vdots & \cdots & \vdots \\ \lambda & \cdots & \lambda & \frac{\epsilon_{1_a}}{\epsilon_{1_a}^2 - v_L^2} & \cdots & \frac{\epsilon_{N_a}}{\epsilon_{N_a}^2 - v_L^2} \end{pmatrix}, \tag{6.24}$$

where the columns only contain those single particle energies that are excited in $|\{i_a\}\rangle$. The per stands for the permanent of the matrix, which differs from the determinant in that the signature of the permutations are not taken into account. Calculating the permanent of a matrix is a computationally intensive task, since it scales exponentially with the matrix size [58]. This is because, unlike for the determinant which is invariant under certain algebraic transformations, one can not use algebraic manipulations to make the computation easier. Fortunately, we can rewrite this particular permanent as a determinant to reduce the complexity of the calculation. One can prove that equation (6.24) can be rewritten as [50, 56]

$$\langle\{i_a\}|\{v_\alpha\}\rangle = \lambda^{L-N}\prod_{j=1}^{N}\epsilon_{j_a}\det J^{a\beta}, \tag{6.25}$$

with J given by

$$\begin{aligned} J_{ij}^{a\beta} &= \begin{cases} \sum_{\beta=1}^{L}\frac{1}{\epsilon_{i_a}^2 - v_\beta^2} - \sum_{j\neq i}^{N}\frac{1}{\epsilon_{i_a}^2 - \epsilon_{j_a}^2} & \text{if } i = j \\ \frac{1}{\epsilon_{i_a}^2 - \epsilon_{j_a}^2} & \text{if } i \neq j \end{cases} \\ &= \begin{cases} \Lambda_i^\beta - \sum_{j\neq i}^{N}\frac{1}{\epsilon_{i_a}^2 - \epsilon_{j_a}^2} & \text{if } i = j \\ \frac{1}{\epsilon_{i_a}^2 - \epsilon_{j_a}^2} & \text{if } i \neq j \end{cases} \end{aligned} \tag{6.26}$$

We have thus succeeded in finding a computationally efficient way of finding the overlap of a direct product state with an eigenstate. In the following subsection, we will use Greek letters to label the eigenstates and Greek letters with a prime to label the dual eigenstates.

6.3.2 Normalization

The eigenstates we used in the previous section were not yet normalized. We will describe the procedure for the normalization in this subsection. We introduce the notations $|\{v_\alpha\}\rangle_N = N_\alpha |\{v_\alpha\}\rangle$, with $|\{v_\alpha\}\rangle_N$ the normalized ket. Similarly, we write $|\{v_{\mu'}\}\rangle_N = N_{\mu'} |\{v_{\mu'}\}\rangle$. We clearly have that

$$\frac{\langle\{i_a\}|\{v_\alpha\}\rangle}{\langle\{i_a\}|\{v_{\mu'}\}\rangle} = \frac{N_\alpha}{N_{\mu'}}, \tag{6.27}$$

with $\langle\{i_a\}|$ an arbitrary direct product state. Using a similar reasoning as for the overlaps, we also have that

$$
\begin{aligned}
N^*_{\alpha'} N_\alpha &= \langle\{v_{\alpha'}\}|\{v_\alpha\}\rangle \qquad (6.28)\\
&= \langle\uparrow \dots \uparrow | \prod_{\alpha'=1}^{L} (-\gamma^* + \sum_{k=1}^{L} \frac{\epsilon_k \hat{S}_k^\dagger}{\epsilon_k^2 - v_{\alpha'}^2}) \prod_{\alpha=1}^{L} (\lambda + \sum_{j=1}^{L} \frac{\epsilon_j \hat{S}_j^\dagger}{\epsilon_j^2 - v_\alpha^2}) | \downarrow \dots \downarrow\rangle \\
&= \frac{1}{L!} \mathrm{per} \begin{pmatrix}
\lambda & \cdots & \lambda & \frac{\epsilon_1}{\epsilon_1^2 - v_1^2} & \cdots & \frac{\epsilon_L}{\epsilon_L^2 - v_1^2} \\
\lambda & \cdots & \lambda & \frac{\epsilon_1}{\epsilon_1^2 - v_2^2} & \cdots & \frac{\epsilon_L}{\epsilon_L^2 - v_2^2} \\
\vdots & \cdots & \vdots & \vdots & \cdots & \vdots \\
\lambda & \cdots & \lambda & \frac{\epsilon_1}{\epsilon_1^2 - v_L^2} & \cdots & \frac{\epsilon_L}{\epsilon_L^2 - v_L^2} \\
-\gamma^* & \cdots & -\gamma^* & \frac{\epsilon_1}{\epsilon_1^2 - v_1'^2} & \cdots & \frac{\epsilon_L}{\epsilon_L^2 - v_1'^2} \\
-\gamma^* & \cdots & -\gamma^* & \frac{\epsilon_1}{\epsilon_1^2 - v_1'^2} & \cdots & \frac{\epsilon_L}{\epsilon_L^2 - v_1'^2} \\
\vdots & \cdots & \vdots & \vdots & \cdots & \vdots \\
-\gamma^* & \cdots & -\gamma^* & \frac{\epsilon_1}{\epsilon_1^2 - v_L'^2} & \cdots & \frac{\epsilon_L}{\epsilon_L^2 - v_L'^2}
\end{pmatrix} \\
&= \frac{\left(\prod_j^L \epsilon_j\right) \lambda^L}{L!} \mathrm{per} \begin{pmatrix}
1 & \cdots & 1 & \frac{1}{\epsilon_1^2 - v_1^2} & \cdots & \frac{1}{\epsilon_N^2 - v_1^2} \\
1 & \cdots & 1 & \frac{1}{\epsilon_1^2 - v_2^2} & \cdots & \frac{1}{\epsilon_N^2 - v_2^2} \\
\vdots & \cdots & \vdots & \vdots & \cdots & \vdots \\
1 & \cdots & 1 & \frac{1}{\epsilon_1^2 - v_L^2} & \cdots & \frac{1}{\epsilon_N^2 - v_L^2} \\
1 & \cdots & 1 & \frac{1}{\epsilon_1^2 - v_1'^2} & \cdots & \frac{1}{\epsilon_N^2 - v_1'^2} \\
1 & \cdots & 1 & \frac{1}{\epsilon_1^2 - v_1'^2} & \cdots & \frac{1}{\epsilon_N^2 - v_1'^2} \\
\vdots & \cdots & \vdots & \vdots & \cdots & \vdots \\
1 & \cdots & 1 & \frac{1}{\epsilon_1^2 - v_L'^2} & \cdots & \frac{1}{\epsilon_N^2 - v_L'^2}
\end{pmatrix} \\
&= \left(\prod_j^L \epsilon_j\right) \lambda^L \det J \qquad (6.29)
\end{aligned}
$$

with

$$
\begin{aligned}
J_{ab}^\alpha &= \begin{cases} \sum_{\kappa=\beta'\cup\beta} \frac{1}{\epsilon_a^2 - v_\kappa^2} - \sum_{k\neq a}^N \frac{1}{\epsilon_a^2 - \epsilon_k^2} & \text{if } a = b \\ \frac{1}{\epsilon_a^2 - \epsilon_b^2} & \text{if } a \neq b \end{cases} \\
&= \begin{cases} 2\Lambda_a^\beta + \frac{\alpha}{\epsilon_a^2} - \sum_{j\neq a}^N \frac{1}{\epsilon_a^2 - \epsilon_j^2} & \text{if } a = b \\ \frac{1}{\epsilon_a^2 - \epsilon_b^2} & \text{if } a \neq b \end{cases}
\end{aligned} \qquad (6.30)
$$

In equation(6.29), we have imposed that $\gamma = -\lambda^*$, which is equivalent with demanding that the Hamiltonian be hermitian. From equations (6.27) and (6.28) it is now possible to

derive the Normalization constants. Note that only the amplitude of these constants are fixed, so that the phase factor can be freely chosen.

6.3.3 Expectation value of $\hat{S}_i^\dagger$

In this section we wish to investigate how $\langle\{i_a\}(t)|\hat{S}_i^\dagger|\{i_a\}(t)\rangle$ evolves through time. We will follow a similar approach as in [56]. We start by introducing completeness relations to get rid of the time dependency within the brakets such that

$$|\{i_a\}(t)\rangle = e^{-\frac{i\hat{H}t}{\hbar}}|\{i_a\}\rangle = \sum_\alpha e^{-\frac{iE_\alpha t}{\hbar}}\langle\{v_\alpha\}|\{i_a\}\rangle \tag{6.31}$$

$$\langle\{i_a\}(t)|\hat{S}_i^\dagger|\{i_a\}(t)\rangle = \sum_{\mu',\beta}\exp i(E_{\mu'}-E_\beta)t\,\langle\{i_a\}|x_{\mu'}\rangle\langle x_{\mu'}|\hat{S}_i^\dagger|x_\beta\rangle\langle x_\beta|\{i_a\}\rangle\,. \tag{6.32}$$

From the previous subsection it is easy to see that the last factor is given by

$$\langle\{v_\alpha\}|\{i_a\}\rangle = (\lambda^*)^{L-N}\left(\prod_{j=1}^{N}\epsilon_{j_a}\right)\det J^{\alpha a} \tag{6.33}$$

with

$$J_{ij}^{\alpha a} = \begin{cases}\Lambda_i^\beta - \sum_{j\neq i}^{N}\frac{1}{\epsilon_{i_a}^2-\epsilon_{j_a}^2} & \text{if } i=j\\ \frac{1}{\epsilon_{i_a}^2-\epsilon_{j_a}^2} & \text{if } i\neq j\end{cases} \tag{6.34}$$

For the overlap of a braket and a dual eigenstate we can derive in a completely similar fashion that

$$\langle\{i_a\}|\{v_{\mu'}\}\rangle = (-\gamma)^N\left(\prod_{j\not\subset i_a}\epsilon_j\right)\det J^{a\mu'} \tag{6.35}$$

with

$$J_{ij}^{a\mu'} = \begin{cases}\Lambda_i^{\mu'} + \frac{\alpha}{\epsilon_{i_a}^2} - \sum_{j\neq i}^{L-N}\frac{1}{\epsilon_{i_a}^2-\epsilon_{j_a}^2} & \text{if } i=j\\ \frac{1}{\epsilon_{i_a}^2-\epsilon_{j_a}^2} & \text{if } i\neq j\end{cases} \tag{6.36}$$

where α is the coefficient in front of $\hat{S}^0$ in the operators $\hat{R}_i$. Using the same kind of combinatorics as we used to derive the overlap, we can derive an expression for

$$\begin{aligned}
\langle\{v_{\mu'}\}|\hat{S}_i^\dagger|\{v_\beta\}\rangle &= \langle\uparrow ... \uparrow | \prod_{\mu'=1}^{L}(-\gamma^* + \sum_{k=1}^{L}\frac{\epsilon_k \hat{S}_k^\dagger}{\epsilon_k^2 - v_{\mu'}^2}) \prod_{\beta=1}^{L}(\lambda + \sum_{j=1}^{L}\frac{\epsilon_j \hat{S}_j^\dagger}{\epsilon_j^2 - v_\beta^2})\hat{S}_i^\dagger | \downarrow ... \downarrow\rangle \\
&= \langle\uparrow ... \uparrow | \prod_{\mu'=1}^{L}(-\gamma^* + \sum_{k=1}^{L}\frac{\epsilon_k}{\epsilon_k^2 - v_{\mu'}^2}) \prod_{\beta=1}^{L}(\lambda + \sum_{j=1}^{L}\frac{\epsilon_j}{\epsilon_j^2 - v_\beta^2})| \downarrow ... \uparrow_i ... \downarrow\rangle \\
&= \frac{1}{(L+1)!}\mathrm{per}\begin{pmatrix}
\lambda & \cdots & \lambda & \frac{\epsilon_1}{\epsilon_1^2-v_1^2} & \cdots & \frac{\epsilon_L}{\epsilon_L^2-v_1^2} \\
\lambda & \cdots & \lambda & \frac{\epsilon_1}{\epsilon_1^2-v_2^2} & \cdots & \frac{\epsilon_L}{\epsilon_L^2-v_2^2} \\
\vdots & \cdots & \vdots & \vdots & \cdots & \vdots \\
\lambda & \cdots & \lambda & \frac{\epsilon_1}{\epsilon_1^2-v_L^2} & \cdots & \frac{\epsilon_L}{\epsilon_L^2-v_L^2} \\
-\gamma^* & \cdots & -\gamma^* & \frac{\epsilon_1}{\epsilon_1^2-v_1'^2} & \cdots & \frac{\epsilon_L}{\epsilon_L^2-v_1'^2} \\
-\gamma^* & \cdots & -\gamma^* & \frac{\epsilon_1}{\epsilon_1^2-v_1'^2} & \cdots & \frac{\epsilon_L}{\epsilon_L^2-v_1'^2} \\
\vdots & \cdots & \vdots & \vdots & \cdots & \vdots \\
-\gamma^* & \cdots & -\gamma^* & \frac{\epsilon_1}{\epsilon_1^2-v_L'^2} & \cdots & \frac{\epsilon_L}{\epsilon_L^2-v_L'^2}
\end{pmatrix} \\
&= \frac{(\prod_{a\neq i}\epsilon_a)\lambda^{L+1}}{(L+1)!}\mathrm{per}\begin{pmatrix}
1 & \cdots & 1 & \frac{1}{\epsilon_1^2-v_1^2} & \cdots & \frac{1}{\epsilon_N^2-v_1^2} \\
1 & \cdots & 1 & \frac{1}{\epsilon_1^2-v_2^2} & \cdots & \frac{1}{\epsilon_L^2-v_2^2} \\
\vdots & \cdots & \vdots & \vdots & \cdots & \vdots \\
1 & \cdots & 1 & \frac{1}{\epsilon_1^2-v_L^2} & \cdots & \frac{1}{\epsilon_L^2-v_L^2} \\
1 & \cdots & 1 & \frac{1}{\epsilon_1^2-v_1'^2} & \cdots & \frac{1}{\epsilon_L^2-v_1'^2} \\
1 & \cdots & 1 & \frac{1}{\epsilon_1^2-v_1'^2} & \cdots & \frac{1}{\epsilon_L^2-v_1'^2} \\
\vdots & \cdots & \vdots & \vdots & \cdots & \vdots \\
1 & \cdots & 1 & \frac{1}{\epsilon_1^2-v_L'^2} & \cdots & \frac{1}{\epsilon_L^2-v_L'^2}
\end{pmatrix} \\
&= (\prod_{a\neq i}\epsilon_a)\lambda^{L+1}\det J^{\mu'\beta}, \qquad (6.37)
\end{aligned}$$

where $\lambda = -\gamma^*$ was again imposed. Here the matrix J is given by

$$\begin{aligned}
J_{ab}^{\mu'\beta} &= \begin{cases} \sum_{\kappa=\mu'\cup\beta}\frac{1}{\epsilon_a^2-v_\kappa^2} - \sum_{j\neq a, j\neq i}^{N}\frac{1}{\epsilon_a^2-\epsilon_j^2} & \text{If } a = b \\ \frac{1}{\epsilon_a^2-\epsilon_b^2} & \text{If } a \neq b \end{cases} \\
&= \begin{cases} \Lambda_a^\beta + \Lambda_a^{\mu'} + \frac{\alpha}{\epsilon_a^2} - \sum_{j\neq a, j\neq i}^{N}\frac{1}{\epsilon_a^2-\epsilon_j^2} & \text{If } a = b \\ \frac{1}{\epsilon_a^2-\epsilon_b^2} & \text{If } a \neq b \end{cases} \qquad (6.38)
\end{aligned}$$

and $a, b \neq i$. All terms in this summation can be efficiently calculated within the eigenvalue-based formalism.

6.3.4 Expectation value of $\hat{S}_i^0$

In this section we will derive an expression for the time evolution of $\langle\{i_a\}(t)|\hat{S}_i^0|\{i_a\}(t)\rangle$.Before starting the derivation, we will introduce a rescaled version of $\hat{R}_i$, see equation (6.9), to simplify the notations in this section

$$\hat{R}_i' = \frac{\hat{R}_i}{g} = \alpha\left(\hat{S}_i^0 + \frac{1}{2}\right) + \gamma\epsilon_i\hat{S}_i^\dagger - \lambda\epsilon_i\hat{S}_i + \sum_{k\neq i}\left[\frac{\epsilon_i\epsilon_k}{\epsilon_i^2-\epsilon_k^2}(\hat{S}_i^\dagger\hat{S}_k + \hat{S}_i\hat{S}_k^\dagger) + \frac{2\epsilon_i^2}{\epsilon_i^2-\epsilon_k^2}(\hat{S}_i^0\hat{S}_k^0 - \frac{1}{4})\right], \tag{6.39}$$

with $\alpha = \frac{1}{g}$.
By introducing completeness relations we obtain a similar equation as in (6.32). The starting point for the derivation will be $\langle x_{\mu'}(\alpha)|\hat{S}_i^0|x_\beta(\alpha+d\alpha)\rangle$, which can rewriting using the observation that $\frac{\partial\hat{R}_i'}{\partial\alpha} = \hat{S}_i^0 + \frac{1}{2}$, yielding

$$\begin{aligned}\langle\{v_{\mu'}\}(\alpha)|\hat{S}_i^0 + \frac{1}{2}|\{v_\beta\}(\alpha+d\alpha)\rangle &= \langle\{v_{\mu'}\}(\alpha)|\frac{\partial\hat{R}_i'}{\partial\alpha}|\{v_\beta\}(\alpha+d\alpha)\rangle \\ &= \langle\{v_{\mu'}\}(\alpha)|\frac{\hat{R}_i'(\alpha+d\alpha)-\hat{R}_i'(\alpha)}{d\alpha}|\{v_\beta\}(\alpha+d\alpha)\rangle \\ &= (r_i^\beta(\alpha+d\alpha) - r_i^{\mu'}(\alpha))\frac{\langle\{v_{\mu'}\}(\alpha)|\{v_\beta\}(\alpha+d\alpha)\rangle}{d\alpha}.\end{aligned} \tag{6.40}$$

In order to further simplify the expression, we will have to make a distinction between the diagonal and the off-diagonal elements.

Diagonal elements

From the previous section we know that we can write the eigenvalues in terms of the eigenvalue based variables as $r_i^\beta = -\epsilon_i^2\Lambda_i^\beta$. We now Taylor expand $r_i^\beta(\alpha+d\alpha)$ in equation (6.40) to the first order and make use of the continuity of the scalar product to obtain

$$\begin{aligned}\langle\{v_{\beta'}\}(\alpha)|\hat{S}_i^0|\{v_\beta\}(\alpha)\rangle &= \frac{\partial r_i}{\partial\alpha}\langle\{v_{\beta'}\}(\alpha)|\{v_\beta\}(\alpha)\rangle \\ &= -\epsilon_i^2\frac{\partial\Lambda_i^\beta}{\partial\alpha}\langle\{v_{\beta'}\}(\alpha)|\{v_\beta\}(\alpha)\rangle\,.\end{aligned} \tag{6.41}$$

This can be rewritten as

$$\frac{\langle\{v_{\beta'}\}(\alpha)|\hat{S}_i^0|\{v_\beta\}(\alpha)\rangle}{\langle\{v_{\beta'}\}(\alpha)|\{v_\beta\}(\alpha)\rangle} = -\epsilon_i^2\frac{\partial\Lambda_i^\beta}{\partial\alpha}. \tag{6.42}$$

It might seem as if little progress has been made, since $\frac{\partial \Lambda_i^\beta}{\partial \alpha}$ is still unknown. However, we will demonstrate later on in this subsection how these partial derivatives can easily be determined.

Off-diagonal elements

To find an expression for the off-diagonal elements, we start by writing the eigenvalues in terms of the eigenvalue based variables

$$\langle \{v_{\mu'}\}(\alpha)|\hat{S}_i^0|\{v_\beta\}(\alpha)\rangle = (\epsilon_i^2 \Lambda_i^\beta(\alpha) - \epsilon_i^2 \Lambda_i^{\mu'}(\alpha)) \frac{\langle \{v_{\mu'}\}(\alpha)|\{v_\beta\}(\alpha + d\alpha)\rangle}{d\alpha}. \tag{6.43}$$

The braket can be rewritten by using the by now usual procedure

$$\begin{aligned}
&\langle \{v_{\mu'}\}(\alpha)|\{v_\beta\}(\alpha + d\alpha)\rangle \\
&= \langle \uparrow ... \uparrow | \prod_{\mu'=1}^{L} \left(-\gamma^* + \sum_{k=1}^{L} \frac{\epsilon_k \hat{S}_k^\dagger}{\epsilon_k^2 - v_{\mu'}^2} \right) \Bigg|_\alpha \prod_{\beta=1}^{L} \left(\lambda + \sum_{j=1}^{L} \frac{\epsilon_j \hat{S}_j^\dagger}{\epsilon_j^2 - v_\beta^2} \right) \Bigg|_{\alpha + d\alpha} | \downarrow ... \downarrow \rangle \\
&= \frac{1}{L!} \mathrm{per} \begin{pmatrix}
\lambda & \cdots & \lambda & \frac{\epsilon_1}{\epsilon_1^2 - v_1^2} & \cdots & \frac{\epsilon_N}{\epsilon_N^2 - v_1^2} \\
\lambda & \cdots & \lambda & \frac{\epsilon_1}{\epsilon_1^2 - v_2^2} & \cdots & \frac{\epsilon_N}{\epsilon_N^2 - v_2^2} \\
\vdots & \cdots & \vdots & \vdots & \cdots & \vdots \\
\lambda & \cdots & \lambda & \frac{\epsilon_1}{\epsilon_1^2 - v_L^2} & \cdots & \frac{\epsilon_N}{\epsilon_N^2 - v_L^2} \\
-\gamma^* & \cdots & -\gamma^* & \frac{\epsilon_1}{\epsilon_1^2 - v_1'^2} & \cdots & \frac{\epsilon_N}{\epsilon_N^2 - v_1'^2} \\
-\gamma^* & \cdots & -\gamma^* & \frac{\epsilon_1}{\epsilon_1^2 - v_1'^2} & \cdots & \frac{\epsilon_N}{\epsilon_N^2 - v_1'^2} \\
\vdots & \cdots & \vdots & \vdots & \cdots & \vdots \\
-\gamma^* & \cdots & -\gamma^* & \frac{\epsilon_1}{\epsilon_1^2 - v_L'^2} & \cdots & \frac{\epsilon_N}{\epsilon_N^2 - v_L'^2}
\end{pmatrix} \\
&= \frac{(\prod_a \epsilon_a)\lambda^L}{L!} \mathrm{per} \begin{pmatrix}
1 & \cdots & 1 & \frac{1}{\epsilon_1^2 - v_1^2} & \cdots & \frac{1}{\epsilon_N^2 - v_1^2} \\
1 & \cdots & 1 & \frac{1}{\epsilon_1^2 - v_2^2} & \cdots & \frac{1}{\epsilon_N^2 - v_2^2} \\
\vdots & \cdots & \vdots & \vdots & \cdots & \vdots \\
1 & \cdots & 1 & \frac{1}{\epsilon_1^2 - v_L^2} & \cdots & \frac{1}{\epsilon_N^2 - v_L^2} \\
1 & \cdots & 1 & \frac{1}{\epsilon_1^2 - v_1'^2} & \cdots & \frac{1}{\epsilon_N^2 - v_1'^2} \\
1 & \cdots & 1 & \frac{1}{\epsilon_1^2 - v_1'^2} & \cdots & \frac{1}{\epsilon_N^2 - v_1'^2} \\
\vdots & \cdots & \vdots & \vdots & \cdots & \vdots \\
1 & \cdots & 1 & \frac{1}{\epsilon_1^2 - v_L'^2} & \cdots & \frac{1}{\epsilon_N^2 - v_L'^2}
\end{pmatrix} \\
&= (\prod_a \epsilon_a)\lambda^L \det J,
\end{aligned} \tag{6.44}$$

with again $\lambda = -\gamma^*$ and with

$$J_{ij}^{\mu'\beta} = \begin{cases} \sum_{\kappa=\mu\cup\beta} \frac{1}{\epsilon_i^2 - v_\kappa^2} - \sum_{k\neq i}^N \frac{1}{\epsilon_i^2-\epsilon_k^2} & \text{if } i = j \\ \frac{1}{\epsilon_i^2-\epsilon_j^2} & \text{if } a \neq b \end{cases}$$
$$= \begin{cases} \Lambda_i^\mu\Big|_\alpha + \Lambda_i^\beta\Big|_{\alpha+d\alpha} + \frac{\alpha}{\epsilon_i^2} - \sum_{k\neq i}^N \frac{1}{\epsilon_i^2-\epsilon_k^2} & \text{if } i = j \\ \frac{1}{\epsilon_i^2-\epsilon_j^2} & \text{if } i \neq j \end{cases} \tag{6.45}$$

The obtained expression is can be seen as a polynomial in $d\alpha$. We can now proceed by explicitly determining the zeroth and first order coefficients. Since the eigenstates are orthogonal, the zeroth order in $d\alpha$ drops out. To find the first order coefficient, we start by noting that only the diagonal elements contain terms in $d\alpha$. We can find the contribution of a diagonal element J_{aa} by Taylor expanding $\Lambda_a^\beta\Big|_{\alpha+d\alpha}$ to the first order and by only considering the zeroth order of the other remaining diagonal elements. Doing this for each of the diagonal elements, the first order in $d\alpha$ becomes

$$\langle\{v_{\mu'}\}(\alpha)|\hat{S}_i^0|\{v_\beta\}(\alpha)\rangle = (\epsilon_i^2\Lambda_i^\beta(\alpha) - \epsilon_i^2\Lambda_i^{\mu'}(\alpha))(\prod_a \epsilon_a)\lambda^L \sum_{k=1}^L \frac{\partial\Lambda_k^\beta}{\partial\alpha} \det \widetilde{J}^k \tag{6.46}$$

with

$$\widetilde{J}_{ij}^{\mu'\beta j} = \begin{cases} \sum_{\kappa=\mu'\cup\beta} \frac{1}{\epsilon_i^2 - v_\kappa^2} - \sum_{k\neq i}^N \frac{1}{\epsilon_i^2-\epsilon_k^2} & \text{if } i = j \\ \frac{1}{\epsilon_i^2-\epsilon_j^2} & \text{if } i \neq j \end{cases}$$
$$= \begin{cases} \Lambda_i^\beta + \Lambda_i^\mu + \frac{\alpha}{\epsilon_i^2} - \sum_{k\neq a}^N \frac{1}{\epsilon_i^2-\epsilon_k^2} & \text{if } i = j \\ \frac{1}{\epsilon_i^2-\epsilon_j^2} & \text{If } i \neq j \end{cases} \tag{6.47}$$

with $i, j \neq k$.

Hence, we again need the partial derivatives to α. These can be obtained by considering the closed set of equations for eigenvalue based variables

$$\epsilon_i^2\Lambda_i^2 = -\alpha\Lambda_i + \sum_{j\neq i} \frac{\epsilon_i^2\Lambda_i - \epsilon_j^2\Lambda_j}{\epsilon_i^2 - \epsilon_j^2} - \gamma\lambda, \tag{6.48}$$

and by taking the partial derivative to α

$$2\epsilon_i^2\Lambda_i\frac{\partial\Lambda_i}{\partial\alpha} = -\Lambda_i - \alpha\frac{\partial\Lambda_i}{\partial\alpha} + \sum_{j\neq i} \frac{\epsilon_i^2\frac{\partial\Lambda_i}{\partial\alpha} - \epsilon_j^2\frac{\partial\Lambda_j}{\partial\alpha}}{\epsilon_i^2 - \epsilon_j^2}. \tag{6.49}$$

The latter equation can be rewritten to give

$$(2\epsilon_i^2\Lambda_i + \alpha - \sum_{j\neq i} \frac{\epsilon_i^2}{\epsilon_i^2 - \epsilon_j^2})\frac{\partial\Lambda_i}{\partial\alpha} + \sum_{j\neq i} \frac{\epsilon_j^2}{\epsilon_i^2 - \epsilon_j^2}\frac{\partial\Lambda_j}{\partial\alpha} = -\Lambda_i, \tag{6.50}$$

which is a linear equation in $\frac{\partial\Lambda_i}{\partial\alpha}$ and can as such be easily solved.

Chapter 7

Numerical analysis of the p+ip model interacting with a bath

7.1 Introduction

In this chapter we will numerically analyze the properties of the $p + ip$ Hamiltonian interacting with a bath using the formulas derived in the previous chapter. In section 7.3 we will examine the static properties such as the eigenenergies, the overlaps and the expectation values with respect to the eigenstates as a function of the coupling strength. In section 7.4 we consider the dynamical properties of the system. We start from a direct product state and observe how the expectation value of $\hat{S}^{\dagger}$ and $\hat{S}^{0}$ evolve through time. Special attention will be paid to the Moore-Read and Read-Green lines. In section 7.2 we briefly discuss how we expect the behavior to change at these points when the number of particles is no longer conserved.

7.2 Avoided crossing

When the number of particles is conserved, there is no interaction possible between states containing a different number of particles. This was the case for the $p + ip$ model we considered in chapter 5. However, when breaking the particle conservation, interaction between the degenerate eigenstates becomes possible and avoided crossing might occur [59]. This is shown in Figure 7.1. Due to the additional system-bath interaction the degeneracy is lifted, but the character of the eigenstates is still changed. From chapter 5 we know that these degeneracies occur at the Read-Green and the Moore-read points in the $p + ip$ model. We thus expect to observe avoided crossing at these points. We

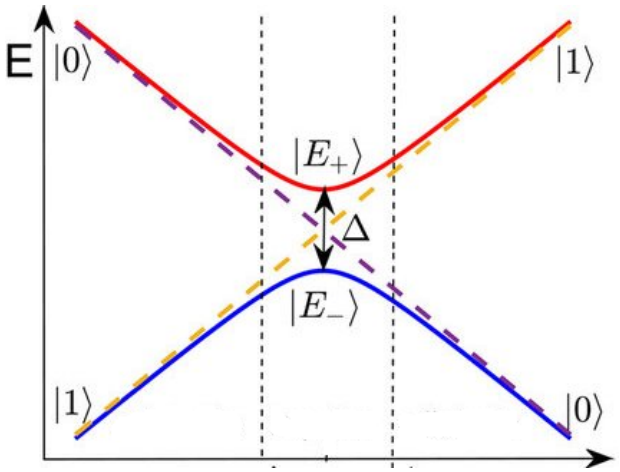

Figure 7.1: An illustration of avoided crossing. The parameter on the x-axis is the coupling strength in this case [60].

can show that the gap between the two states involved in the crossing, Δ in Figure 7.1, is proportional to the interaction strength between the two involved states. Consider a two-level Hamiltonian of the form

$$\hat{H} = \begin{bmatrix} E_1 & V \\ V & E_2 \end{bmatrix}, \tag{7.1}$$

where all matrix elements are considered to be real and V can be considered to be a perturbation, linking the two states. The eigenenergies are

$$E_+ = \frac{(E_1 + E_2)}{2} + \frac{1}{2}\sqrt{(E_1 - E_2)^2 + 4|V|^2} \tag{7.2}$$

$$E_- = \frac{(E_1 + E_2)}{2} - \frac{1}{2}\sqrt{(E_1 - E_2)^2 + 4|V|^2}. \tag{7.3}$$

We thus find for the gap

$$\Delta = E_+ - E_- = \sqrt{(E_1 - E_2)^2 + 4|V|^2}. \tag{7.4}$$

When the two-state system is degenerate in the unperturbed situation, $E_1 = E_2$, we find that $\Delta = 2|V|$. The interaction between the states thus lifts the degeneracy. Although we only discussed a two-level system, the above conclusions are often valid for more levels systems as well. This is because around the degeneracy the interactions between the states involved in the no-crossing region is strong enough so that the interactions with the other states can be neglected. In what follows, we can consider the terms in the Hamiltonian 6.10 that are proportional to γ as the perturbation and therefore we expect that in case of non-crossing the gap will be proportional to γ.

7.3 Statics

7.3.1 Total System

The ground state

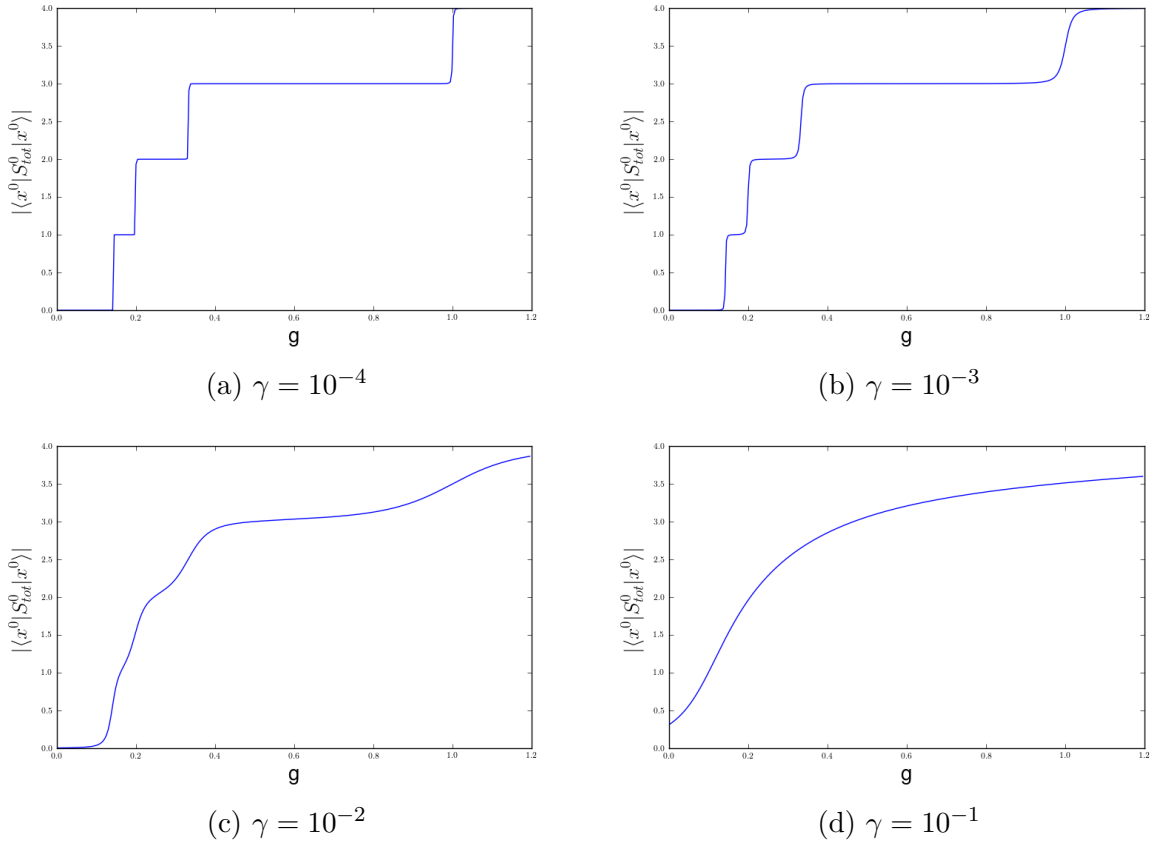

(a) $\gamma = 10^{-4}$ (b) $\gamma = 10^{-3}$

(c) $\gamma = 10^{-2}$ (d) $\gamma = 10^{-1}$

Figure 7.2: The occupation of the ground state as a function of the coupling strength.

All the numerical results throughout the remainder of this chapter were obtained with the single-particle energies $\epsilon_i^2 = i$ for $i = 1, ..., L$. In Figure 7.2b we see how the number of pairs in the ground state changes strongly around $g = \frac{1}{7}$, $g = \frac{1}{5}$, $g = \frac{1}{3}$ and $g = 1$. Not surprisingly, these values correspond to the Read-Green points. We also see that the transition is more abrupt as γ decreases. This is because for small γ the interaction between states with a different number of pairs will be very weak and hence the states involved in the transition will only interact in a very small interval around the Read-Green points. For very large γ, see Figure 7.2d, we no longer get clear transitions in

the number of pairs. At this point the terms proportional to γ in the Hamiltonian play a more important role than the pairing terms. The system then becomes reminiscent of the third regime we have encountered before in subsection 2.2.1, which can be given the interpretation of a mean field theory where particle fluctuations are dominant. The terms proportional to γ are also very similar to the mean-field Hamiltonian encountered in the BCS theory [40]. For the expectation value of $\hat{S}^\dagger_{tot}$ with respect to the ground

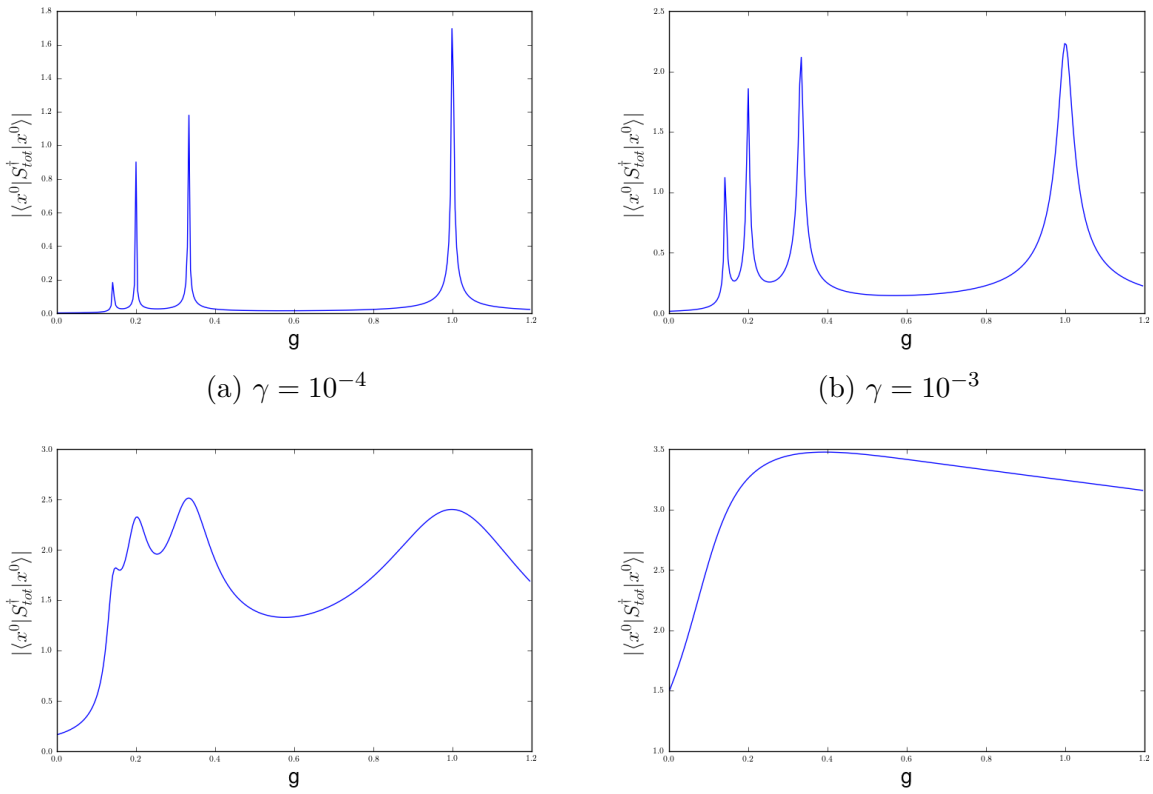

(a) $\gamma = 10^{-4}$ (b) $\gamma = 10^{-3}$

(c) $\gamma = 10^{-2}$ (d) $\gamma = 10^{-1}$

Figure 7.3: The expectation value of $\hat{S}^\dagger_i$ of the ground state as a function of the coupling strength.

state, shown in Figure 7.3, we find that for small γ there are only significant peaks around the Read-Green points, indicating that there is indeed a strong interaction between the ground state and the excited states at these points. At these crossings, the eigenstates are approximately given by $\frac{1}{\sqrt{2}}(|\psi_n\rangle + |\psi_{n+1}\rangle)$, with n denoting the number of pairs in the state, and a such $\langle \hat{S}^\dagger_{tot}\rangle = \langle \psi_{n+1}|\hat{S}^\dagger_{tot}|\psi_n\rangle$. Farther from the crossing the eigenstates are approximately unperturbed and $\langle \hat{S}^\dagger_{tot}\rangle = \langle \psi_n|\hat{S}^\dagger_{tot}|\psi_n\rangle = 0$. Away from the Read-Green points, we see that for small γ the expectation value is close to zero, which is the same

as what we found for the particle conserving $p + ip$ model, see section 5.4. For larger γ, the peaks start to spread out and they become less pronounced. For $\gamma = 10^{-1}$ they have completely disappeared. This is again an indication that at $\gamma = 10^{-1}$ the model has entered a different regime. It is clear that the number of excitations in an eigenstate no longer has a clear meaning, as the states belonging to different excitation sectors[1] interact strongly with each other. The peaks in Figure 7.3 suggest that there is a strong interaction between

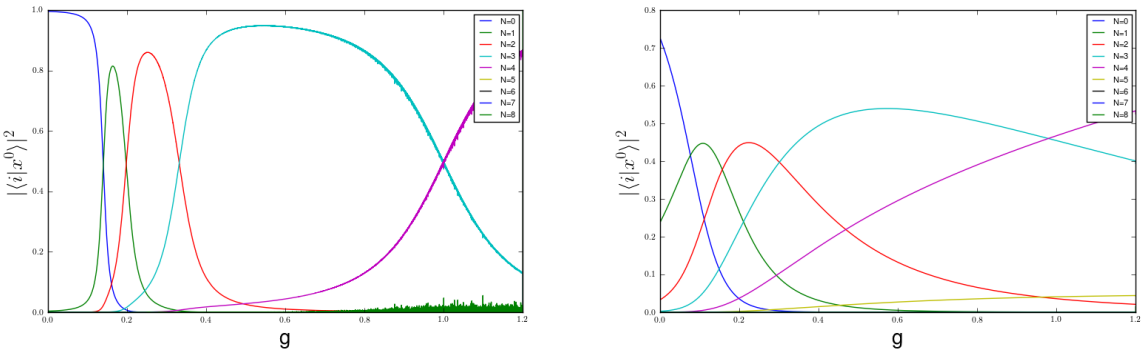

(a) $\gamma = 10^{-2}$ (b) $\gamma = 10^{-1}$

Figure 7.4: The squared overlap of the groundstate with the groups of direct products states having the same number of excitations.

states with a different number of excitations. To further investigate this, we look at the overlap of the groundstate with the direct product states containing a definite number of particles. For clarity of the plot, we first group all direct product states with the same number of excitations. The result for $\gamma = 10^{-2}$ is shown in Figure 7.4. At each of the Read-Green points the dominant number of excitations changes, leading to an effective change of the number of particles in the system. This is consistent with what we saw in Figure 7.15. It is also remarkable to see that the overlap with $N = 3$ sector is dominant in a much larger interval than the $N = 1$ and $N = 2$ sectors. When we compare the $\gamma = 10^{-2}$ to the $\gamma = 10^{-1}$, we see that in the latter case the contribution of the dominant sector is smaller than in the former case.

The alert reader might notice that the graph of $N = 8$ for $\gamma = 10^{-2}$ exhibits a rough behavior at higher coupling strength, as can be seen in the lower right corner in Figure 7.4a. This is probably because of numerical noise. From equation (6.24) it is clear that we are dealing with factors of the order γ^N. If $\gamma = 10^{-2}$ we can have an order of 10^{16}

[1]We define an excitation sector to be the collection of states that can be adiabatically connected to the set of direct product states with the same number of particles.

difference in the computations[2]. For smaller values of γ it was found that the noise was too big to produce reliable results. Fortunately, we are mainly interested in the lower excited states, for which the numerical noise is not present. We have anticipated the occurrence

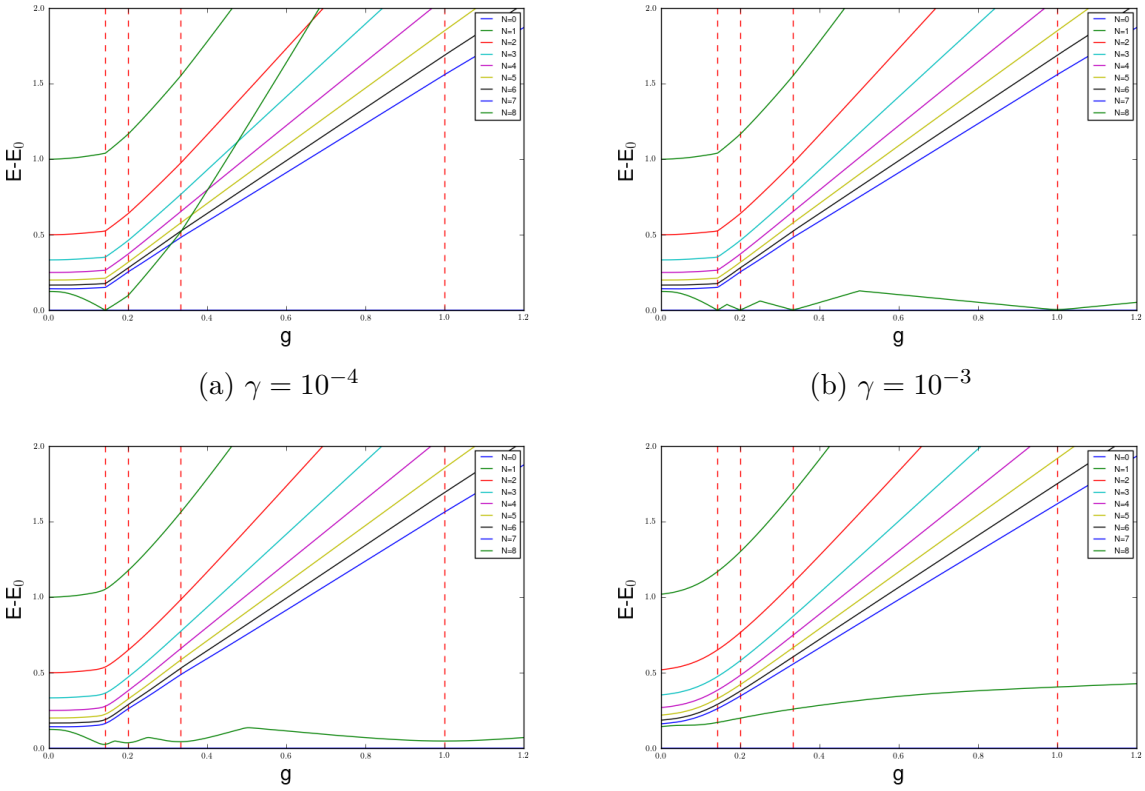

(a) $\gamma = 10^{-4}$ (b) $\gamma = 10^{-3}$

(c) $\gamma = 10^{-2}$ (d) $\gamma = 10^{-1}$

Figure 7.5: The eigenenergies of the first excitation sector with respect to the ground state energy.

of avoided crossings in section 7.2. The strong interactions between the different sectors in combination with the change of (dominant) number of excitations at the Read-Green points, suggest that at these points there is indeed an avoided crossing. To confirm this, we look at the eigenenergies of the states in the first excitation sector, see Figure 7.5. We indeed see that the state $|\uparrow\downarrow\downarrow\downarrow\downarrow\downarrow\downarrow\downarrow\rangle_g$ avoids crossing with the ground state. This is the eigenstate with the lowest eigenenergy in the zero-coupling limit. The other states of the sector have no tendency to interact with the ground state and the difference between

[2]One might also think that the noise is be caused by the computation of the determinant an 8×8 matrix containing small number. However, performing the calculations without the factor γ^N yielded smooth graphs, indicating that no noise is present and that the determinant is computed correctly.

the ground state energy and the eigenenergy of these states increases monotonically with increasing coupling strength. The gap between the no-crossing states is proportional to γ, being of the order 10^{-2} for $\gamma = 10^{-4}$ and of the order 1 for $\gamma = 10^{-2}$. For $\gamma = 10^{-2}$ the $|\uparrow\downarrow\downarrow\downarrow\downarrow\downarrow\downarrow\downarrow\rangle_g$ state exhibits avoided crossing with the ground state at each Read-Green point, $g = \frac{1}{7}$, $g = \frac{1}{5}$, $g = \frac{1}{3}$ and $g = 1$. This is clearly not the case for $\gamma = 10^{-4}$, where avoided crossing only occurs at $g = \frac{1}{7}$. Because Figure 7.3a clearly indicates that the ground state is involved in interactions with other eigenstates at each of the Read-Green points, we can presume that this is caused by other excitation sectors. Figure 7.6a confirms this: the eigenstates from other excitation sectors also exhibit avoided crossing with the ground state. From Figure 7.6c it is clear that indirectly the other excitation sectors are responsible for the repeated avoided crossing of the state $|\uparrow\downarrow\downarrow\downarrow\downarrow\downarrow\downarrow\downarrow\downarrow\rangle_g$ with the ground state. Because of the stronger interaction between the different excitation sectors, avoided crossing can now also occur between two excitation sectors with both at least one excitation. We see that the one-excitation sector eigenstate is repelled by the two-excitations sector eigenstate and is thus "pushed back" towards the ground state. The two-excitations sector eigenstate is at its turn repelled by the three-excitation sector. It is remarkable that for higher excitations sectors, for instance the four-excitation sector and the five-excitation sector, there is no avoided crossing present. For $\gamma = 10^{-1}$, we see that avoided crossing with the ground state is no longer present. From section 7.2 we know that the character of the eigenstates changes when they are involved in an avoided crossing. This change in character is reflected in the occupancy of the state. This helps to explains the results shown in Figure 7.7. At each avoided crossing, which occur at the Read-Green points, the occupancy of state $|\uparrow\downarrow\downarrow\downarrow\downarrow\downarrow\downarrow\downarrow\downarrow\rangle_g$ changes to the occupancy of the state with which it is involved in the non-crossing. For instance, for the $\gamma = 10^{-3}$ case, we see that the occupancy is 1 before $g = \frac{1}{7}$, the first Read-Green point. As the state $|\uparrow\downarrow\downarrow\downarrow\downarrow\downarrow\downarrow\downarrow\rangle_g$ belongs to the first excitation sector, this is what we would expect. At $g = \frac{1}{7}$ there is an avoided crossing with the ground state, that has zero occupancy, see Figure 7.2b. The occupancy of both eigenstates is exchanged. At $g = \frac{1}{6}$ the state $|\uparrow\downarrow\downarrow\downarrow\downarrow\downarrow\downarrow\downarrow\rangle_g$ has an avoided crossing with a state from the second excitation sector and thus its occupancy becomes 2. It is remarkable how abrupt the occupancy changes at this point. This indicates that both states interact very weakly with each other. This weak interaction is probably the reason why for $\gamma = 10^{-4}$ we don't see any changes: the numerical accuracy is insufficient to capture this very weak interaction. At $g = \frac{1}{5}$ there is again an avoided crossing with the ground state, that has an occupancy of 1 from its previous interaction with the state $|\uparrow\downarrow\downarrow\downarrow\downarrow\downarrow\downarrow\downarrow\rangle_g$.

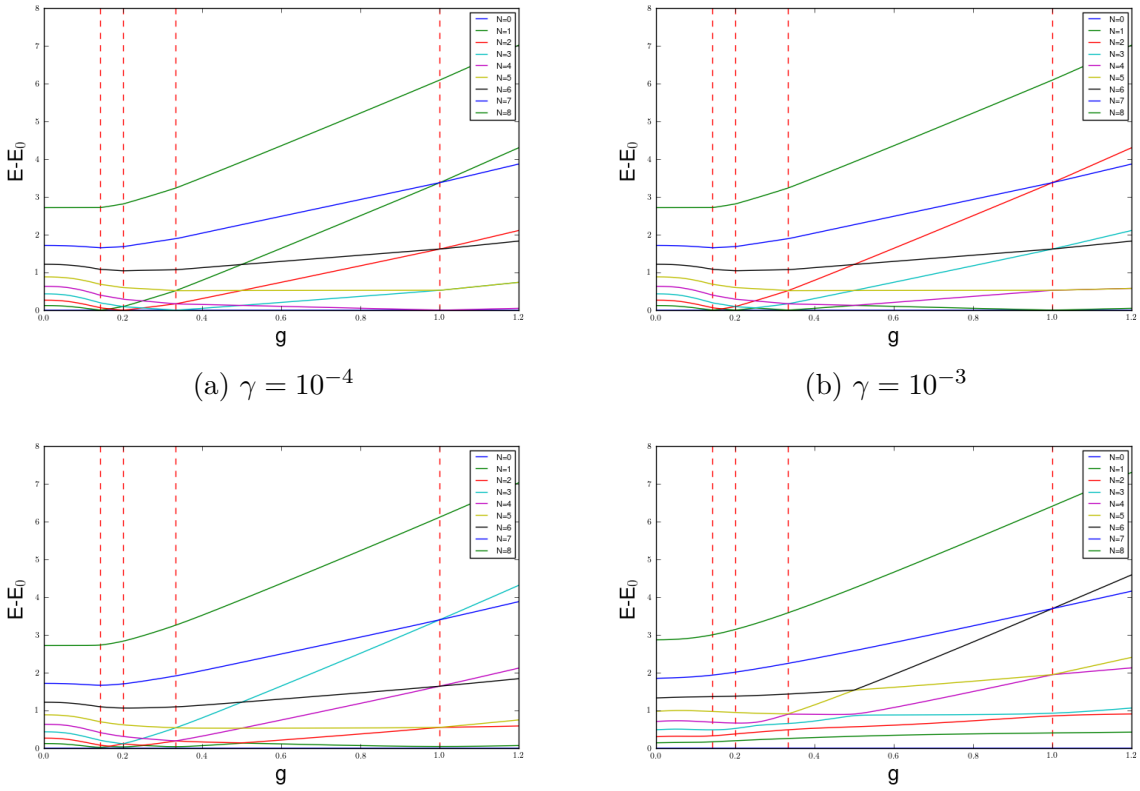

(a) $\gamma = 10^{-4}$ (b) $\gamma = 10^{-3}$

(c) $\gamma = 10^{-2}$ (d) $\gamma = 10^{-1}$

Figure 7.6: The eigenenergy of the eigenstate that, for each excitation sector, interacts most strongly with the vacuum state as a function of the coupling strength.

The vacuum state

We know that the vacuum state is involved in the transition at the Read-Green points. It is therefore interesting to look at the overlap of the vacuum state with the most important eigenstates. To get an idea of what eigenstate are most important, we plot the maximal overlap encountered for each of the eigenstates while sweeping the coupling strength from 0 to 1.2. This is shown in Figure 7.8d. We see that as γ increases, there appear more high peaks. The overlaps are shown in Figure 7.9. We see that for higher γ, there are more states involved. It is remarkable how the number of excitations in the vacuum state in the strong-coupling limit seems to depend on strongly γ. Of course, it might be that for coupling strengths higher than 1.2 there are still changes in the number of excitations of the vacuum state, but considering that from $g = 1$ onwards all excitation sectors have entered the strong coupling regime this seems highly unlikely.

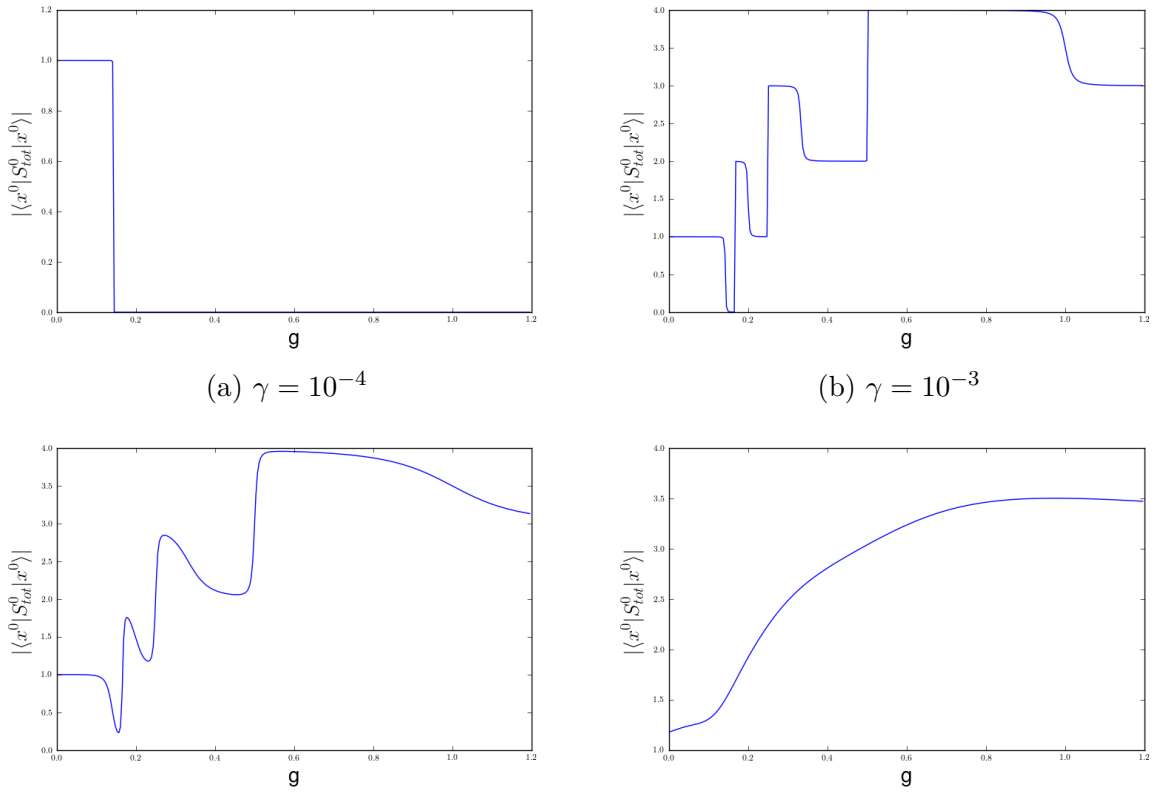

(a) $\gamma = 10^{-4}$

(b) $\gamma = 10^{-3}$

(c) $\gamma = 10^{-2}$

(d) $\gamma = 10^{-1}$

Figure 7.7: The occupation of the lowest exited state,$|\uparrow\downarrow\downarrow\downarrow\downarrow\downarrow\downarrow\downarrow\rangle_g$, as a function of the coupling strength.

In Figure 7.9c we see that at $g = \frac{1}{4}$ the overlap of state x^{92}, $|\downarrow\downarrow\downarrow\downarrow\downarrow\uparrow\uparrow\uparrow\rangle_{\frac{1}{4}}$[3], suddenly drops and that of $|\downarrow\downarrow\downarrow\downarrow\uparrow\uparrow\uparrow\uparrow\rangle_{\frac{1}{4}}$ peaks. Looking a the energies of these two eigenstates, see Figure 7.10, we find that the states are degenerate at this value of the coupling strength. For lower values of γ, we also find this degeneracy, but for numerical reasons the overlaps with the vacuum state are too small to draw reliable conclusions on whether the overlap behaves in the same manner as for the $\gamma = 10^{-2}$ case.

[3]We introduce the notation $|\downarrow\downarrow\downarrow\downarrow\downarrow\uparrow\uparrow\uparrow\rangle_a$ to indicate the eigenstate at $g = a$ that can be adiabatically connected to the direct product state $|\downarrow\downarrow\downarrow\downarrow\downarrow\uparrow\uparrow\uparrow\rangle$

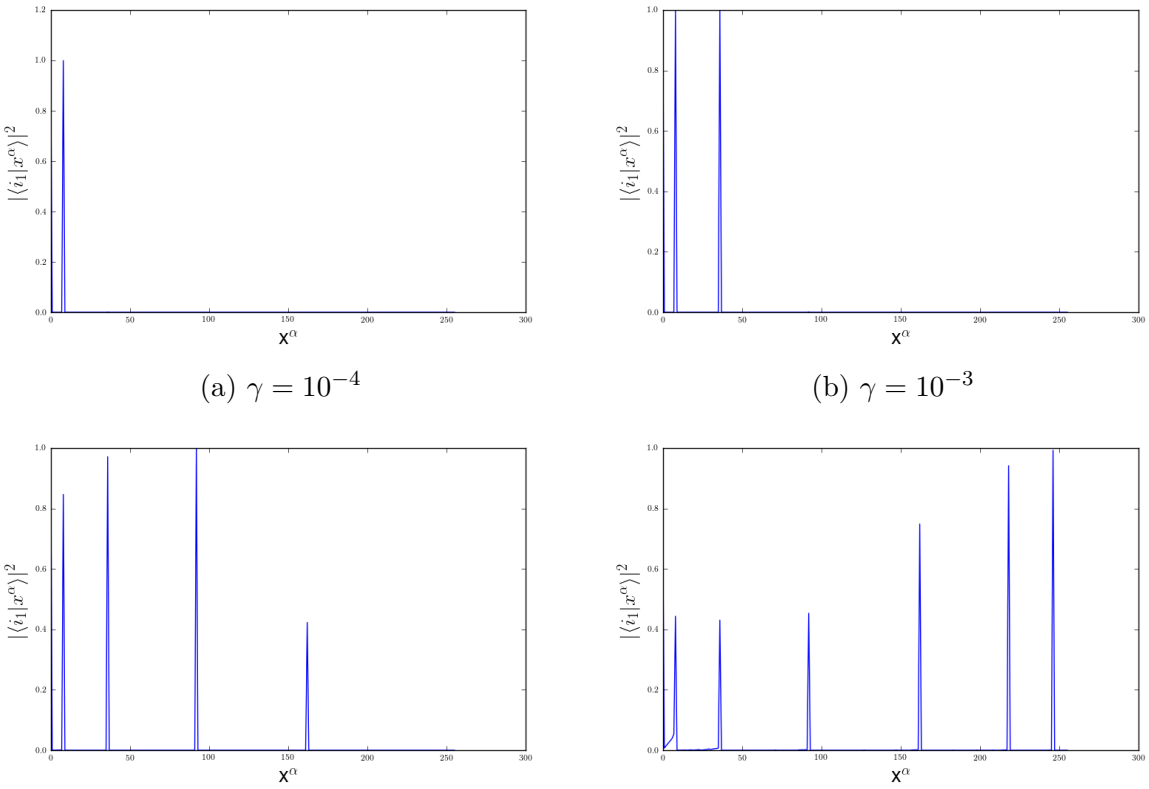

(a) $\gamma = 10^{-4}$ (b) $\gamma = 10^{-3}$

(c) $\gamma = 10^{-2}$ (d) $\gamma = 10^{-1}$

Figure 7.8: The maximal encountered overlap of the vacuum with each of the eigenstates when sweeping the coupling strength from 0 to 1.2.

7.3.2 A single excited state

In the previous subsection, we examined the properties of the entire system. We will now look at the properties of a single state. We choose to discuss the state with single particle energy ϵ_8, because of its importance in the avoided crossing with the ground state.
In Figure 7.11 we see that the occupancy of the single level with respect to the ground state behaves in a very similar manner as that of the total system. At the Read-Green points, the occupancy of the orbital changes abruptly. Between these points the occupancy drops, which is different from the entire system, where the occupancy remains constant.
For the interaction strength between the different excitation sectors, we also find a demeanor almost identical to the entire system. This suggests that the decreasing occupancy between the Read-Green points is caused by the interactions of the states belonging to the same excitation sector.

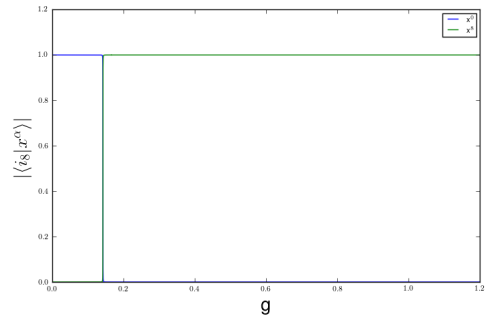

(a) $\gamma = 10^{-4}$

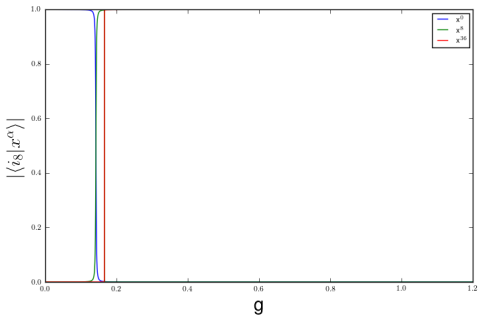

(b) $\gamma = 10^{-3}$

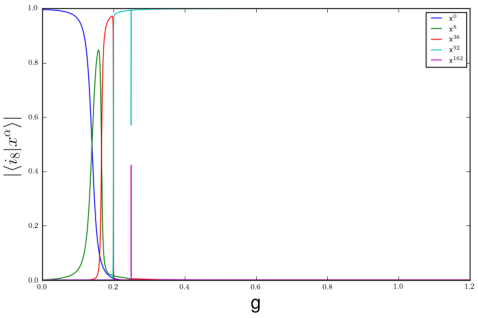

(c) $\gamma = 10^{-2}$

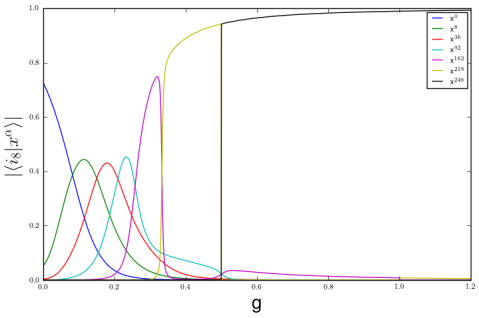

(d) $\gamma = 10^{-1}$

Figure 7.9: The overlap of the vacuum with the most important eigenstates as a function of the coupling strength.

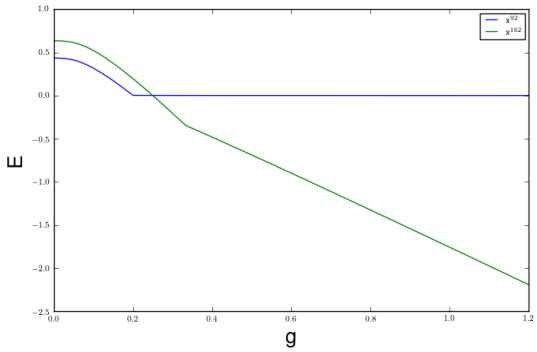

(a) $\gamma = 10^{-2}$

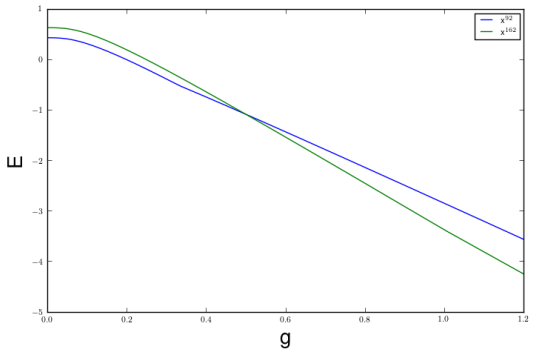

(b) $\gamma = 10^{-4}$

Figure 7.10: The eigenenergies of states x^{92} and x^{162}.

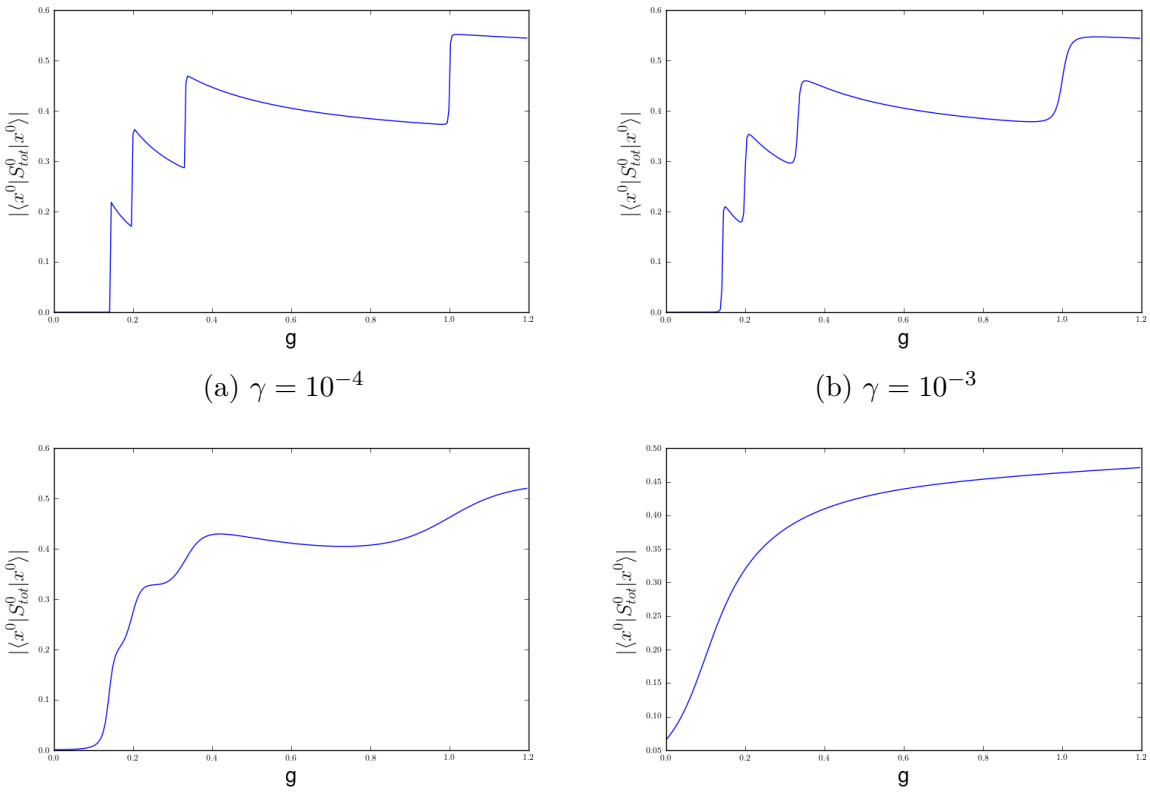

(a) $\gamma = 10^{-4}$ (b) $\gamma = 10^{-3}$

(c) $\gamma = 10^{-2}$ (d) $\gamma = 10^{-1}$

Figure 7.11: The occupation of the ground state as a function of the coupling strength.

7.4 Dynamics

In this section we will numerically analyze the behavior of $\langle i(t)|\hat{S}^\dagger|i(t)\rangle$ and $\langle i(t)|\hat{S}^0|i(t)\rangle$ with $|i(t=0)\rangle$ a direct product state. The first expectation value is an indication for how strong states within different excitation sectors interact with each other. The second will learn us more about the occupancy of the system. These properties enable us to better understand the dynamics of the model. We will consider both an eight level system and a four level system.

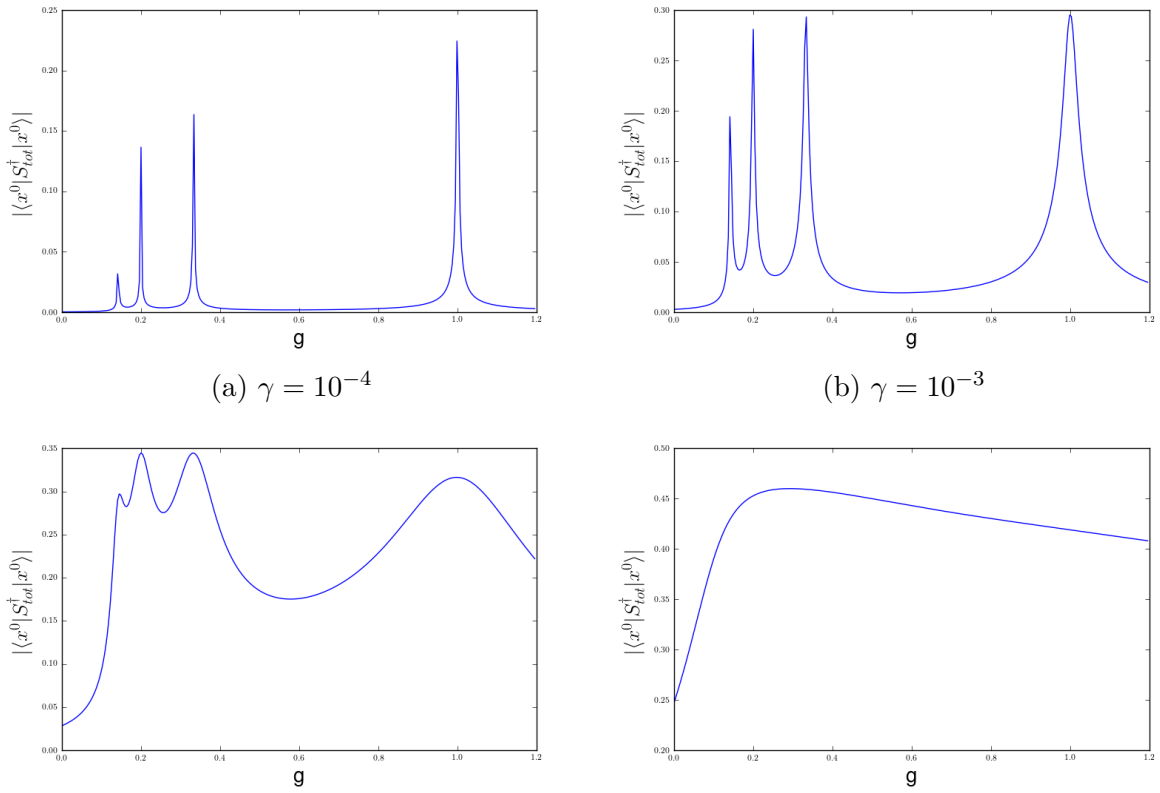

(a) $\gamma = 10^{-4}$ (b) $\gamma = 10^{-3}$

(c) $\gamma = 10^{-2}$ (d) $\gamma = 10^{-1}$

Figure 7.12: The expectation value of $\hat{S}_i^\dagger$ of the ground state as a function of the coupling strength.

7.4.1 The eight level system

The vacuum state

In Figure 7.14 the time evolution of the vacuum is shown. We see a periodical behavior suggesting the presence of quantum revival effects. For $\gamma = 10^{-4}$, see Figure 7.13c, the figure somewhat resembles a modulated *sine* function. However, we should point out that the magnitude of the occupancy in this case is about 10^{-8}, which might be lower than the numerical accuracy of the the computations[4]. For $\gamma = 10^{-2}$, we still find an occupancy of the order 10^{-5}, indicating that the expectation value for the occupancy with respect to the vacuum differs very little from that of the isolated $p + ip$ model, even for $\gamma = 10^{-2}$. For $\gamma = 10^{-1}$, we find an order of magnitude of 10^{-2}, indicating a much stronger variance

[4]By comparing the values of the matrix elements at $t = 0$ to their exact values, we find an accuracy of at least 10^{-6}.

in the occupancy over time. As discussed before, for this value of γ the system exhibits a fundamentally different behavior.

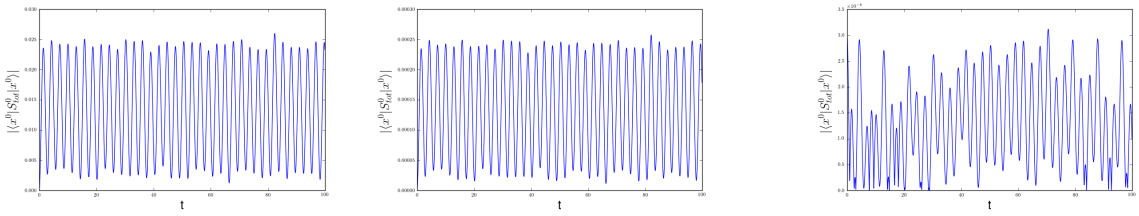

(a) $\gamma = 10^{-1}$ (b) $\gamma = 10^{-2}$ (c) $\gamma = 10^{-4}$

Figure 7.13: The occupation the vacuum state as a function of time at $g = -1.2$.

In figure 7.14, we again see a more or less periodic behavior. The magnitude of the expectation value is proportional to the value of γ, ranging from 10^{-1} for $\gamma = 10^{-1}$ to 10^{-4} for $\gamma = 10^{-4}$. Here, the behavior of the $\gamma = 10^{-4}$ case is very similar to that of the other values of γ. In Figure 7.15a we see that at small timescales, the figure resembles a $sinc^2$

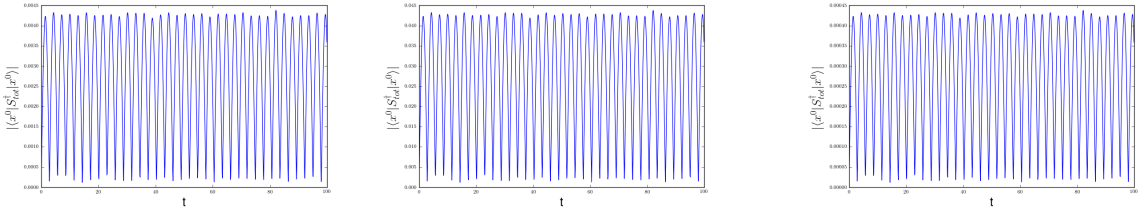

(a) $\gamma = 10^{-1}$ (b) $\gamma = 10^{-2}$ (c) $\gamma = 10^{-4}$

Figure 7.14: The expectation value of $\hat{S}^{\dagger}_{tot}$ the vacuum state as a function of the time at $g = -1.2$.

function with the peak centered around $\frac{1}{8}$, independent of the value of γ. For larger time scales the graph becomes less smooth and for $\gamma = 10^{-1}$ there is a peak at $g = \frac{1}{3}$, which is a Read-Green point. From Figures 7.17l and 7.15c it is clear that the magnitude of this peak oscillates strongly through time. For $\gamma = 10^{-2}$ we observe similar peaks at the values $g = \frac{1}{5}$, $g = \frac{1}{6}$ and $g = \frac{1}{7}$. For smaller values of γ, only the $\frac{1}{6}$ peak can be observed and for $\gamma = 10^{-4}$ there is also a small peak at $g = 1$. The occupancy again exhibits a periodic behavior through time for each value of the coupling strength[5].

[5]This cannot be observed based on the plots shown. When we make a movie showing the evolution through time, we can however clearly discern periodicity through time.

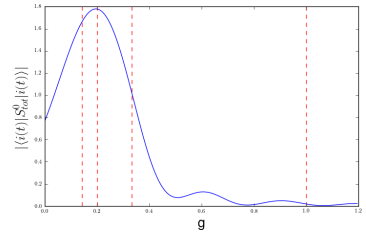

(a) $\gamma = 10^{-1}$ and $t = 100$

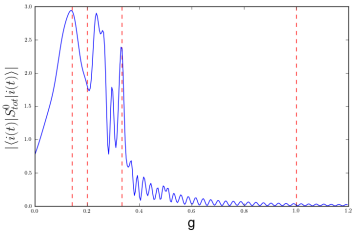

(b) $\gamma = 10^{-1}$ and $t = 1000$

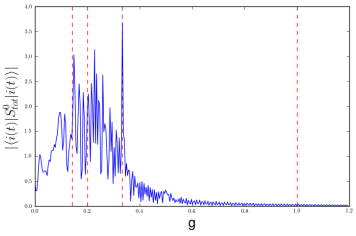

(c) $\gamma = 10^{-1}$ and $t = 10000$

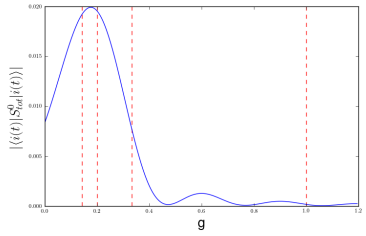

(d) $\gamma = 10^{-2}$ and $t = 100$

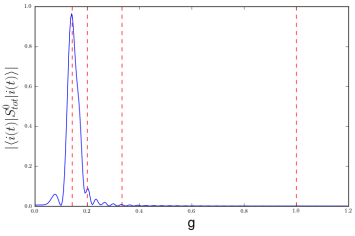

(e) $\gamma = 10^{-2}$ and $t = 1000$

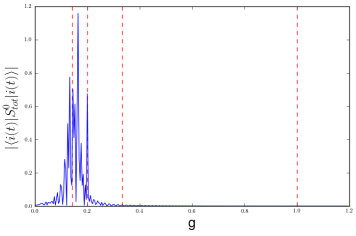

(f) $\gamma = 10^{-2}$ and $t = 10000$

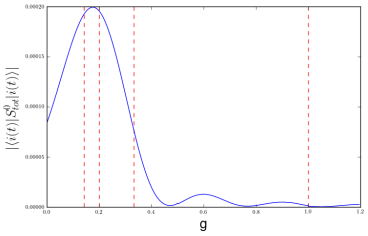

(g) $\gamma = 10^{-3}$ and $t = 100$

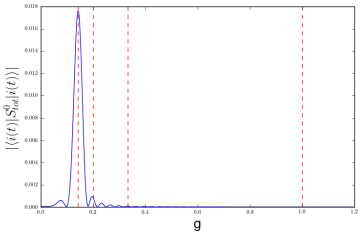

(h) $\gamma = 10^{-3}$ and $t = 1000$

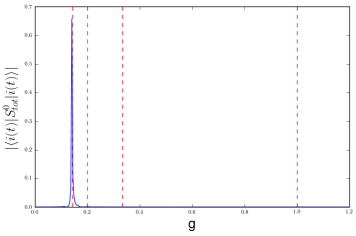

(i) $\gamma = 10^{-3}$ and $t = 10000$

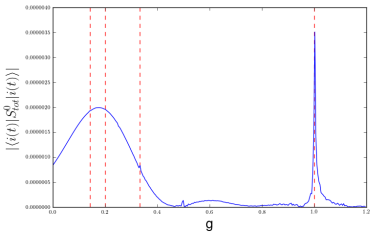

(j) $\gamma = 10^{-4}$ and $t = 100$

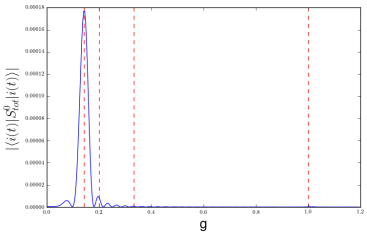

(k) $\gamma = 10^{-4}$ and $t = 1000$

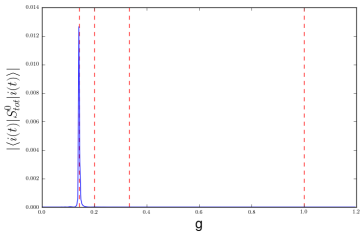

(l) $\gamma = 10^{-4}$ and $t = 10000$

Figure 7.15: The occupation of the vacuum state as a function of the coupling strength and at several times.

For the expectation value of $\hat{S}^{\dagger}_{tot}$, see Figure 7.16 we find that for small t the behavior is very similar for each value of γ. For larger t, however, there is a clear difference in behavior between the $g = 10^{-1}$ case and the other value of γ. For $g = 10^{-1}$ no clear peaks can be discerned. For $\gamma = 10^{-2}$ there are oscillating peaks at $g = \frac{1}{7}, \frac{1}{6}, \frac{1}{5}$. For smaller values of γ there is only a peak at $g = \frac{1}{7}$.

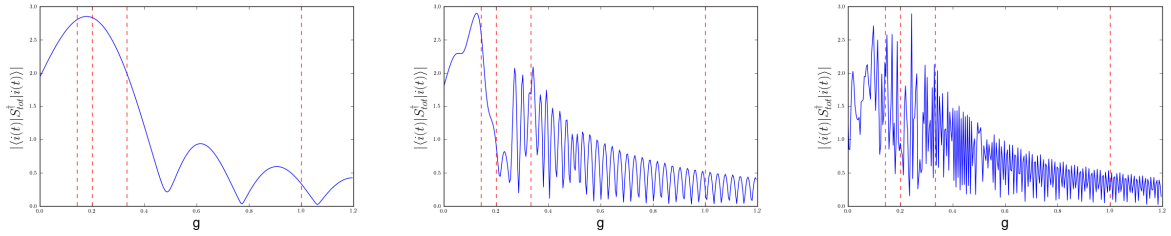

(a) $\gamma = 10^{-2}$ and $t = 100$ (b) $\gamma = 10^{-2}$ and $t = 1000$ (c) $\gamma = 10^{-1}$ and $t = 10000$

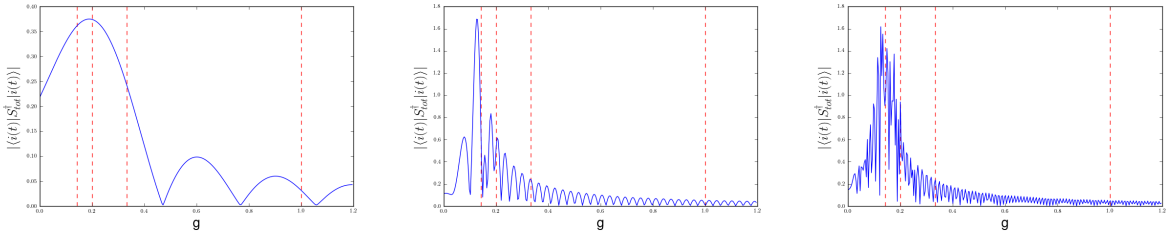

(d) $\gamma = 10^{-2}$ and $t = 100$ (e) $\gamma = 10^{-2}$ and $t = 1000$ (f) $\gamma = 10^{-2}$ and $t = 10000$

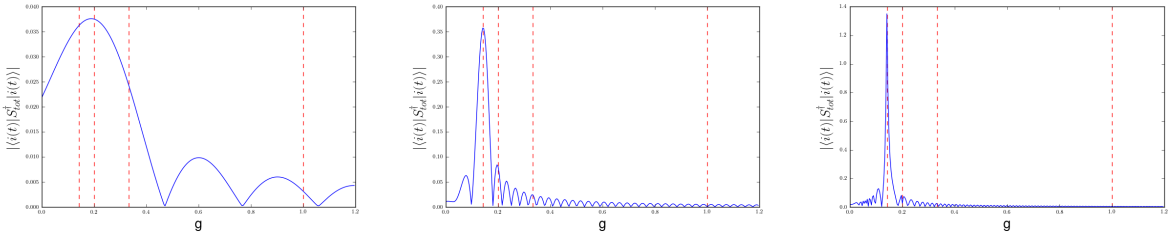

(g) $\gamma = 10^{-3}$ and $t = 100$ (h) $\gamma = 10^{-3}$ and $t = 1000$ (i) $\gamma = 10^{-3}$ and $t = 10000$

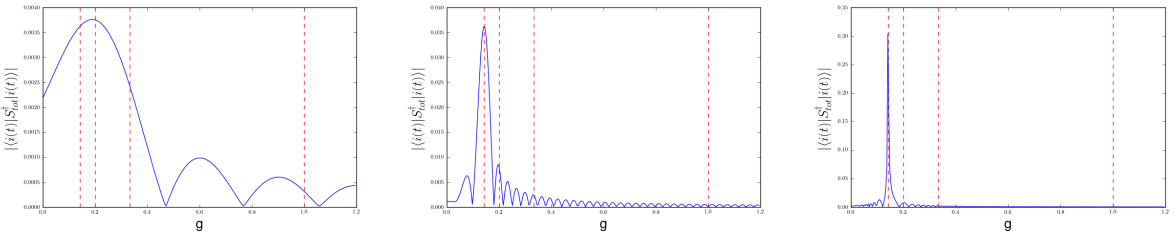

(j) $\gamma = 10^{-4}$ and $t = 100$ (k) $\gamma = 10^{-4}$ and $t = 1000$ (l) $\gamma = 10^{-4}$ and $t = 10000$

Figure 7.16: The expectation value of $\hat{S}^\dagger$ of the vacuum state as a function of the coupling strength and at several times.

7.4.2 The four-level system

In this subsection we examine the dynamics of a four-level system, because there are some remarkable differences between the dynamics of this system and that of the eight-level system. In Figure 7.17 we see that for $\gamma = 10^{-4}$ and $\gamma = 10^{-3}$, there is one small peak at $g = \frac{1}{3}$ that increases monotonously through time. Note that the scaling of the y-axis

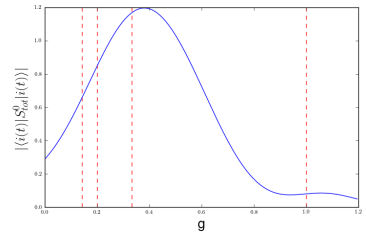

(a) $\gamma = 10^{-1}$ and $t = 100$

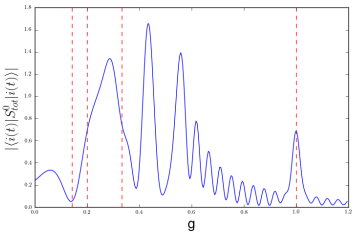

(b) $\gamma = 10^{-1}$ and $t = 1000$

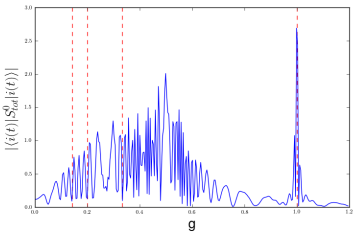

(c) $\gamma = 10^{-1}$ and $t = 10000$

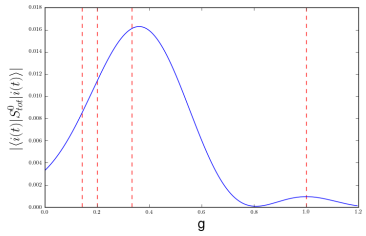

(d) $\gamma = 10^{-2}$ and $t = 100$

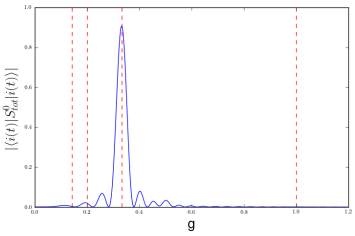

(e) $\gamma = 10^{-2}$ and $t = 1000$

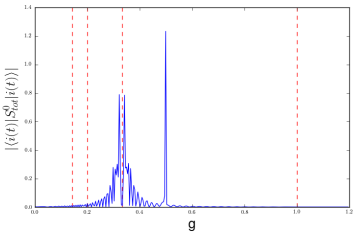

(f) $\gamma = 10^{-2}$ and $t = 10000$

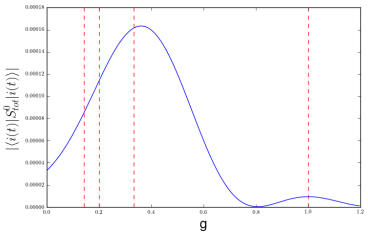

(g) $\gamma = 10^{-3}$ and $t = 100$

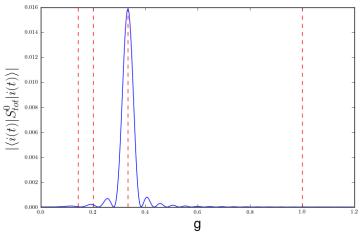

(h) $\gamma = 10^{-3}$ and $t = 1000$

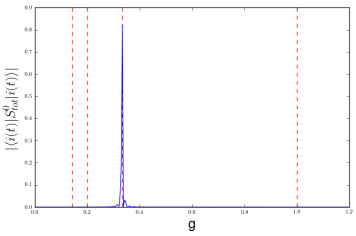

(i) $\gamma = 10^{-3}$ and $t = 10000$

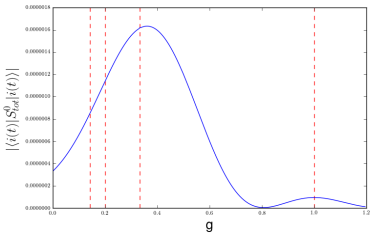

(j) $\gamma = 10^{-4}$ and $t = 100$

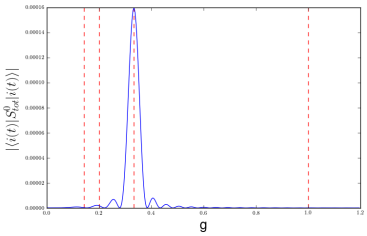

(k) $\gamma = 10^{-4}$ and $t = 1000$

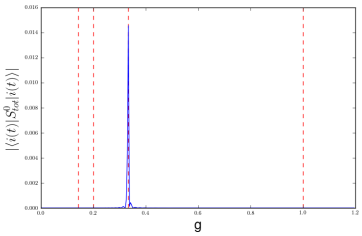

(l) $\gamma = 10^{-4}$ and $t = 10000$

Figure 7.17: The occupation of the vacuum state as a function of the coupling strength and at several times.

increases by roughly a factor 10 for each plot when going from left to right. For $\gamma = 10^{-2}$, there is a broad peak at $g = \frac{1}{3}$ and a small one at $g = \frac{1}{2}$. The magnitude of the small peak oscillates through time. For $\gamma = 10^{-1}$, there is a small peak at $g = 1$ and a very broad peak at $g = \frac{1}{2}$. The behavior for $\gamma = 10^{-1}$ and $\gamma = 10^{-2}$ is clearly very different from that of the eight-level system, where no small peaks were present at those values of the coupling strength. In Figure 7.18, we see that there is a peak at $g = \frac{1}{3}$ for $\gamma = 10^{-4}$, $\gamma = 10^{-3}$ and $\gamma = 10^{-2}$. The broadness of the peak increases for increasing values of γ. For $\gamma = 10^{-1}$ the peak has become so broad that is no longer clearly distinguishable. In contrast to the occupancy, the points $g = \frac{1}{2}$ and $g = 1$ don't seem to play an important role here.
The appearance of the small peaks in the expectation value of $\hat{S}^0_{tot}$ for $\gamma = 10^{-1}$ and $\gamma = 10^{-2}$ is a feature that was not present in the eight-level system. It is unclear whether this discrepancy has a physical reason or it is due to a lack of accuracy in the computations for the eight-level system.

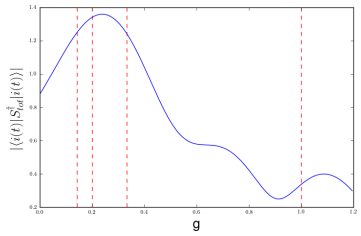

(a) $\gamma = 10^{-2}$ and $t = 100$

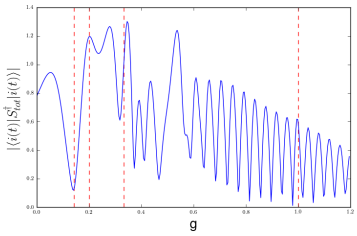

(b) $\gamma = 10^{-2}$ and $t = 1000$

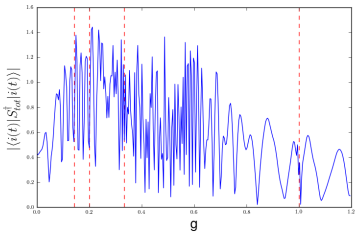

(c) $\gamma = 10^{-1}$ and $t = 10000$

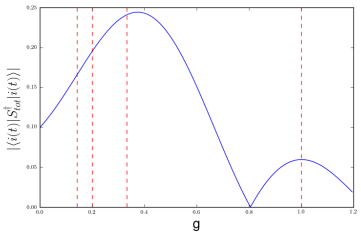

(d) $\gamma = 10^{-2}$ and $t = 100$

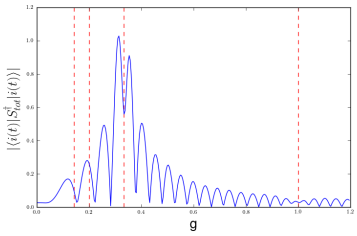

(e) $\gamma = 10^{-2}$ and $t = 1000$

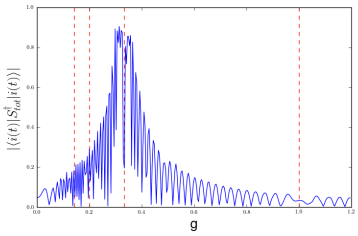

(f) $\gamma = 10^{-2}$ and $t = 10000$

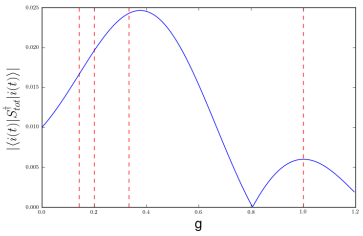

(g) $\gamma = 10^{-3}$ and $t = 100$

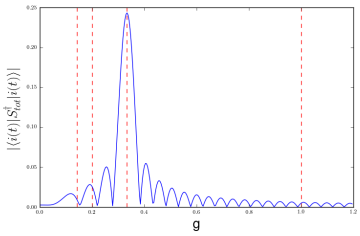

(h) $\gamma = 10^{-3}$ and $t = 1000$

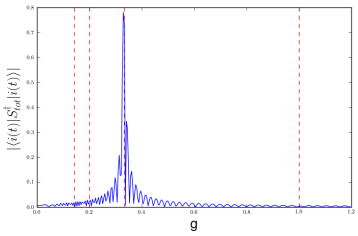

(i) $\gamma = 10^{-3}$ and $t = 10000$

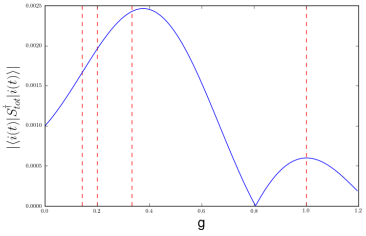

(j) $\gamma = 10^{-4}$ and $t = 100$

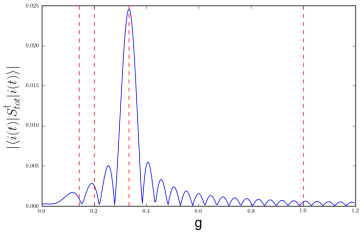

(k) $\gamma = 10^{-4}$ and $t = 1000$

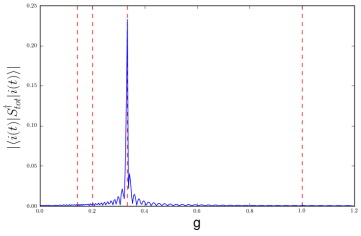

(l) $\gamma = 10^{-4}$ and $t = 10000$

Figure 7.18: The expectation value of $\hat{S}^{\dagger}$ of the vacuum state as a function of the coupling strength and at several times.

Chapter 8

Conclusion and outlook

The aim of this thesis was to extend the integrable $p + ip$ model by adding terms that are linear in the creation and annihilation operator to the Hamiltonian in order to break the particle-number conservation and to study the dynamics of this system. The model can then be considered to interact with an environment, allowing for dissipative effects. These dissipative effects can for instance be used to model spin decoherence in two state systems, which is useful for quantum computing.

From our study of the harmonic oscillator, we have learned that it is possible to obtain damping or amplification by adding linear terms in the creation and annihilation operators to the Hamiltonian. However, to obtain this we had to give up the hermicity of the Hamiltonian. This leads to a time evolution operator that is no longer unitary and therefore the norm of the wavefunction is not longer conserved through time. As we were unable to give a clear interpretation to this unnormalized wavefunction, we proceeded to consider other methods to include interaction with an environment in a quantum system. We found that the density operator formalism is a very natural method for describing these open quantum systems.

We have discussed the Richardson-Gaudin models in general and illustrated it with the reduced BCS Hamiltonian, which is a historically important example. We then proceeded to discuss the phase diagram in the $p+ip$ model and briefly discussed some of the dynamics of the model, making use of the particle-number conservation to separate the Hilbert space.

In chapter 6 we derived formulas for the overlap of a direct product state with an eigenstate, for the expectation value of the creation operator with respect to a time-dependent

direct product state and for the expectation value of the occupancy of an orbital with respect to that state. Using these formulas we can numerically analyze the dynamics of the model. We found that avoided crossing plays a very important role at the Read-Green points and that for small values of γ avoided crossings only occur when the ground state is involved. For larger γ we also observe repulsion between the states of different non-zero excitation sectors.

It would be interesting to discuss the $p + ip$ model interacting with a bath within the density operator formalism, as it is more natural to describe open quantum systems. It would also be interesting to study the properties of the system when γ is time-dependent. To do this an approach similar as in [61] can be taken. This approach seems promising when γ is small and the terms in the Hamiltonian that break particle conservation can be treated as a perturbation. The intrinsic disadvantage of this approach is that (i) it is approximative, so we no longer obtain exact solutions (ii) the error increases as time propagates.

The study of the time evolution of (open) quantum systems is a very actual and interesting subject with many questions left to be answered. Hopefully, the findings in this thesis can contribute to a better understanding of this fascinating topic.

Appendix A

The classical harmonic oscillator

A.1 The classical harmonic oscillator

The Hamiltonian of a single harmonic oscillator is given by

$$H = \frac{p^2}{2m} + \frac{m\omega^2 x^2}{2}. \tag{A.1}$$

The coordinate x and the momentum p are called the canonical variables of the system. Using these variables, we can define the Poisson bracket

$$\{f, g\} = \frac{\partial f}{\partial q}\frac{\partial g}{\partial p} - \frac{\partial f}{\partial p}\frac{\partial g}{\partial q}. \tag{A.2}$$

Clearly, we have that

$$\{q, q\} = \{p, p\} = 0 \tag{A.3}$$

$$\{q, p\} = 1. \tag{A.4}$$

These relations should hold for each set of canonical variables.
Applying Hamilton's equation

$$\frac{dp}{dt} = -\frac{\partial H}{\partial x} \tag{A.5}$$

$$\frac{dx}{dt} = \frac{\partial H}{\partial p} \tag{A.6}$$

we find

$$\frac{dp}{dt} = -m\omega^2 x \tag{A.7}$$

$$\frac{dx}{dt} = \frac{p}{m}, \tag{A.8}$$

which can be combined to obtain the familiar equation of motion

$$\frac{d^2x}{dt^2} = -\omega^2 x. \tag{A.9}$$

Imposing the boundary conditions $x(0) = A$ and $\frac{dx}{dt}(0) = 0$, we find as solution

$$x(t) = A\cos(\omega t). \tag{A.10}$$

A.2 A set of coupled oscillators

The Hamiltonian is now given by

$$H = \sum_i^N \frac{p_i^2}{2m_i} + \frac{1}{2}\sum_{i,j}^N K_{ij}x_i x_j. \tag{A.11}$$

Making use of Hamilton's equations, we find the following equation of motion

$$M\frac{d^2x}{dt^2} = -Kx. \tag{A.12}$$

To solve for the eigenmodes, we propose a solution of the kind $x = c\cos(\omega t + \phi)$, with c a real vector. The equation becomes

$$M\omega^2 c = Kc \tag{A.13}$$

or, with $K^{'} = M^{-1/2}KM^{-1/2}$ and $c^{'} = M^{1/2}c$

$$K^{'}c^{'} = \omega^2 c^{'}, \tag{A.14}$$

which is a regular eigenvalue problem. We therefore obtain that $c^{'}$ has to be an eigenvalue of $K^{'}$ or, equivalently, c has to be an eigenvalue of $M^{-1}K$. The general form of the solution is therefore, with the notation from before

$$x_k = \sum_{i=1}^N c_i \frac{V_{ki}}{\sqrt{m_k}}\cos(\omega_i t + \phi_i) \tag{A.15}$$

We impose the following initial conditions

$$\left.\frac{dx}{dt}\right|_{t=0} = 0, \tag{A.16}$$

$$x_k(0) = A\delta_{k,0}. \tag{A.17}$$

The first condition leads to $\phi_i = 0$, $\forall i$, whereas the second leads to

$$b_i = AV_{0i}\sqrt{m_0}. \tag{A.18}$$

We thus obtain

$$x_k = A\sqrt{\frac{m_0}{m_k}}\sum_{i=1}^{N} V_{0i}V_{ki}\cos(\omega_i t) = A\sqrt{\frac{m_0}{m_k}}\sum_{i=1}^{N} V_{ik}V_{i0}cos(\omega_i t). \tag{A.19}$$

Appendix B

The Baker–Campbell–Hausdorff formula

Throughout this appendix capital letters will represent operators. The most general form of the Baker–Campbell–Hausdorff formula reads

$$\log(\exp X \exp Y) = \sum_{n>0} \frac{(-1)^{n-1}}{n} \sum_{\substack{r_i+s_i>0 \\ 1\leq i\leq n}} \frac{(\sum_{i=1}^{n}(r_i+s_i))^{-1}}{r_1!s_1!\cdots r_n!s_n!}[X^{r_1}Y^{s_1}X^{r_2}Y^{s_2}\ldots X^{r_n}Y^{s_n}], \tag{B.1}$$

where s_n and r_n are non-negative integers and we have used the following notation

$$[X^{r_1}Y^{s_1}\ldots X^{r_n}Y^{s_n}] = [\underbrace{X,[X,\ldots[X}_{r_1},[\underbrace{Y,[Y,\ldots[Y}_{s_1},\ \ldots\ [\underbrace{X,[X,\ldots[X}_{r_n},[\underbrace{Y,[Y,\ldots Y}_{s_n}]]\ldots]]. \tag{B.2}$$

This term is zero if $s_n > 1$ or if $s_n = 0$ and $r_n > 1$ [62]. Explicitly writing out the first few terms, we find

$$\log(\exp X \exp Y) \tag{B.3}$$

$$= X + Y + \frac{1}{2}[X,Y] + \frac{1}{12}([X,[X,Y]] + [Y,[Y,X]]) \tag{B.4}$$

$$- \frac{1}{24}[Y,[X,[X,Y]]] \tag{B.5}$$

$$- \frac{1}{720}([Y,[Y,[Y,[Y,X]]]] + [X,[X,[X,[X,Y]]]]) \tag{B.6}$$

$$+ \frac{1}{360}([X,[Y,[Y,[Y,X]]]] + [Y,[X,[X,[X,Y]]]]) \tag{B.7}$$

$$+ \frac{1}{120}([Y,[X,[Y,[X,Y]]]] + [X,[Y,[X,[Y,X]]]]) + \cdots . \tag{B.8}$$

This formula is very general, but rather unwieldy. We will make use of a more specific and compact version of the Baker–Campbell–Hausdorff formula:

$$e^X Y e^{-X} = Y + [X, Y] + \frac{1}{2!}[X, [X, Y]] + \frac{1}{3!}[X, [X, [X, Y]]] + \cdots . \tag{B.9}$$

This formula can be proven, see [63], by assuming that $e^{sX} Y e^{-sX}$ with s real can be written as $e^{sX} Y e^{-sX} = f(s)Y$. Taking the derivative to s on both sides of the equation, we find

$$\frac{d}{ds} f(s)Y = X e^X Y e^{-sX} - e^{sX} Y e^{-sX} X = [X, f(s)Y]. \tag{B.10}$$

Denoting $[X, Y]$ as $\mathrm{ad}_X Y$ and using the fact that $f(s = 0) = 1$, we find that

$$f(s) = e^{s\,\mathrm{ad}_X}, \tag{B.11}$$

which after putting $s = 1$ proves equation (B.9).

Appendix C

The Newton-Raphson method

The Newton-Raphson is an iterative method to numerically determine the roots of a differentiable function. Suppose we have a function $f(x)$ of which we want to determine a root. We start by making an initial guess, x_0. If we know the numeric values of $f(x_0)$ and $f^{'}(x_0)$, we can find an improved guess

$$x_1 = x_0 - \frac{f(x_0)}{f^{'}(x_0)}. \tag{C.1}$$

This formula is derived found by linearly approximating $f(x)$ around x_0 and by looking for the root of this approximation

$$f(x_1) \approx f(x_0) + (x_1 - x_0)f^{'}(x_0) = 0. \tag{C.2}$$

Solving this for x_1, we indeed find equation C.1. Repeating this procedure for the new guess x_1, we find that in general

$$x_{n+1} = x_n - \frac{f(x_n)}{f^{'}(x_n)}. \tag{C.3}$$

Figure C.1 illustrates the algorithm. We indeed see that method can converge very quickly under the right circumstances. However, the above discussion applies only to a function in one variable. For a set of k functions in k variables, the above generalizes to

$$J(x_n)(x_{n+1} - x_n) = -F(x_n), \tag{C.4}$$

where $J(x_n)$ is the Jacobian and F is the vector function consisting out of the k functions. It can be proven that, under certain conditions, the method converges quadratically, meaning that the error in iteration $n + 1$ is proportional to the square of the error in iteration n [65]. The method has a few disadvantages. The function under consideration should be differentiable and it has to be possible to efficiently evaluate the first derivative. Also, if a bad initial guess is made the method might not converge.

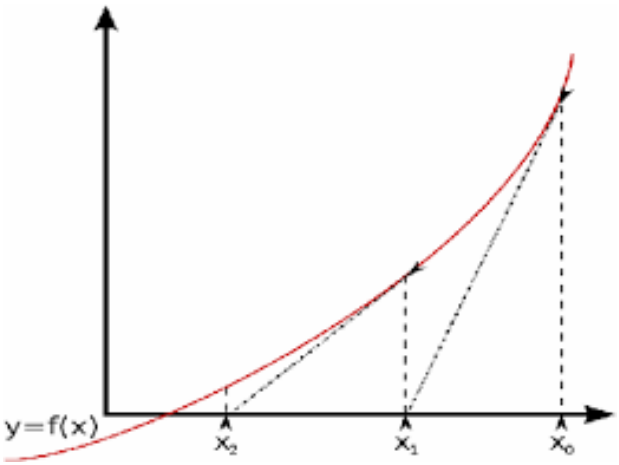

Figure C.1: A graphical illustration of the Newton-Raphson method. [64]

Bibliography

[1] W. H. Zurek, "Decoherence, einselection, and the quantum origins of the classical," *Rev. Mod. Phys.*, vol. 75, pp. 715–775, May 2003.

[2] R. Hanson, L. P. Kouwenhoven, J. R. Petta, S. Tarucha, and L. M. K. Vandersypen, "Spins in few-electron quantum dots," *Rev. Mod. Phys.*, vol. 79, pp. 1217–1265, Oct 2007.

[3] E. Schrödinger, "An Undulatory Theory of the Mechanics of Atoms and Molecules," *Physical Review*, vol. 28, pp. 1049–1070, Dec. 1926.

[4] W. Dickhoff and D. Van Neck, *Many-body Theory Exposed!: Propagator Description of Quantum Mechanics in Many-body Systems*. World Scientific, 2008.

[5] A. Faribault, P. Calabrese, and J.-S. Caux, "Quantum quenches from integrability: the fermionic pairing model," *Journal of Statistical Mechanics: Theory and Experiment*, vol. 2009, no. 03, p. P03018, 2009.

[6] M. Schlosshauer, "Decoherence, the measurement problem, and interpretations of quantum mechanics," *Rev. Mod. Phys.*, vol. 76, pp. 1267–1305, Feb 2005.

[7] H. Breuer and F. Petruccione, *The Theory of Open Quantum Systems*. Oxford University Press, 2002.

[8] A. Steane, "Quantum computing," *Reports on Progress in Physics*, vol. 61, no. 2, p. 117, 1998.

[9] A. Edmonds, U. D'Haenens-Johansson, R. Cruddace, M. Newton, K. Fu, C. Santori, R. Beausoleil, D. Twitchen, and M. Markham, "Production of oriented nitrogen-vacancy color centers in synthetic diamond," *prb*, vol. 86, p. 035201, July 2012.

[10] D. D. Awschalom, "The diamond age of spintronics: Room temperature spin control," in *Device Research Conference, 2008*, pp. 215–216, June 2008.

[11] N. Bar-Gill, L. M. Pham, A. Jarmola, D. Budker, and R. L. Walsworth, "Solid-state electronic spin coherence time approaching one second," *Nature Communications*, vol. 4, p. 1743, Apr. 2013.

[12] L. J. Rogers, M. W. Doherty, M. S. J. Barson, S. Onoda, T. Ohshima, and N. B. Manson, "Singlet levels of the nv centre in diamond," *New Journal of Physics*, vol. 17, no. 1, p. 013048, 2015.

[13] M. W. Doherty, N. B. Manson, P. Delaney, F. Jelezko, J. Wrachtrup, and L. C. L. Hollenberg, "The nitrogen-vacancy colour centre in diamond," *physrep*, vol. 528, pp. 1–45, July 2013.

[14] Y. Hamdouni and F. Petruccione, "Time evolution and decoherence of a spin-$\frac{1}{2}$ particle coupled to a spin bath in thermal equilibrium," *Phys. Rev. B*, vol. 76, p. 174306, Nov 2007.

[15] "http://www.christianhill.co.uk/teaching/tutorials/qm2/the-harmonic-oscillator/introduction/the-harmonic-oscillator/solution/."

[16] R. Bertlmann, "Theoretical physics t2 quantum mechanics."

[17] J. Klauder, "B.-s. skagerstam coherent states," 1985.

[18] J.-P. Gazeau, *Coherent states in quantum physics*. Wiley, 2009.

[19] W.-M. Zhang, R. Gilmore, *et al.*, "Coherent states: theory and some applications," *Reviews of Modern Physics*, vol. 62, no. 4, p. 867, 1990.

[20] R. Loudon, *The quantum theory of light*. OUP Oxford, 2000.

[21] "http://chemwiki.ucdavis.edu/@api/deki/files/9218/=slide1.png?revision=1."

[22] B. Nagel, *Modern Group Theoretical Methods in Physics: Proceedings of the Conference in Honour of Guy Rideau*, ch. Spectra and Generalized Eigenfunctions of the One- and Two-Mode Squeezing Operators in Quantum Optics, pp. 211–220. Dordrecht: Springer Netherlands, 1995.

[23] N. Bogoliubov, "A new method in the theory of superconductivity. 1.," *SOVIET PHYSICS JETP-USSR*, vol. 7, no. 1, pp. 41–46, 1958.

[24] J. Valatin, "Comments on the theory of superconductivity," *Il Nuovo Cimento (1955-1965)*, vol. 7, no. 6, pp. 843–857, 1958.

[25] C. Um, I. Kim, S. Hong, K. Yeon, and D. Kim, "Quantum mechanical treatment of the general damped harmonic oscillator," *JOURNAL OF THE KOREAN PHYSICAL SOCIETY*, vol. 30, no. 1, pp. 1–6, 1997.

[26] R. Puri and S. Lawande, "Time-dependent invariants and stable coherent states," *Physics Letters A*, vol. 70, no. 2, pp. 69–70, 1979.

[27] U. Weiss, "Quantum dissipative systems," pp. 20–22, World Scientific, 2012.

[28] F. Kazuyuki, "Quantum damped harmonic oscillators1.".

[29] K. Hornberger, "Introduction to decoherence theory," in *Entanglement and Decoherence*, pp. 221–276, Springer, 2009.

[30] L. Amico, A. D. Lorenzo, and A. Osterloh, "Integrable models for confined fermions: applications to metallic grains," *Nuclear Physics B*, vol. 614, no. 3, pp. 449 – 466, 2001.

[31] S. Tewari, S. Das Sarma, C. Nayak, C. Zhang, and P. Zoller, "Quantum computation using vortices and majorana zero modes of a $p_x + ip_y$ superfluid of fermionic cold atoms," *Phys. Rev. Lett.*, vol. 98, p. 010506, Jan 2007.

[32] J. D. Sau, R. M. Lutchyn, S. Tewari, and S. Das Sarma, "Generic new platform for topological quantum computation using semiconductor heterostructures," *Phys. Rev. Lett.*, vol. 104, p. 040502, Jan 2010.

[33] J.-S. Caux and J. Mossel, "Remarks on the notion of quantum integrability," *Journal of Statistical Mechanics: Theory and Experiment*, vol. 2011, no. 02, p. P02023, 2011.

[34] J. Dukelsky, S. Pittel, and G. Sierra, "Colloquium: Exactly solvable richardson-gaudin models for many-body quantum systems," *Reviews of modern physics*, vol. 76, no. 3, p. 643, 2004.

[35] D. Rowe and J. Wood, *Fundamentals of Nuclear Models: Foundational Models*. World Scientific, 2010.

[36] M. Gaudin, *La fonction d'onde de Bethe*. Collection du Commissariat a l'Energie Atomique / Ser. scientifique, Masson, 1983.

[37] G. Ortiz, R. Somma, J. Dukelsky, and S. Rombouts, "Exactly-solvable models derived from a generalized gaudin algebra," *Nuclear Physics B*, vol. 707, no. 3, pp. 421 – 457, 2005.

[38] H. Bethe, "Zur theorie der metalle," *Zeitschrift für Physik*, vol. 71, no. 3, pp. 205–226.

[39] M. Van Raemdonck, S. De Baerdemacker, and D. Van Neck, "Perturbations on the superconducting state of metallic nanoparticles: influence of geometry and impurities," *EUROPEAN PHYSICAL JOURNAL D*, vol. 67, p. 7, 2013.

[40] J. Bardeen, L. N. Cooper, and J. R. Schrieffer, "Theory of superconductivity," *Phys. Rev.*, vol. 108, pp. 1175–1204, Dec 1957.

[41] C. C. Tsuei and J. R. Kirtley, "Pairing symmetry in cuprate superconductors," *Rev. Mod. Phys.*, vol. 72, pp. 969–1016, Oct 2000.

[42] R. Richardson, "A restricted class of exact eigenstates of the pairing-force hamiltonian," *Physics Letters*, vol. 3, no. 6, pp. 277 – 279, 1963.

[43] M. Cambiaggio, A. Rivas, and M. Saraceno, "Integrability of the pairing hamiltonian," *Nuclear Physics A*, vol. 624, no. 2, pp. 157–167, 1997.

[44] R. Richardson and N. Sherman, "Exact eigenstates of the pairing-force hamiltonian," *Nuclear Physics*, vol. 52, pp. 221 – 238, 1964.

[45] S. Rombouts, D. Van Neck, and J. Dukelsky, "Solving the richardson equations for fermions," *Phys. Rev. C*, vol. 69, p. 061303, Jun 2004.

[46] F. Domínguez, C. Esebbag, and J. Dukelsky, "Solving the richardson equations close to the critical points," *Journal of Physics A: Mathematical and General*, vol. 39, no. 37, p. 11349, 2006.

[47] A. Faribault, O. El Araby, C. Sträter, and V. Gritsev, "Gaudin models solver based on the correspondence between bethe ansatz and ordinary differential equations," *Physical Review B*, vol. 83, no. 23, p. 235124, 2011.

[48] S. De Baerdemacker, "Richardson-gaudin integrability in the contraction limit of the quasispin," *Physical Review C*, vol. 86, no. 4, p. 044332, 2012.

[49] P. W. Claeys, S. De Baerdemacker, M. Van Raemdonck, and D. Van Neck, "Eigenvalue-based method and form-factor determinant representations for integrable xxz richardson-gaudin models," *Phys. Rev. B*, vol. 91, p. 155102, Apr 2015.

[50] A. Faribault and D. Schuricht, "On the determinant representations of gaudin models' scalar products and form factors," *Journal of Physics A: Mathematical and Theoretical*, vol. 45, no. 48, p. 485202, 2012.

[51] J. Xia, Y. Maeno, P. T. Beyersdorf, M. M. Fejer, and A. Kapitulnik, "High resolution polar kerr effect measurements of sr_2ruo_4: Evidence for broken time-reversal symmetry in the superconducting state," *Phys. Rev. Lett.*, vol. 97, p. 167002, Oct 2006.

[52] A. P. Mackenzie and Y. Maeno, "The superconductivity of sr_2ruo_4 and the physics of spin-triplet pairing," *Rev. Mod. Phys.*, vol. 75, pp. 657–712, May 2003.

[53] S. M. Rombouts, J. Dukelsky, and G. Ortiz, "Quantum phase diagram of the integrable p x+ i p y fermionic superfluid," *Physical Review B*, vol. 82, no. 22, p. 224510, 2010.

[54] S. De Baerdemacker, "Notes on the richardson-gaudin systems."

[55] I. Lukyanenko, P. S. Isaac, and J. Links, "An integrable case of the p + i p pairing hamiltonian interacting with its environment," *Journal of Physics A: Mathematical and Theoretical*, vol. 49, no. 8, p. 084001, 2016.

[56] P. W. Claeys, S. De Baerdemacker, M. Van Raemdonck, and D. Van Neck, "Eigenvalue-based determinants for scalar products and form factors in Richardson-Gaudin integrable models coupled to a bosonic mode," *Journal of Physics A Mathematical General*, vol. 48, p. 425201, Oct. 2015.

[57] P. W. Claeys, "Notes on the xxz model interacting with a bath.."

[58] N. Linial, A. Samorodnitsky, and A. Wigderson, "A deterministic strongly polynomial algorithm for matrix scaling and approximate permanents," in *Proceedings of the Thirtieth Annual ACM Symposium on Theory of Computing*, STOC '98, (New York, NY, USA), pp. 644–652, ACM, 1998.

[59] L. D. Landau and E. M. Lifshitz, "Quantum mechanics non-relativistic theory," 1981.

[60] M. Gong, X. Wen, G. Sun, D.-W. Zhang, D. Lan, Y. Zhou, Y. Fan, Y. Liu, X. Tan, H. Yu, Y. Yu, S.-L. Zhu, S. Han, and P. Wu, "Simulating the Kibble-Zurek mechanism of the Ising model with a superconducting qubit system," *Scientific Reports*, vol. 6, p. 22667, Mar. 2016.

[61] R. van den Berg, G. P. Brandino, O. El Araby, R. M. Konik, V. Gritsev, and J.-S. Caux, "Competing interactions in semiconductor quantum dots," *Phys. Rev. B*, vol. 90, p. 155117, Oct 2014.

[62] A. Sagle and R. Walde, *Introduction to Lie Groups and Lie Algebras*. No. v. 51 in Introduction to Lie groups and Lie algebras, Academic Press, 1973.

[63] W. Rossmann, *Lie Groups: An Introduction Through Linear Groups*. Oxford graduate texts in mathematics, Oxford University Press, 2006.

[64] "http://astarmathsandphysics.com/a-level-maths-notes/193-fp1/3441-the-newton-raphson-method-of-finding-roots-of-equations.html."

[65] V. Ryaben'kii and S. Tsynkov, *A Theoretical Introduction to Numerical Analysis*. Taylor & Francis, 2006.

List of Figures